This is to certify that the
dissertation entitled

THE VERTICAL DISTRIBUTION OF PHYTOPLANKTON:
OBSERVATIONS, THEORY, EXPERIMENTS

presented by

JARAD P. MELLARD

has been accepted towards fulfillment
of the requirements for the

Ph.D.	degree in	Plant Biology and Ecology, Evolutionary Biology, and Behavior

Major Professor's Signature

5/12/10

Date

THE VERTICAL DISTRIBUTION OF PHYTOPLANKTON: OBSERVATIONS, THEORY, EXPERIMENTS

By

Jarad P. Mellard

A DISSERTATION

Submitted to
Michigan State University
in partial fulfillment of the requirements
for the degree of

DOCTOR OF PHILOSOPHY

Plant Biology
Ecology, Evolutionary Biology, and Behavior

2010

ABSTRACT

THE VERTICAL DISTRIBUTION OF PHYTOPLANKTON: OBSERVATIONS, THEORY, EXPERIMENTS

By

Jarad P. Mellard

Extrinsic and intrinsic factors have been shown to determine spatial pattern formation of populations and we show how both of these factors interact to determine spatial patterns in phytoplankton communities. Determinants of the spatial (vertical) distribution of phytoplankton remain under-investigated and untested. One of the leading hypotheses to explain phytoplankton vertical distribution patterns is that competition for essential resources, nutrients and light, in opposing gradients determines vertical distribution. We used a combination of mathematical modeling, experiments in plankton towers, and lake surveys across major environmental gradients to study what determines the vertical distribution of phytoplankton, focusing on competition for nutrients and light.

In chapter 2, we combined two previous bodies of theory on well-mixed and poorly-mixed water columns to develop a model for a stratified water column. In addition, we considered multiple nutrient sources- one source to the bottom of the water column and one source to the surface mixed layer. Employing this combination of stratification and multiple nutrient sources in our model, we found eight distinct evolutionarily stable strategy (ESS) distributions. The predicted ESS distributions from our model accurately reflected phytoplankton distributions we have observed in lakes. Algae can exist in the mixed layer, deep layer, or in the mixed layer and deep layer together. Algae in either of these locations can be limited by nutrients or colimited by nutrients and light, but counterintuitively, only the mixed layer can be light limited. We predict how the ESS distribution should change as a function of relevant major environmental parameters known to vary across bodies of water.

In chapter 3, we conducted experiments to examine how spatial patterns in algae form as the result of interacting processes: active movement and habitat selection, growth, and depletion of resources. These experiments were conducted to test prior theory that predicted that algae will aggregate into a thin layer at a depth and that that depth depends on resource supply rates. In all experimental plankton towers, algae formed thin layers at the surface, which disappeared at low-nutrient supply by the end of the experiment. Higher nutrient supply rates created more biomass and made the algae relatively more light limited. Thus, results qualitatively supported many of our theoretical predictions. In addition, algae exhibited spatial dynamics consistent with niche construction processes, i.e. modification of their environment and responses to these modifications through behavioral movement. These experiments explain how intraspecific competition can drive vertical distributions.

In chapter 4, we surveyed stratified lakes to measure the variation in vertical distributions of phytoplankton and ascribe environmental conditions to the vertical distributions. A primary purpose was to evaluate model predictions of the vertical distribution of phytoplankton in stratified lakes with multiple nutrient sources, while also considering that the phytoplankton communities are made up of many different species. Lakes with single pronounced peaks of algal biomass mostly conformed with model predictions of how environmental variables affect vertical distribution. Phytoplankton also frequently formed multiple peaks in biomass within a water column. The number of peaks that formed depended on the physical space available and the amount of resource heterogeneity in that space. Peaks were typically dominated by a single species and each peak in a water column existed at different nutrient and light conditions. Taxonomic groups sorted across lakes and with depth within lakes and surface and deep vertical niches could be filled by different taxonomic groups and species. Competition for nutrients and light appears to be a primary driver of phytoplankton community structure and vertical distribution.

DEDICATION

I dedicate this work to my family, thank you for supporting me through the years, and to all those who toil in obscurity.

ACKNOWLEDGMENT

First and foremost, I would like to thank my advisors, Chris Klausmeier and Elena Litchman. This work is very much influenced by and in collaboration with them. I would also really like to thank another collaborator, Kohei Yoshiyama, for all the good detailed work and ideas contributed to these studies. I would like to thank Mary Anne Evans for her hard field work and Don Schoolmaster for much conceptual help in analyses. I would like to thank Pam Woodruff, Darice Shumway, and Ally Hutchens for help with lab and field work. I would also like to thank Paula Tezanos for help in identification of phytoplankton species and Stuart Jones for providing many useful comments on the thesis and helping in statistical analyses used in chapter 4. This work could not have been completed without the help of all of you.

In addition, I would like to thank Kelly Amrhein, Paula Tezanos, Chris Steiner, Anne Schwaderer, and Claes Becker for contributing in discussions of chapter 3, and Stuart Jones and Jay Lennon for helpful discussions of analyses used in chapter 4. Comments from Jim Grover, and several anonymous reviewers greatly improved chapter 2 and I would like to thank Jason Cepela, Emily Grman, and Todd Robinson for helpful comments on chapter 3 and Emily Grman, Kali Bird, and Colin Kremer for comments on chapter 4. This work was supported by funding from National Science Foundation Division of Environmental Biology 06-10531 and 06-10532 and the J.S. McDonnell Foundation.

TABLE OF CONTENTS

LIST OF TABLES

LIST OF FIGURES

Chapter 1

Introduction

> "Space complicates ecological interactions by two fundamental mechanisms: it allows for non-uniform patterns of environment and population density, and for movement (dispersal or migration) from one location to another."
> -S. Levin

Ecological communities are structured in space across multiple scales. The heterogeneous nature of the environment (Burrough 1981) translates to community compositional patterns at local, regional, and even global scales (MacArthur 1972). Different ecological processes may determine species distributions at different scales and these processes can feed back on one another (Levin 1992, Tilman and Kareiva 1997, Leibold et al. 2004). A community is comprised of individual populations and each is distributed in space according to its tolerances to stresses and requirements for resources (Levin 1976, Tilman and Pacala 1993). Spatial heterogeneity may be key to explaining the coexistence of many similar species (Hutchinson 1961).

Spatially heterogeneous distributions of populations have important consequences for ecosystem-level processes (Loreau et al. 2003*a*). Production can vary in space which influences the spatial distributions of consumers and transfer of energy to higher trophic levels (Johnsen and Jakobsen 1987) as well as spatial coupling between

systems due to consumer behavior (McCann et al. 2005). Populations distributed in space also change the flux of matter, energy, and nutrients between ecosystem components and ecosystems, creating meta-ecosystems (Loreau et al. 2003*b*).

I will use phytoplankton (algae) to illustrate how spatial heterogeneity can be generated. Algae exhibit striking spatial patterns that are likely the result of opposing resource supply gradients (Fee 1976, Klausmeier and Litchman 2001). Light is supplied from the surface and declines exponentially with depth due to abiotic and biotic absorbance and scattering (Kirk 1975*a*). Nutrients usually enter the water column from the sediments at the bottom (Wetzel 1975). These opposing resource gradients create a dilemma for algae, as they require both resources for growth. Many algae are motile (Reynolds 1984) or have other ways to control their location in the water column, such as regulation of buoyancy (Cullen and MacIntyre 1998), and thus are not passively drifting about as the name plankton suggests. Where is the optimal location in an environment with opposing resource gradients?

For algae, the optimal location within the water column is the depth where an individual is equally limited by both light and nutrients (Klausmeier and Litchman 2001). This depth of colimitation depends on the resource supply rates. It also depends on all the other algae in the water column. Algae can be at different depths in the water column; physiological traits may determine each species depth of colimitation or "strategy." As they grow, algae modify their environment due to resource depletion, taking up nutrients and shading one another. These processes of movement, resource depletion, and growth create feedbacks among algal strategies in the aquatic environment. This is what I will refer to as algal games (Klausmeier and Litchman 2001). This game will be key to my approach in understanding studying vertical distributions.

The spatial distribution of algae is important because it controls ecosystem processes such as whole-system primary production (Fee 1976), the flux of carbon to

deeper parts of a water body (Suess 1980), the flux of nutrients from the deep to shallower waters (Garside 1985), and even the thermal properities and physical structure of the water body (Mazumder et al. 1990). Spatial heterogeneity in the aquatic environment may also impact community-level processes and patterns such as resource competition and species coexistence (Tilman 1982). Observed spatial distributions may be the result of resource competition interactions within the community and vertical niche partitioning between species may result in their coexistence (Carney et al. 1988).

Before I outline my dissertation work, I will review relevant literature to provide a context for my graduate research. Then I will briefly introduce each of my dissertation chapters.

1.1 Context

The major axis of heterogeneity in lakes and oceans is the vertical dimension. Depth-varying irradiance and turbulent mixing are prominent forms of vertical heterogeneity. The foundations for present day ecosystem-level investigations focused on how light and mixing impact phytoplankton populations and I will focus on studies that consider these processes.

Phytoplankton spatial models generally focus on one-dimensional water columns and come in two forms: well-mixed and poorly-mixed water columns. Phytoplankton spatial models of light competition began with considering well-mixed populations for simplicity, but include the underlying spatial heterogeneity in light. In well-mixed water columns, algae are homogenized, hence no spatial patterns can form. In poorly-mixed water columns, algae can be distributed heterogeneously with depth and may aggregate into a thin layer. I consider a model to address poorly-mixed conditions if it allows for any heterogeneous distribution of algae. Some of these studies that

address poorly-mixed conditions varied mixing levels to create conditions between well-mixed and extremely poorly-mixed, where algae can still form patterns but the mixing prevents the population from forming a thin layer. Although I have categorized light competition studies into well-mixed and poorly-mixed water column categories, note that many of the studies contain other aspects that makes them different from each other, such as whether they include competition for nutrients, multiple species, and traits related to buoyancy and swimming.

I will introduce theoretical developments and empirical tests of theory, emphasizing those studies that consider mixing and competition for light. Many of the theoretical studies have been tested empirically. This is an area in ecology that has advanced significantly, likely due to the close relationship between the modeling being conducted and the explicit tests of predictions from those models. Of course it helps that phytoplankton populations are amenable to experiments due to their small size and fast generation time.

1.1.1 Well-mixed water columns

Phytoplankton spatial models of light competition start with well-mixed populations (Huisman and Weissing 1994), but include heterogeneity in the form of the underlying light gradient. Many later models and experiments build on these well-mixed-population results.

1.1.1.1 Observations

Early observations of phytoplankton populations in the surface layer focused on the importance of water column stability, specifically mixed layer depth, as a primary determinant of spring algal blooms in temperate waters (Riley 1942). One of the first examinations of how light sets the conditions for population growth showed that for phytoplankton in a well-mixed layer, there is a critical depth for the mixed layer in

order for a population to persist there. That critical depth is set by the metabolic balance between energy production and destruction (respiration) (Sverdrup 1953).

1.1.1.2 Theory and empirical tests of theory

Several very influential theoretical studies on effects of light competition and mixing on phytoplankton populations were published in the mid-1990s. Huisman and Weissing (1994,1995) put forth the theory of how light acts as a resource in a well-mixed environment, which is similar but not identical to a nutrient: the light at the bottom of a water column at equilibrium, I_{out}, predicts the outcome of competition for light in a well-mixed water column, that is, the species with the lowest I_{out} wins in competition, similar to R^*. However it differs from R^* in nutrient competition in two ways: 1) I_{out} depends on the light supply, I_{in}. 2) I_{out} is a global measure of the effects of a population on light, which is not the same as the local measure of the effects of a population on light, I^*. Actually, $I_{\text{out}} < I^*$, which means that part of the population is experiencing negative growth. How can the population be maintained then, without going extinct? It can be maintained because the losses from that negative growth rate at depth are balanced by production above it (Huisman and Weissing 1994). However, if the water column is too deep, the population can go extinct because there is not enough production to balance those losses.

Light competition theory was tested and verified for monocultures (Huisman 1999) and multispecies mixtures (Huisman et al. 1999*a*). Huisman and Weissing (1994,1995) also examined competition for light and nutrients and those predictions were tested and verified as well (Passarge et al. 2006).

An in-depth analysis of how mixing depth, nutrient supply, light, biomass, sinking, and recycling was undertaken by Diehl (2002) in a model that built on Huisman and Weissing (1994,1995), and thus assumes a well-mixed phytoplankton population. Diehl (2002) predicts biomass in the mixed layer to show a unimodal response to

mixed layer depth. Model predictions from Diehl (2002) were evaluated in several field enclosure experiments (Diehl et al. 2002, Ptacnik et al. 2003). Predictions of how mixing depth affects phytoplankton production, sedimentation, and resource levels (Diehl 2002) were tested and verified, as well as how mixing depth differentially affects sinking and nonsinking taxa (Ptacnik et al. 2003). Kunz and Diehl (2003) also showed some evidence that consistent with field observations in lakes differing in mixed layer depth.

1.1.2 Poorly-mixed water columns

Poorly-mixed conditions are necessary to examine spatial pattern formation. General spatial models of continuous space start with the relatively simple (Skellam 1951) and increase in complexity as outlined in Okubo (1980). Spatial models for phytoplankton populations are related to these general models (Huisman et al. 1999*c*), and in some ways, mimic their development.

1.1.2.1 Observations

Heterogeneous depth distributions of phytoplankton were observed and shown to be a significant component of the ecosystem (Fee 1976). Fee (1976) showed that significant phytoplankton populations and primary production occur below the mixed layer in lakes. Fee (1976) explained how light and nutrient gradients could lead to the formation of a deep chlorophyll maximum, DCM, which is a peak in chlorophyll well below the surface, often at apparently suboptimal light levels (Camacho 2006). Fee (1976) emphasized that the position of the DCM should be related to light penetration, but also hypothesized that sedimentation, grazing, and minimization of loss due to respiration could be responsible for the large amount of deep layer biomass. Since then, numerous hypotheses for DCM formation and vertical distribution patterns of phytoplankton have been proposed (see Lindholm 1992 and references therein. For

example, offshore advection (Cullen et al. 1982), near-inertial internal wave shear (Franks 1995), sinking in a density stratified water column (Condie and Bormans 1997), depth dependent grazing by zooplankton (Johnsen and Jakobsen 1987) or mixotrophs (Tittel et al. 2003), lateral intrusions of nutrient rich water that may stimulate growth (S. MacIntyre pers. comm.), diel vertical migration of algae (Sommer and Gliwicz 1986, Gasol et al. 1991), preferential movement of algae to depth that favors growth (Klausmeier and Litchman 2001), in situ growth (Fee 1976), and behavioral responses to chemoclines or other information acting as sensory cues (Gervais 1998, Clegg et al. 2007) have all been proposed to explain DCM formation.

1.1.2.2 Theory and empirical tests of theory

Spatial heterogeneity of a population was examined by relaxing the assumption of a well-mixed water column and examining neutrally buoyant species in this environment. Huisman et al. (1999*c*) used numerical simulations of a spatially explicit model to show how bloom formation depends on physical mixing: if the water column depth is less than a critical depth and turbulent mixing is less than a critical turbulence level, then blooms can form. In this poorly-mixed environment, multispecies competition for light showed that neutrally buoyant species competing for light should always decline with depth, hence no DCM formation should occur under these conditions (Huisman et al. 1999*b*). In addition, species were not likely to vertically segregate, and in this kind of environment with just light competition, there are very limited opportunities for coexistence (Huisman et al. 1999*b*).

Under poorly-mixed conditions, the species or individuals that obtain the best position in the water column are favored (Huisman et al. 1999*b*, Klausmeier and Litchman 2001). Considering a motile species competing for light and nutrients in a poorly mixed water column, Klausmeier and Litchman (2001) showed there is an evolutionarily stable strategy (ESS) depth that prevents growth in the rest of the

water column. Of note, Klausmeier and Litchman (2001) assume that the system is adaptive, i.e. algae move to where conditions are best for growth. This adaptive strategy can lead to non-intuitive results. For example, algae in a benthic layer are far from their light source so one might predict them to be limited by light. However, with adaptive movement, if there was not enough light at the bottom, the algae would not move there. Therefore, Klausmeier and Litchman (2001) predict algae in a benthic layer to be limited by nutrients, not light.

Studies that explicitly test the theory of how opposing resource gradients in poorly-mixed water columns can generate vertical distributions of phytoplankton were needed. I, in collaboration with Kohei Yoshiyama, Christopher Klausmeier, and Elena Litchman, tested this theory (Klausmeier and Litchman 2001) in experimental water columns (Chapter 3). We examined the dynamics and equilibrium vertical distribution of phytoplankton along a gradient in nutrient loading and found evidence for many of our dynamic and some equilibrium theoretical predictions in our experiment.

Huisman et al. (2002) builds on previous work (Huisman et al. 1999*c*) by adding sinking to a light-limited population in a uniformly mixed water column, effectively adding sinking to the arguments of Riley (1942). Previous work (Huisman et al. 1999*c*) showed there was a maximal water column depth and a maximal turbulent mixing level for a population to persist, but with the addition of sinking, there is also a minimal turbulent mixing level in order to keep the population from sinking out of the photic zone. A theoretical study that varied sinking rate demonstrated the maximal sinking rate in different environments (Huisman and Sommeijer 2002). Theory predicts that the outcome of competition for light between sinking and buoyant species can depend on turbulent mixing, with sinking species dominating at high turbulent mixing levels and buoyant species dominating at low turbulent mixing levels (Huisman and Sommeijer 2002, Huisman et al. 2004). An artificially mixed lake

that could be intermittently mixed was used to test this prediction. Comparison of periods with artificial mixing versus periods without verified the predicted shift in species dominance (Huisman et al. 2004).

More recently, an empirical study (Jaeger et al. 2008) examined some of the predictions related to Huisman et al. (2002) of how mixing intensity, water column depth, sinking, and light affect phytoplankton populations. However, this study was also complicated by the fact that there were community-level interactions and responses. The combination of low mixing intensities, deep water columns, and different species with different motility and buoyancy related traits was shown to create vertical niche partitioning in the experimental enclosures in the lake (Jaeger et al. 2008). Furthermore, Jaeger et al. (2010) conducted a theoretical study that extended the interactive effects of mixing intensity, water column depth, sinking, and light (Huisman et al. 2002) to include nutrients. In these uniformly mixed water columns, Jaeger et al. (2010) predicts that the population could be light or nutrient limited, depending on the mixing intensity and water column depth.

1.1.3 Stratified water columns

Many bodies of water stratify, resulting in division of the ecosystem into distinct parts: a well-mixed surface layer and a poorly-mixed deep layer. However, few theoretical studies that include the feedbacks between phytoplankton and light have considered the impacts of stratification on the vertical distribution of phytoplankton.

1.1.3.1 Theory and empirical tests of theory

Studies mentioned previously have generally focused on phytoplankton only in the mixed layer (Huisman and Weissing 1994,1995, Diehl 2002). However, some considered a completely poorly-mixed water column (Huisman et al. 1999*c*, 1999*b*, Klausmeier and Litchman 2001) and one considered a stratified water column (Yoshiyama

and Nakajima 2002). Illustrating some of the complications that spatially-explicit competition for nutrients and light can create, Yoshiyama and Nakajima (2002) used numerical simulations of a sinking population to show bistability of alternative vertical equilibria in a coupled well-mixed surface layer and poorly-mixed deep layer separated by a thin thermocline region that reduced exchange between the two layers. The bistability of surface layer maxima and deep layer maxima is created by positive feedback in both layers. This positive feedback is due to asymmetric competition, as phytoplankton in the surface layer reduce light supply to phytoplankton in the deep layer and phytoplankton in the deep layer decrease nutrient supply to phytoplankton in the surface layer (Yoshiyama and Nakajima 2002).

In order to get more insight into stratified bodies of water, I, in collaboration with Kohei Yoshiyama, Christopher Klausmeier, and Elena Litchman, combined elements from these previous studies to show how spatially-varying mixing (stratification), can drive the vertical distribution of phytoplankton (Chapter 2). In addition we used analytical results from our game theoretical model to better define and analyze parameter space. Stratification was not the only extra environmental complexity we added. We also added multiple nutrient sources, which can create previously unpredicted depth distributions. Specifically, multiple nutrient sources allows for multiple vertical biomass maxima.

Multiple species may compete for nutrients and light in poorly-mixed environments. Huisman et al. (2006) examined how sinking species with different nutrient and light competitive abilities may coexist in a nonequilibrium environment caused by seasonal changes in incoming light. Yoshiyama et al. (2009) delineated the areas in parameter space where two species competing for nutrients and light in stratified water columns may coexist. Yoshiyama et al. (2009) use the same ESS approach as Chapter 2, extending it to multiple species, but including just one nutrient source. Yoshiyama et al. (2009) provide another explanation for bimodal phytoplankton dis-

tributions, hence when we observe two modes, then according to our theory, it could be one species (Chapter 2) or two species (Yoshiyama et al. 2009). Yoshiyama et al. (2009) show that for two species with a tradeoff in light and nutrient competitive abilities, the species can divide the water column according to their requirements. In addition, stratification in combination with multiple species creates distinct disjunct niches of the same species. For example, along an environmental gradient of nutrient loading or mixed layer depth, one species can live under the shade of the other, then disappear completely at higher nutrient loading or deeper mixed layer depth, but then reinvade and outcompete the other species to take over the mixed layer at even higher nutrient loading or deeper mixed layer depth conditions.

In 2007, I, in collaboration with Mary Anne Evans, Kohei Yoshiyama, Christopher Klausmeier, and Elena Litchman, set out to examine how model predictions, specifically Chapter 2 and Yoshiyama et al. (2009), are upheld in the field (Chapter 4). We found a great deal of variation in vertical distributions of phytoplankton in lakes and that major environmental variables explained much of this variation as theory predicted (Chapter 2). In addition we uncovered pronounced community compositional patterns across lakes and within lakes with depth that should fuel further studies, both theoretical and empirical.

A recent community study has shown how groups of phytoplankton that differ in their pigment composition are distributed differently with depth. Across lakes, the environmental variables of color (DOC), total phosphorus, and CV of temperature were shown to determine vertical distribution of the bulk community of phytoplankton as well as individual groups of phytoplankton distinguished by their pigment composition (Longhi and Beisner 2009).

1.2 Outline

The aim of this dissertation was to determine what drives vertical distributions of phytoplankton. To this end, we developed generalized theory and rigorously tested theoretical predictions in experimental water columns and in lakes existing across environmental gradients. No experimental tests had been conducted of how intraspecific competition for nutrients and light in poorly-mixed water columns could create different vertical distributions of phytoplankton. Most of the previous theory was limited to the two extremes of completely well-mixed or poorly-mixed water columns and could not replicate real vertical distributions of phytoplankton. In addition, few previous studies had explicitly tested predictions from previous theory on how competition for nutrients and light determines vertical distributions of phytoplankton in many lakes along environmental gradients.

In Chapter 2, we combine two bodies of theory, that of well-mixed and poorly-mixed water columns, into one theoretical framework in order to describe stratified water columns. I, in collaboration with Kohei Yoshiyama, Elena Litchman, and Christopher Klausmeier, made previous theory more realistic, by extending previous models of spatially heterogeneous competition for nutrients and light to include stratification and multiple nutrient sources. We asked, how does stratification affect vertical distribution and how do multiple nutrient sources, in addition to stratification, affect vertical distribution? A key issue we faced was how to create stratification in a simplified model that would provide analytical results. We created stratification by merging two theories, that of a completely well-mixed water column with that of a completely poorly-mixed water column. We found the ESS distribution of algae to be a function of different environmental parameters. A difference with a previous study that considered motile algae (Klausmeier and Litchman 2001), is that the algae in the surface layer are well mixed, hence cannot aggregate at their ESS depth. In this

situation, if the depth of colimitation is in the mixed layer, the shallower part of the population is limited by nutrients and the deeper part of the population is limited by light.

We also add depth-dependent nutrient sources, which can create previously unpredicted depth distributions. Specifically, multiple nutrient sources can create multiple vertical biomass maxima. Perhaps counter intuitively (especially considering previous theory that predicts a single best location for growth (Klausmeier and Litchman 2001)), a vertical distribution with multiple maxima is an ESS under some conditions. When this additional environmental complexity of multiple nutrient sources is coupled with stratification, phytoplankton can exist in the mixed layer and deep layer simultaneously. Although the same species is in the mixed layer and deep layer, they are not necessarily the same physiologically: the mixed layer algae are nutrient limited and the deep layer algae are nutrient limited or colimited if in a benthic layer or DCM respectively. The goal of our contribution was not to further obfuscate what is already known about phytoplankton in vertical light and nutrient gradients but rather provide an encompassing picture of many of the possible outcomes by generalizing previous models. We provided detailed mathematical descriptions of the environment and how the organism interacts with it, explicitly considering vertical strategies in that environment.

In Chapter 3, I, in collaboration with Kohei Yoshiyama, Christopher Klausmeier, and Elena Litchman, tested the algal games theory (Klausmeier and Litchman 2001) in experimental plankton towers designed to mimic poorly-mixed water columns. In this experiment, we asked, will algae form a thin layer and will the depth of the thin layer be related to resource conditions? Specifically, will the thin layer be shallower under higher nutrient conditions? We also extended the theoretical predictions to include predictions of spatio-temporal dynamics. For example, we asked, where should the algae aggregate initially? One might think it depends on environmental condi-

situation, if the depth of colimitation is in the mixed layer, the shallower part of the population is limited by nutrients and the deeper part of the population is limited by light.

We also add depth-dependent nutrient sources, which can create previously unpredicted depth distributions. Specifically, multiple nutrient sources can create multiple vertical biomass maxima. Perhaps counter intuitively (especially considering previous theory that predicts a single best location for growth (Klausmeier and Litchman 2001)), a vertical distribution with multiple maxima is an ESS under some conditions. When this additional environmental complexity of multiple nutrient sources is coupled with stratification, phytoplankton can exist in the mixed layer and deep layer simultaneously. Although the same species is in the mixed layer and deep layer, they are not necessarily the same physiologically: the mixed layer algae are nutrient limited and the deep layer algae are nutrient limited or colimited if in a benthic layer or DCM respectively. The goal of our contribution was not to further obfuscate what is already known about phytoplankton in vertical light and nutrient gradients but rather provide an encompassing picture of many of the possible outcomes by generalizing previous models. We provided detailed mathematical descriptions of the environment and how the organism interacts with it, explicitly considering vertical strategies in that environment.

In Chapter 3, I, in collaboration with Kohei Yoshiyama, Christopher Klausmeier, and Elena Litchman, tested the algal games theory (Klausmeier and Litchman 2001) in experimental plankton towers designed to mimic poorly-mixed water columns. In this experiment, we asked, will algae form a thin layer and will the depth of the thin layer be related to resource conditions? Specifically, will the thin layer be shallower under higher nutrient conditions? We also extended the theoretical predictions to include predictions of spatio-temporal dynamics. For example, we asked, where should the algae aggregate initially? One might think it depends on environmental condi-

tions such as nutrient loading. Perhaps non-intuitively, our theory predicts that algae should always swim to the top because they should be light limited initially for the reasonable range of nutrients explored in our experiment. Once sufficient growth has occurred, the nutrients should be depleted at the surface in low-nutrient treatments so that the algae swim down to acquire more nutrients.

We found that algae formed a thin layer at the surface during the first part of our experiment in all treatments because that is the best location for growth. This thin layer persisted throughout the experiment in high-nutrient treatments, but in low-nutrient treatments, the thin layer dissipated midway through the experiment as algae redistributed throughout the water column. We found qualitative support for predictions of equilibrium biomass and resource limitation status across our treatments.

In Chapter 4, I, in collaboration with Mary Anne Evans, Kohei Yoshiyama, Christopher Klausmeier, and Elena Litchman, conducted a lake survey to measure vertical distributions of phytoplankton and environmental variables. We focused on environmental variables predicted from Chapter 2 to be important in determining phytoplankton vertical distributions. We asked, what phytoplankton vertical distributions exist in different lakes and what determines them across major environmental gradients? On the empirical side, theory on how mixing and light interact to affect phytoplankton populations had already had some success in explaining whole lake systems across lakes (Kunz and Diehl 2003) and within a lake that was experimentally manipulated (Huisman et al. 2004). However, we wanted to better know how well it can describe other situations, particularly when other factors are involved, such as nutrients, stratification, and motility, that recent theory had shown to be important in being able to replicate patterns in the field. We aimed to test predictions across large environmental gradients to examine how nutrient and light competition can drive patterns in different lakes. In addition, with the many complications

presented by stratification and multiple species with presumably different motility, nutrient, and light traits (Yoshiyama et al. 2009), we wondered if we would see any evidence supporting our predictions for how vertical distribution should change across environmental gradients.

We found a great deal of variation in vertical distributions of phytoplankton in lakes and that major environmental variables explain much of this variation as theory predicted (Chapter 2). We found that multiple peaks of algae within the water column is a common phenomenon and that these peaks exist at different light and nutrient resource levels. Across all peaks, there is a negative relationship between nutrient and light levels. We found that taxonomic groups of phytoplankton are distributed across lakes according to environmental variables, exhibit contrasting depth distributions between lakes, and respond differently to nutrient and light levels within lakes. Furthermore, vertical niches such as DCMs, are composed of many different species across lakes but each DCM is usually dominated by a single species.

Chapter 2

The vertical distribution of phytoplankton in stratified water columns

Jarad P. Mellard

with

Kohei Yoshiyama, Elena Litchman, and Christopher A. Klausmeier

2.1 Abstract

What determines the vertical distribution of phytoplankton in different aquatic environments remains an open question. To address this question, we develop a model to explore how phytoplankton respond through growth and movement to opposing resource gradients and different mixing conditions. We assume stratification creates a well-mixed surface layer on top of a poorly-mixed deep layer and nutrients are supplied from multiple depth-dependent sources. Intraspecific competition leads to a unique strategic equilibrium for phytoplankton, which allows us to classify the dis-

tinct vertical distributions that can exist. Biomass can occur as a benthic layer (BL), a deep chlorophyll maximum (DCM), or in the mixed layer (ML), or as a combination of BL+ML or DCM+ML. The ML biomass can be limited by nutrients, light, or both. We predict how the vertical distribution, relative resource limitation, and biomass of phytoplankton will change across environmental gradients. We parameterized our model to represent potentially light and phosphorus limited freshwater lakes, but the model is applicable to a broad range of vertically stratified systems. Increasing nutrient input from the sediments or to the mixed layer increases light limitation, shifts phytoplankton towards the surface, and increases total biomass. Increasing background light attenuation increases light limitation, shifts the phytoplankton towards the surface, and generally decreases total biomass. Increasing mixed layer depth increases, decreases, or has no effect on light limitation and total biomass. Our model is able to replicate the diverse vertical distributions observed in nature and explain what underlying mechanisms drive these distributions.

2.2 Introduction

The aquatic environment of phytoplankton creates an opportune situation to study the feedbacks between resource gradients, behavioral movement, population dynamics, and passive dispersal. The major axis of spatial heterogeneity for phytoplankton is the vertical dimension. The vertical distribution of phytoplankton affects primary production as well as energy transfer to higher trophic levels (Leibold 1990; Williamson et al. 1996; Lampert et al. 2003). Therefore, there is an immediate need to understand the fundamental principles that govern the vertical distribution of phytoplankton, ecologically important organisms that contribute roughly half of global net primary productivity (NPP) (Field et al. 1998) and continue to be affected by climate change (Hays et al. 2005).

A dizzying diversity of phytoplankton vertical distributions have been observed (*see* Fig. 2.1 for a few examples). Density stratification breaks the water column into distinct strata resulting in non-uniform mixing, often with a well-mixed surface layer on top of a poorly-mixed deep layer (Wetzel 1975; Wüest et al. 2000). Phytoplankton may be found in high abundance in the mixed layer, in the deep layer, directly on the bottom, or in some combination of these locations. What determines their vertical distribution in stratified water columns? Light is in greatest supply at the top of the mixed layer and phytoplankton are hypothesized to exist there when there is adequate nutrient supply (Reynolds 1984; Paerl 1988). Frequently, phytoplankton form a peak in abundance known as a deep chlorophyll maximum, or DCM, in the deep layer. Low turbulence and sufficient light penetration have been hypothesized as necessary for a DCM to persist (Fee 1976) and the light and nutrient gradients control the depth of the peak (Fee 1976; Klausmeier and Litchman 2001). Under low nutrient concentrations and if sufficient light penetrates to the bottom, phytoplankton may form a benthic layer on the sediments and access nutrients diffusing through the

sediment pore water before it enters the water column (Sand-Jensen and Borum 1991).

Figure 2.1. Example phytoplankton vertical distributions observed in stratified lakes in Southern Michigan. A) Benthic layer biomass only. B) DCM biomass only. C) Mixed layer biomass only. D) Benthic layer and mixed layer biomass. E) DCM and mixed layer biomass. Vertical distributions are chlorophyll *a* fluorescence profiles and mixed layer depth, z_{m}, is defined from the temperature profile to be the depth 1 °C cooler than the surface temperature. Profile A) is from Sherman Lake, Kalamazoo County MI, October 12, 2007. Profile B) is from Bristol Lake, Barry County MI, October 3, 2007. Profile C) is from Fine Lake, Barry County MI, October 3, 2007. Profile D) is from Hogsett Lake, Kalamazoo County MI, October 22, 2007. Profile E) is from Bassett Lake, Barry County MI, October 15, 2007.

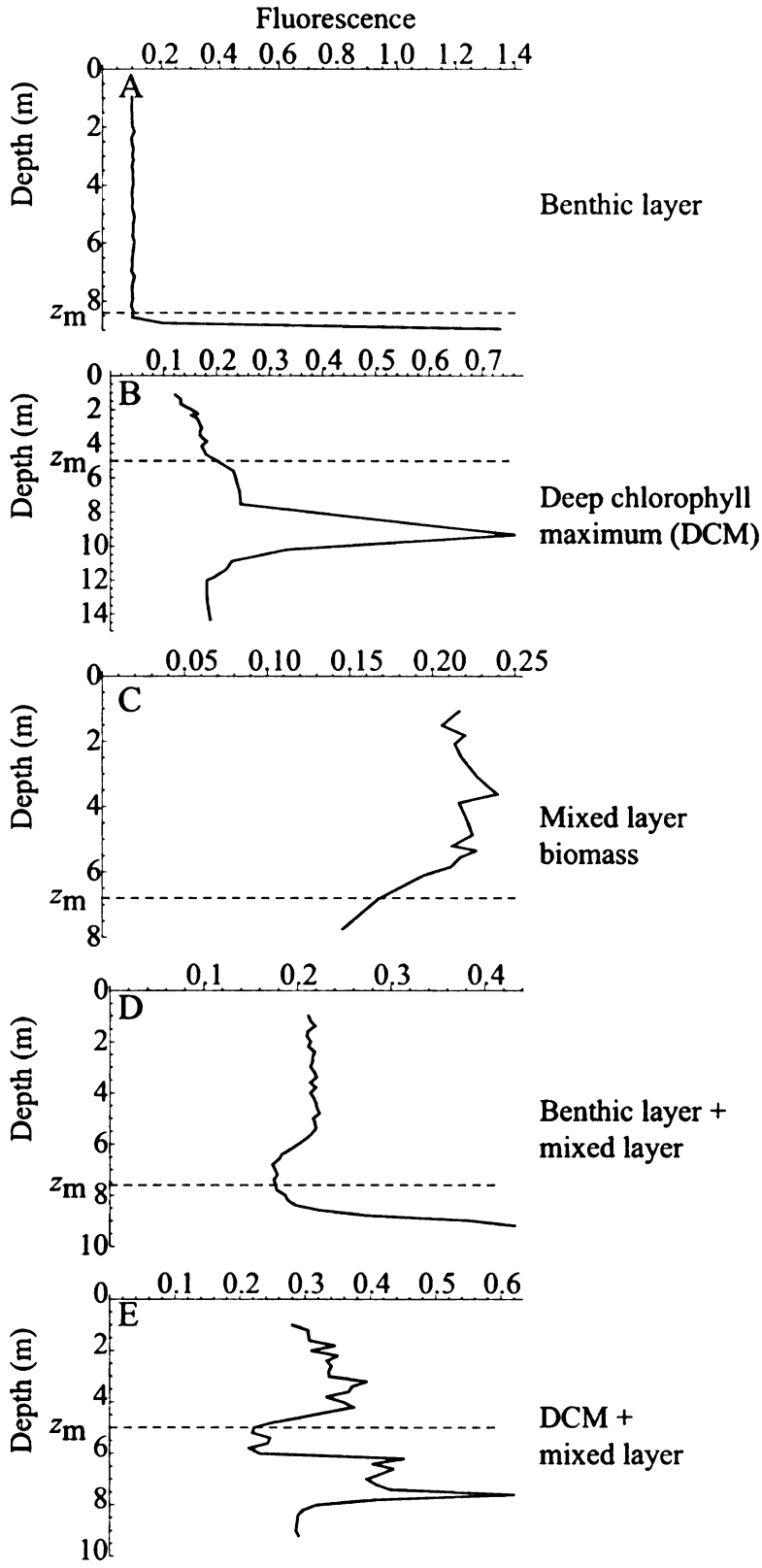

Figure 2.1: Example phytoplankton vertical distributions observed in stratified lakes.

In a well-mixed water column, phytoplankton and nutrients are homogenized throughout the water column; however a light gradient is inevitable. As a consequence, phytoplankton experience varying local light levels and therefore varying growth rates. The light level at the bottom of the water column, I_{out}, predicts the outcome of competition for light (Huisman and Weissing 1994, 1995) in a way similar to R^* for nutrients (Tilman 1982). In contrast, in a poorly-mixed water column, motile phytoplankton can be thought of as playing a competitive game in opposing essential resource gradients. A shallower position allows a cell to shade those below it but a deeper position allows it to intercept nutrients mixing up from below. Eventually phytoplankton will aggregate at their evolutionarily stable strategy (ESS) depth z^*, which is the depth of equal limitation by nutrients and light and prevents growth elsewhere in the water column (Klausmeier and Litchman 2001). These studies are applicable to the two extremes of whole water columns, one of well-mixed and one of poorly-mixed.

Many bodies of water stratify. Several models have considered stratified water columns, ranging from complex simulation models particular to specific ecosystems (Lucas et al. 1998; Fennel and Boss 2003; Peeters et al. 2007; Ross and Sharples 2007) to simpler models aimed at general understanding. Condie and Bormans (1997) and Hodges and Rudnick (2004) included sinking but neglect the feedback of phytoplankton on light. Huisman and Sommeijer (2002a,b) incorporate the feedback of phytoplankton on light, but omit nutrients and assume no mixing in the hypolimnion. Yoshiyama and Nakajima (2002), Yoshiyama et al. (2009), and Ryabov et al. (2009) do not include nutrient loading to the mixed layer. Our study systematically explores the different vertical distributions of phytoplankton that can arise from intraspecific competition for nutrients and light in a stratified water column.

In this paper, we build on previous work by considering a stratified water column with a well-mixed surface layer on top of a poorly-mixed deep layer, a combination

of approaches by Huisman and Weissing (1994, 1995) and Klausmeier and Litchman (2001). We relax the assumption of an infinitely thin layer (Klausmeier and Litchman 2001) to a layer of finite depth and show what resources limit growth at different depths within the layer. Furthermore, we consider multiple nutrient inputs, including input directly to the mixed layer, expanding on Diehl (2002). Current models for poorly-mixed water columns consider only nutrient supply from below (Klausmeier and Litchman 2001; Huisman et al. 2006; Beckmann and Hense 2007). We enumerate the possible equilibrium algal vertical strategies and show under what conditions each should occur.

2.3 Methods

2.3.1 Full Model

The full model consists of partial differential equations for biomass, $b(z,t)$ and nutrients, $R(z,t)$ which in our examples represents phosphorus, and an integral equation for light, $I(z,t)$. We consider a one-dimensional water column where z is depth with the surface at $z = 0$ and the bottom at $z = z_b$.

Phytoplankton biomass b grows according to Liebig's law of the minimum, so gross growth rate at depth z is $g(R,I) = \min(f_I(I(z,t)), f_R(R(z,t)))$. Functions $f_I(I)$ and $f_R(R)$ are the potential growth rates as a function of the resource I or R when that resource is limiting. We use the Michaelis-Menten form for the functions in our numerical solutions, $f_I(I) = rI/(I+K_I)$ and $f_R(R) = rR/(R+K_R)$ where r is the maximum growth rate and K_I and K_R are half-saturation constants for light and nutrients respectively. Our qualitative results, however, should hold for other bounded, strictly increasing functions. Biomass is lost at density independent rate m, which encompasses all sources of mortality. Net growth rate is $g(z) - m$. Net growth at depth z is only possible if both I is greater than the break even light

level, $I^* = f_I^{-1}(m)$, and R is greater than the break even nutrient concentration, $R^* = f_R^{-1}(m)$ (Tilman 1982).

A depth-dependent turbulent eddy diffusion coefficient $D(z)$ describes passive movement. Active movement is described by a taxis term (Okubo 1980). Phytoplankton behavior is governed by simple rules. They move up if conditions immediately above are better than immediately below, move down if conditions immediately below are better than immediately above, and do not move if conditions are worse immediately above and below. To describe this behavior, we let phytoplankton velocity v depend on the gradient in growth rate, $\partial g/\partial z$. We assume v to be an odd decreasing function that approaches $v_{\max}$ as $\partial g/\partial z$ approaches negative infinity (positive v is upward), approaches $-v_{\max}$ as $\partial g/\partial z$ approaches positive infinity, and $v(0) = 0$. See the section titled Assumptions, limitations, and extensions in the Discussion for how relaxing the assumption of active motility affects results.

Change in biomass at depth z is the balance of growth, death, and passive and active movement.

$$\frac{\partial b}{\partial t} = (g(R, I) - m)b + \frac{\partial}{\partial z}\left(D(z)\frac{\partial b}{\partial z} + v\left(\frac{\partial g}{\partial z}\right)b\right) \tag{2.1}$$

Nutrients R are taken up by phytoplankton with a yield of Y biomass per unit nutrient consumed, are mixed with eddy diffusion coefficient $D(z)$, are supplied directly to the water column at depth z at rate $R_{\text{in}}(z)$, and are recycled from dead phytoplankton with proportion ε.

$$\frac{\partial R}{\partial t} = -g(R, I)\frac{b}{Y} + \frac{\partial}{\partial z}\left(D(z)\frac{\partial R}{\partial z}\right) + R_{\text{in}}(z) + \varepsilon m\frac{b}{Y} \tag{2.2}$$

Light follows Lambert-Beer's law, decreasing due to attenuation from biomass and background turbidity (Kirk 1975*a*). The attenuation coefficient due to biomass is a

and due to background is a_{bg}.

$$I(z,t) = I_{\text{in}} e^{-\left(a_{\text{bg}} z + \int_0^z ab(Z,t)dZ\right)} \tag{2.3}$$

Phytoplankton do not leave or enter the water column, so boundary conditions are:

$$\left(D(z)\frac{\partial b}{\partial z} + v\left(\frac{\partial g}{\partial z}\right)b\right)\Big|_{z=0,z_{\text{b}}} = 0 \tag{2.4}$$

Nutrients have no surface flux but diffuse into the water column from the sediments where they have fixed concentration R_{sed} at a rate proportional to the concentration difference across the interface. The permeability of the interface is described by h.

$$\frac{\partial R}{\partial z}\Big|_{z=0} = 0 \quad \text{and} \quad \frac{\partial R}{\partial z}\Big|_{z=z_{\text{b}}} = h(R_{\text{sed}} - R(z_{\text{b}})) \tag{2.5}$$

See Table 2.1 for a list of variables and Table 2.2 for a list of parameters and their default values.

Table 2.1: Variables in the model.

Variable	Units	Meaning
$b(z,t)$	cells mL^{-1}	biomass concentration
B_{ML}	cells cm^{-2}	biomass in ML
B_{DL}	cells cm^{-2}	biomass in DL
z^*	m	depth of co-limitation in DL
z_{e}	m	depth of co-limitation in ML
$R(z,t)$	μg P L^{-1}	phosphorus concentration
$\bar{R}_{\text{ML}}$	μg P L^{-1}	average phosphorus concentration in ML
$I(z,t)$	μmol photons $\text{m}^{-2}\text{s}^{-1}$	irradiance
$g(R,I)$	d^{-1}	growth rate
$\bar{g}_{\text{ML}}$	d^{-1}	average growth rate in ML

Table 2.2: Parameter values unless noted otherwise. Ranges explored here are in parentheses.

Parameter	Value (range)	Units	Meaning	Reference
r	0.4	d^{-1}	maximum growth rate	(1)
m	0.2	d^{-1}	loss rate	(1)
K_R	1.0	μg P L^{-1}	phosphorus half-saturation constant	(1)
K_I	50.0	μmol photons $m^{-2}s^{-1}$	light half-saturation constant	(1)
Y	10^3	cells $mL^{-1}\left[\mu g\ P\ L^{-1}\right]^{-1}$	yield coefficient	(1)
D_{DL}	1.0	m^2d^{-1}	diffusion coefficient in deep layer	(1,2)
I_{in}	1400	μmol photons $m^{-2}s^{-1}$	incoming light	(1)
a_{bg}	0.1 $(10^{-2} - 10)$	m^{-1}	background attenuation coefficient	(1, 4)
a	10^{-5}	$m^{-1}\left[\text{cells } mL^{-1}\right]^{-1}$	algal attenuation coefficient	(1, 4)
z_b	20 $(1 - 10^3)$	m	water column depth	(1, 5)
z_m	5 $(0 - z_b)$	m	mixed layer depth	(5)
R_{sed}	10 $(0 - 10^3)$	μg P L^{-1}	sediment phosphorus concentration	(1, 3, 5, 6)
h	10^{-2}	m^{-1}	sediment-water column interface permeability	(1)
ε	0.9	dimensionless	recycling coefficient	(1,7,8)
v_{max}	10	m d^{-1}	swimming speed	(1)
R_{inML}	1 $(0 - 10^2)$	mg P m^{-2} d^{-1}	mixed layer nutrient input	(9,10)

Sources.- (1) Klausmeier and Litchman 2001. (2) MacIntyre et al. 1999 (3) Jöhnk et al. 2008. (4) Krause-Jensen and Sand-Jensen 1998. (5) Wetzel 1975. (6) Portielje and Lijklema 1999. (7) Peters and Rigler 1973. (8) Depinto and Verhoff 1977. (9) Gonsiorczyk et al. 1998. (10) Sharpley et al. 1996.

2.3.1.1 Simulating the full model

The system of reaction-diffusion equations that define our model (Eqs. 1–5) defies analytical treatment, so we begin with numerical solutions of the model to gain insight into its behavior. We spatially discretized and numerically simulated the full model using VODE (Brown et al. 1989) following Huisman and Sommeijer (2002). The specific equation we use for v is $v = v_{\max} \cdot \frac{\partial g}{\partial z} / \left(\frac{\partial g}{\partial z} + K_{\text{swim}} \right)$, where $K_{\text{swim}} = 0.001\ \text{md}^{-1}$. We simulate a stratified water column with mixed layer depth z_{m}, setting $D(z) = 10^2\ \text{m}^2\text{d}^{-1}$ for $0 \leq z \leq z_{\text{m}}$ and $D(z) = 1\ \text{m}^2\text{d}^{-1}$ for $z_{\text{m}} < z \leq z_{\text{b}}$, realistic values for $D(z)$ in the epilimnion and hypolimnion (MacIntyre et al. 1999). An example equilibrium vertical profile shows that biomass is almost uniformly distributed in the mixed layer and forms a deep chlorophyll maximum (DCM) in the deep layer (Fig. 2.2A). The DCM thickness decreases as the swimming speed of the phytoplankton is increased until it can be approximated by an infinitely thin layer (Klausmeier and Litchman 2001, unpub. results). Nutrients are almost uniformly distributed in the mixed layer, relatively constant below the mixed layer down to the DCM, and increase linearly below the DCM to the sediments. These numerical results and previous research (Huisman and Weissing 1994; Klausmeier and Litchman 2001) suggest that the full model can be approximated by a simplified model (Fig. 2.2B) with a completely homogenous mixed layer above a poorly-mixed layer where phytoplankton can form a thin layer.

2.3.2 Simplified model

In order to obtain analytical results, we use a simplified model to approximate the equilibrium distribution of the full model. Evidence that the full model can be reduced to a simpler model comes from simulations (Klausmeier and Litchman 2001, Mellard et al. unpublished) and a rigorous mathematical proof (Du and Hsu 2008). We later

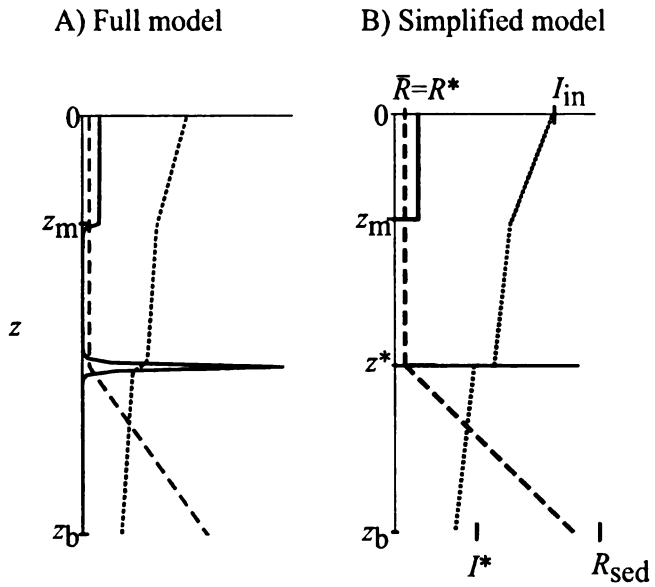

Figure 2.2: A) Example numerical simulation output of full model showing a DCM and nutrient-limited mixed layer at steady-state. Solid line is biomass (cells mL^{-1}), dashed line is nutrient concentration (μg dissolved P L^{-1}), and dotted line is log light (μmol photons $m^{-2}s^{-1}$). Parameters are as in Table 2.1 except $R_{sed} = 220$ μg P L^{-1}; $D_{ML} = 10^2$ m^2 d^{-1}; $R_{in}(z) = 0.6$ μg P L^{-1} d^{-1} for $0 \leq z \leq 5$, $R_{in}(z) = 0$ for $z > 5$. B) Example representation of simplified model showing a DCM and nutrient-limited mixed layer as in the output of the full model.

give criteria for when our simplified model does a good job of approximating the full model as well as discuss specific cases for when it may do a poor job (see Assumptions, limitations, and extensions in the Discussion).

In addition to providing intuitive insight, algebraic expressions, and ease of numerically exploring parameter space, the simplified model provides a skeleton of the full model showing where the peaks in biomass occur, the depth of co-limitation, and the amount of biomass in the mixed layer and deep layer (compare Fig. 2.2B with Fig. 2.2A). We break up the water column into a perfectly-mixed upper layer (Huisman and Weissing 1994) and a poorly-mixed deep layer (Klausmeier and Litchman 2001). This water column approximates stratified temperate lakes (Wetzel 1975; Wüest et al.

2000) and oceans (Osborn 1980; Mann and Lazier 1996).

2.3.2.1 Definitions and assumptions

Well-mixed surface layer (ML)

In the mixed layer, $0 \leq z \leq z_{\mathrm{m}}$, we assume $D(z)$ is large enough to homogenize the nutrients and phytoplankton, overcoming phytoplankton motility, growth, and nutrient consumption ($D(z) \gg v_{\mathrm{max}} z_{\mathrm{m}}$ and $D(z) \gg g z_{\mathrm{m}}^2$ for $0 \leq z \leq z_{\mathrm{m}}$). Phytoplankton and nutrient distributions observed in thermally stratified lakes are often consistent with this assumption (Fig. 2.1, J. Mellard unpublished data).

Define B_{ML} to be the depth-integrated biomass in the mixed layer

$$B_{\mathrm{ML}} = \int_0^{z_{\mathrm{m}}} b(z) dz \tag{2.6}$$

and $\bar{R}_{\mathrm{ML}}$ to be the average nutrient concentration in the mixed layer

$$\bar{R}_{\mathrm{ML}} = \frac{1}{z_{\mathrm{m}}} \int_0^{z_{\mathrm{m}}} R(z) dz \tag{2.7}$$

To explore the effect of changing z_{m} without changing the nutrient supply to the mixed layer, we assume the only source of nutrients besides the sediments is direct surface input by setting $R_{\mathrm{in}}(z)$ as a delta function at $z = 0$ with total nutrient input rate R_{inML}

$$R_{\mathrm{inML}} = \int_0^{z_{\mathrm{m}}} R_{\mathrm{in}}(z) dz \tag{2.8}$$

Define $\bar{g}_{\mathrm{ML}}$ to be the average growth rate in the mixed layer

$$\bar{g}_{\mathrm{ML}} = \frac{1}{z_{\mathrm{m}}} \int_0^{z_{\mathrm{m}}} g(z) dz \tag{2.9}$$

and z_e to be the depth of equal limitation where

$$f_R(R(z_e)) = f_I(I(z_e)) \tag{2.10}$$

Poorly-mixed deep layer (DL)

In the deep layer, $z_m < z \leq z_b$, we assume that phytoplankton motility or growth can overcome mixing to form a thin layer ($v_{max}(z_b - z_m) \gg D(z)$ or $g(z_b - z_m)^2 \gg D(z)$ for $z_m < z \leq z_b$). Following Klausmeier and Litchman (2001), we assume that algae will aggregate at their ESS depth z^*. Note that there are two ways for the algae to achieve their ESS depth z^*. According to the inequalities, either swimming or growth can overcome mixing. For a DCM, $z_e = z^*$. We use a delta function to approximate the biomass distribution at depth z^* (Klausmeier and Litchman 2001),

$$b(z) = B_{DL}\delta(z^*) \tag{2.11}$$

where depth integrated biomass in the deep layer is

$$B_{DL} = \int_{z_m}^{z_b} b(z)dz \tag{2.12}$$

2.3.2.2 Equilibrium conditions

We focus on vertical distribution at both dynamic ($d/dt = 0$) and strategic (ESS) equilibrium. At equilibrium, net growth rate is 0 wherever biomass exists

$$\begin{cases} \bar{g}_{ML} - m = 0 & \text{if } B_{ML} > 0; \\ g(z^*) - m = 0 & \text{if } B_{DL} > 0. \end{cases} \tag{2.13}$$

In other words, at equilibrium, if the population exists in the mixed layer or deep layer, it is neither increasing or decreasing there. For an equilibrium to be an ESS,

$$\begin{cases} \bar{g}_{\mathrm{ML}} - m \leq 0 & \text{and} \\ g(z) - m \leq 0 & \text{for } z_{\mathrm{m}} < z \leq z_{\mathrm{b}}. \end{cases} \tag{2.14}$$

In other words, phytoplankton cannot invade the mixed layer or deep layer. In terms of resource conditions in the deep layer, $I(z^{*+}) = I^*$ and $R(z^*) = R^*$ when $B_{\mathrm{DL}} > 0$ meaning that light is at the break-even level immediately below the thin layer and nutrients are at the break-even level at the depth of the thin layer (Klausmeier and Litchman 2001).

Simplified model derivation

Nutrients are constant in the surface layer ($R(z) \equiv \bar{R}_{\mathrm{ML}}$ for $0 \leq z \leq z_{\mathrm{m}}$), and are linear with depth wherever there is no biomass in the deep layer ($d^2R/dz^2 = 0$ for $z_{\mathrm{m}} < z < z_b$ where $b(z) = 0$). For convenience, we specify vertical diffusion coefficient in the deep layer as D_{DL}.

At steady state, net nutrient flux equals net nutrient consumption by phytoplankton. In the surface layer, we have

$$-\frac{\bar{g}_{\mathrm{ML}} B_{\mathrm{ML}}}{Y} + \frac{\varepsilon m B_{\mathrm{ML}}}{Y} + R_{\mathrm{inML}} + D_{\mathrm{DL}} \left.\frac{dR}{dz}\right|_{z=z_{\mathrm{m}}^+} = 0. \tag{2.15}$$

The first two terms of the left-hand side of (Eq. 2.15) represent consumed and recycled nutrients within the surface layer, and the third and fourth terms, direct nutrient input to the surface layer and nutrient flux from the deep layer, respectively. Because $\bar{g}_{\mathrm{ML}} - m = 0$ when $B_{\mathrm{ML}} > 0$, (Eq. 2.15) can be modified to:

$$-\frac{m\,(1-\varepsilon)\,B_{\mathrm{ML}}}{Y} + R_{\mathrm{inML}} + D_{\mathrm{DL}} \left.\frac{dR}{dz}\right|_{z=z_{\mathrm{m}}^+} = 0. \tag{2.16}$$

Note that (Eq. 2.16) also holds when $B_{\mathrm{ML}} = 0$. Nutrient flux from the deep layer depends on whether biomass is present in the deep layer ($B_{\mathrm{DL}} > 0$) or not ($B_{\mathrm{DL}} = 0$). When $B_{\mathrm{DL}} = 0$, dR/dz is constant in the deep layer:

$$\frac{dR}{dz} = \frac{R(z_{\mathrm{b}}) - \bar{R}_{\mathrm{ML}}}{z_{\mathrm{b}} - z_{\mathrm{m}}}. \tag{2.17}$$

From the boundary condition at $z = z_{\mathrm{b}}$ (5) and (Eq. 2.17) we have

$$\frac{R(z_{\mathrm{b}}) - \bar{R}_{\mathrm{ML}}}{z_{\mathrm{b}} - z_{\mathrm{m}}} = h\left(R_{\mathrm{sed}} - R(z_{\mathrm{b}})\right). \tag{2.18}$$

Rearranging (Eq. 2.18), we obtain $R(z_{\mathrm{b}})$, and substituting $R(z_{\mathrm{b}})$ in (Eq. 2.17), dR/dz is expressed by:

$$\frac{dR}{dz} = \frac{R_{\mathrm{sed}} - \bar{R}_{\mathrm{ML}}}{z_{\mathrm{b}} + 1/h - z_{\mathrm{m}}}. \tag{2.19}$$

According to Klausmeier and Litchman (2001), a stable DCM should be co-limited by nutrients and light (i.e., $R(z^*) = R^*$ and $I(z^{*+}) = I^*$), and a stable benthic layer should be limited by nutrients (i.e., $R(z_{\mathrm{b}}) = R^*$ and $I(z_{\mathrm{b}}^+) \geq I^*$). Therefore, when $B_{\mathrm{DL}} > 0$, $R(z^*) = R^*$, and dR/dz is expressed by:

$$\left.\frac{dR}{dz}\right|_{z=z_{\mathrm{m}}^+} = \frac{R^* - \bar{R}_{\mathrm{ML}}}{z^* - z_{\mathrm{m}}}. \tag{2.20}$$

Substituting dR/dz in (Eq. 2.16) with (Eq. 2.19), and (Eq. 2.20), we have equalities for nutrient balance in the surface layer:

$$\begin{cases} -\frac{m(1-\varepsilon)B_{\mathrm{ML}}}{Y} + R_{\mathrm{inML}} + \frac{D_{\mathrm{DL}}(R_{\mathrm{sed}} - \bar{R}_{\mathrm{ML}})}{z_{\mathrm{b}} + 1/h - z_{\mathrm{m}}} = 0 & \text{when } B_{\mathrm{DL}} = 0, \\ -\frac{m(1-\varepsilon)B_{\mathrm{ML}}}{Y} + R_{\mathrm{inML}} + \frac{D_{\mathrm{DL}}(R^* - \bar{R}_{\mathrm{ML}})}{z^* - z_{\mathrm{m}}} = 0 & \text{when } B_{\mathrm{DL}} > 0. \end{cases} \tag{2.21}$$

Similarly in the deep layer, we have an equality for nutrient balance at a depth

with positive biomass z^*. When $z_m < z^* < z_b$ (DCM), we have

$$-\frac{m(1-\varepsilon)B_{DL}}{Y} + D_{DL}\left.\frac{dR}{dz}\right|_{z=z^*+} - D_{DL}\left.\frac{dR}{dz}\right|_{z=z^*-} = 0. \tag{2.22}$$

The second and third terms of left-hand side of (Eq. 2.22) respectively denote nutrient fluxes from below and above z^*. Because $R(z^*) = R^*$ (Klausmeier and Litchman 2001), these fluxes can be expressed by:

$$\begin{aligned} D_{DL}\left.\frac{dR}{dz}\right|_{z=z^*+} &= \frac{D_{DL}(R_{sed} - R^*)}{z_b + 1/h - z^*}, \\ D_{DL}\left.\frac{dR}{dz}\right|_{z=z^*-} &= \frac{D_{DL}(R^* - \bar{R}_{ML})}{z^* - z_m}. \end{aligned} \tag{2.23}$$

Substituting the fluxes in (Eq. 2.22) with (Eq. 2.23) we have an equality for nutrient balance at depth z^*,

$$-\frac{m(1-\varepsilon)B_{DL}}{Y} + \frac{D_{DL}(R_{sed} - R^*)}{z_b + 1/h - z^*} - \frac{D_{DL}(R^* - \bar{R}_{ML})}{z^* - z_m} = 0. \tag{2.24}$$

When $z^* = z_b$ (benthic layer), net nutrient flux is the sum of nutrient fluxes at sediment-water interface $[hD_{DL}(R_{sed} - R(z_b)) = hD_{DL}(R_{sed} - R^*)]$ and from above z_b. Thus nutrient balance at benthic layer is written as

$$-\frac{m(1-\varepsilon)B_{DL}}{Y} + hD_{DL}(R_{sed} - R^*) - \frac{D_{DL}(R^* - \bar{R}_{ML})}{z_b - z_m} = 0. \tag{2.25}$$

We can see that (Eq. 2.24) implies (Eq. 2.25) when $z^* = z_b$. Therefore the equality (Eq. 2.24) holds for $z_m < z^* \leq z_b$, which expresses nutrient balance at either a DCM or a benthic layer.

The light profile is expressed by

$$I(z) = \begin{cases} I_{\text{in}} e^{-\left(a_{\text{bg}} z + aB_{\text{ML}} z/z_{\text{m}}\right)} & \text{for } 0 \le z \le z_{\text{m}} \\ I_{\text{in}} e^{-\left(a_{\text{bg}} z + aB_{\text{ML}}\right)} & \text{for } z_{\text{m}} < z < z^* \\ I_{\text{in}} e^{-\left(a_{\text{bg}} z + aB_{\text{ML}} + aB_{\text{DL}}\right)} & \text{for } z^* \le z \le z_{\text{b}} \end{cases} . \tag{2.26}$$

Steady state distributions are obtained by solving equations for zero net growth (Eq. 2.13), nutrient balance in the surface layer (Eq. 2.21), and nutrient balance in the deep layer (Eq. 2.24), with the light profile (Eq. 2.26). Conditions (2.14) should be satisfied for a steady state distribution to be an ESS.

2.4 Results

2.4.1 Spatial distribution states

Stratification and multiple nutrient sources lead to a greater diversity of possible equilibrium vertical distributions and resource limitation states of phytoplankton than in previous models. In the mixed layer, four states for phytoplankton are possible: light-limited ($f_R(z) > f_I(z)$ for $0 \le z \le z_{\text{m}}$), nutrient-limited ($f_R(z) < f_I(z)$ for $0 \le z \le z_{\text{m}}$), co-limited ($0 \le z_{\text{e}} \le z_{\text{m}}$), or not present (empty). In the deep layer, three states for phytoplankton are possible: nutrient-limited in a benthic layer, co-limited in a deep chlorophyll maximum, or not present (empty). Combinations of these four mixed layer and three deep layer biomass states result in $4 \times 3 = 12$ logically possible vertical distribution states (Table 2.3). However, four of these vertical distribution states are infeasible. In order to have both mixed layer and deep layer biomass, the mixed layer biomass must be nutrient-limited (if mixed layer biomass is co-limited or light-limited then the light level below the mixed layer is less than I^*). This

eliminates the four combinations of co-limited or light-limited mixed layer biomass states with any deep layer biomass state, leaving eight possible vertical distribution states at equilibrium (for proof *see* Appendix).

Table 2.3: Combinations of equilibrium spatial distribution states of the mixed layer and deep layer. X indicates the combination is infeasible. All other combinations are possible subject to criteria listed and their corresponding figures and sections in the appendix are indicated.

Deep layer	Mixed layer			
	Empty	R-limited	Co-limited	I-limited
Empty	Fig. 3A [1]	Only if $R_{\text{inML}} > 0$ Fig. 6A [2]	Fig. 3D [3]	Fig. 3E [4]
Benthic Layer	Only if $R_{\text{inML}} = 0$ Fig. 3B [5]	Only if $R_{\text{inML}} > 0$ Fig. 6B [6]	X	X
DCM	Only if $R_{\text{inML}} = 0$ Fig. 3C [7]	Only if $R_{\text{inML}} > 0$ Fig. 6C [8]	X	X

[1] Appendix page 61, Case 1: Empty.
[2] Appendix page 67, Case 4: Nutrient-limited mixed layer.
[3] Appendix page 63, Case 2: Co-limited mixed layer.
[4] Appendix page 66, Case 3: Light-limited mixed layer.
[5] Appendix page 71, Case 7: Benthic layer.
[6] Appendix page 68, Case 5: Benthic layer and Nutrient-limited mixed layer.
[7] Appendix page 73, Case 8: DCM.
[8] Appendix page 69, Case 6: DCM and Nutrient-limited mixed layer.

As mentioned above, our model incorporates two new factors beyond Klausmeier and Litchman (2001): 1) stratification and 2) mixed layer nutrient input. We describe the possible distribution states and examine how they depend on environmental conditions. In order to do this, we numerically evaluated expressions for the equilibrium (Eqs. 2.13, 2.21, 2.24, 2.26) and checked the feasibility of each case. We always found a unique vertical distribution state of phytoplankton for a given set of parameters. In addition, we examined how the vertical distribution state changes along

environmental gradients and confirmed these results according to methods in Table 2.4.

Table 2.4: Effect of environmental parameters on state variables.

	Case I: Empty	Case II: BL	Case III: DCM		Case IV: Co-lim. ML			Case V: *I*-lim. ML	Case VI: *R*-lim. ML	Case VII: BL+ML		Case VIII: DCM+ML			
	R_{ML}	B_{DL}	z^*	B_{DL}	z_e	B_{ML}	R_{ML}	B_{ML}	R_{ML}	B_{ML}	B_{DL}	B_{ML}	z^*	B_{DL}	B_{ML}
R_{sed}	(+)[d]	(+)[b]	(-)[b]	(+)[b]	(-)[e]	(+)[a]	(+)[a]	(0)[a]	(+)[a]	(+)[d]	(+)[b]	(0)[d]	(-)[b]	(+)[b]	(0)[d]
a_{bg}	(0)[d]	(0)[b]	(-)[b]	(-)[b]	(-)[e]	(-)[c]	(+)[c]	(-)[c]	(+)[c]	(0)[d]	(0)[b]	(0)[d]	(-)[b]	(-)[b]	(0)[d]
R_{inml}	(+)[d]	(0)[d]	(0)[d]	(0)[d]	(-)[e]	(+)[a]	(+)[a]	(0)[a]	(+)[a]	(+)[d]	(0)[d]	(+)[d]	(-)[e]	(-)[e]	(+)[d]
z_m	(-/0)[d]	(0)[d]	(0)[d]	(0)[d]	(+/-)[e]	(+/-)[e]	(+/-)[e]	(-)[c]	(+)[c]	(-)[d]	(0)[d]	(0)[d]	(0)[d]	(0)[d]	(0)[d]

[a] Huisman & Weissing 1995

[b] Klausmeier & Litchman 2001

[c] Diehl 2002

[d] Implicit differentiation

[e] Extensive numerical exploration

2.4.2 Possible distribution states

There is often appreciable nutrient input directly to the mixed layer, due to riverine inputs, surface runoff, or atmospheric deposition. This mixed layer nutrient input, R_{inML}, can depend on landscape geomorphology and anthropogenic influences surrounding the body of water. Here we consider the case $R_{\mathrm{inML}} > 0$, although some kettle or other glacial lakes that have very small drainage basins might be reasonably approximated by an assumption of no mixed layer nutrient input (Hutchinson 1957).

With mixed layer nutrient input, six equilibrium vertical distribution states are possible (Fig. 2.3, Table 2.3). A benthic layer or DCM by itself are special cases not possible with positive R_{inML} because they form when sufficient light penetrates to the deep layer and reduce nutrient concentration above to R^* so any amount of nutrient input to the mixed layer will sustain a population there (see Two special cases if $R_{\mathrm{inML}} = 0$ below for their description). We describe the equilibrium vertical distribution states below; mathematical details are given in Appendix.

1) *Empty.* An empty state is perhaps trivial because likely all bodies of water have enough nutrients for some biomass to exist but we describe it here as a possibility. No biomass persists in the water column. Light declines exponentially with depth due to background attenuation. Nutrient levels are uniform with depth and at the same concentration as in the sediments ($R(z) = R_{\mathrm{sed}}$). *See* Fig. 2.3A and page 61, Case 1 in Appendix.

2) *Co-limited mixed layer.* A co-limited mixed layer is actually only co-limited at one point in the mixed layer but as a whole, we consider it co-limited because the population is experiencing the entire range of conditions in it. Biomass is uniformly distributed throughout the mixed layer and absent below it. The upper portion of the mixed layer ($z < z_{\mathrm{e}}$) is nutrient-limited and the lower portion ($z > z_{\mathrm{e}}$) is light-limited. Light declines exponentially within the mixed

layer due to algal and background attenuation and in the deep layer below due to background attenuation only. Light at the bottom of the mixed layer is actually less than the break-even level ($I(z_m) = I_{out} \leq I^*$), but the population can persist (Huisman and Weissing 1994). Nutrients in the mixed layer are uniform at or above the break-even concentration ($\bar{R}_{ML} \geq R^*$) and increase linearly with depth in the deep layer. *See* Fig. 2.3B and page 63, Case 2 in Appendix.

3) *Light-limited mixed layer.* In a light-limited mixed layer, the depth of co-limitation for the population would be above the water column if it could exist there. Conditions are the same as a co-limited mixed layer except the entire mixed layer is limited by light ($f_R(\bar{R}_{ML}) > f_I(I_{in})$). *See* Fig. 2.3C and page 66, Case 3 in Appendix.

4) *Nutrient-limited mixed layer* (R-limited ML). A nutrient-limited mixed layer by itself may be somewhat unlikely as most bodies of water have significant nutrient input from the sediments. Conditions are the same as co-limited and light-limited mixed layers except nutrients in the mixed layer are at the break even concentration ($\bar{R}_{ML} = R^*$) and below the mixed layer, are constant or decrease linearly to $R(z_b)$. *See* Fig. 2.3D and page 67, Case 4 in Appendix.

5) *Benthic layer + nutrient-limited mixed layer* (BL+ML). This is an intriguing case with the population divided between two locations but with both locations limited by the same resource. Biomass is uniformly distributed throughout the mixed layer and resides at the sediment-water interface in the deep layer. The entire mixed layer and the benthic layer are limited by nutrients. Light declines exponentially with depth in the mixed layer due to algal and background attenuation and in the deep layer below due to background attenuation only. Light at the bottom of the water column $I(z_b) > I^*$. Nutrients are uniformly distributed throughout the water column at the break-even concentration ($R(z) = R^*$). *See*

Fig. 2.3E and page 68, Case 5 in Appendix.

6) *Deep chlorophyll maximum + nutrient-limited mixed layer* (DCM+ML). This is another intriguing and probably common (Mellard et al. unpublished data) case. Biomass is uniformly distributed throughout the mixed layer and forms a thin layer at depth z^* within the deep layer. The entire mixed layer is limited by nutrients and the DCM is limited by nutrients and light. Light declines exponentially with depth in the mixed layer due to algal and background attenuation. In the deep layer, light declines exponentially above and below the DCM and decreases a finite amount within the DCM. Immediately below z^*, light is at the break-even level ($I(z^{*+}) = I^*$). Nutrients in the mixed layer and below to the DCM are constant at R^*. Below the DCM, nutrients increase linearly with depth. *See* Fig. 2.3F and page 69, Case 6 in Appendix.

2.4.2.1 Two special cases if $R_{\text{inML}} = 0$

Benthic layer and DCM are special cases of BL+ML and DCM+ML where $R_{\text{inML}} = 0$.

7) *Benthic layer* (BL). (Only possible if $R_{\text{inML}} = 0$) The benthic layer is the only location in the water column the population exists in this case. Biomass resides at the sediment-water interface at $z = z_{\text{b}}$. Light declines exponentially with depth due to background attenuation and there is sufficient light at the bottom ($I(z_{\text{b}}) > I^*$). Nutrient levels are uniform throughout the water column at R^*. *See* Fig. 2.3G and page 71, Case 7 in Appendix.

8) *Deep chlorophyll maximum* (DCM). (Only possible if $R_{\text{inML}} = 0$) The conspicuous DCM (Camacho 2006) is considered to form at the ESS depth (of co-limitation) in the deep layer. Biomass forms a thin layer at depth z^* within the deep layer. Light declines exponentially above and below the DCM and

decreases a finite amount at the DCM. Immediately below z^*, $I(z^{*+}) = I^*$. Nutrient levels are at R^* at and above the DCM and increase linearly below the DCM. *See* Fig. 2.3H and page 73, Case 8 in Appendix.

Figure 2.3. Equilibrium vertical profiles A-F) with mixed layer nutrient input ($R_{\text{inML}} > 0$). G) and H) are special cases where $R_{\text{inML}} = 0$. A) Empty. Here, there is not sufficient nutrients for biomass to persist. B) Co-limited mixed layer. The solid lines enveloping the mixed layer represents the biomass there. $\bar{R}_{\text{ML}}$ is the nutrient concentration in the mixed layer. C) Light-limited mixed layer. The mixed layer biomass is completely light-limited due to increased R_{sed}. D) Nutrient-limited mixed layer. Primary nutrient source is directly to the mixed layer ($R_{\text{sed}} < R^*$). The entire mixed layer is nutrient limited because $I(z_{\text{m}}) > I^*$. E) Benthic layer and nutrient-limited mixed layer. The solid line at the bottom represents biomass in the benthic layer. $I(z_{\text{b}}^+) > I^*$. $R = R^*$ in both layers. F) DCM and nutrient-limited mixed layer. The solid line representing biomass in the DCM is at z^*, where $R = R^*$ and $I(z^{*+}) = I^*$. $R = R^*$ in both layers. G) Benthic Layer. The solid line at the bottom represents biomass in the benthic layer. There are enough nutrients from sediment ($R_{\text{sed}} > R^*$) for biomass to exist at the bottom of the water column and also enough light ($> I^*$). Nutrients above the benthic layer are constant at R^*. H) DCM. The solid line representing biomass in the DCM is at z^*, where $R = R^*$ and $I = I^*$.

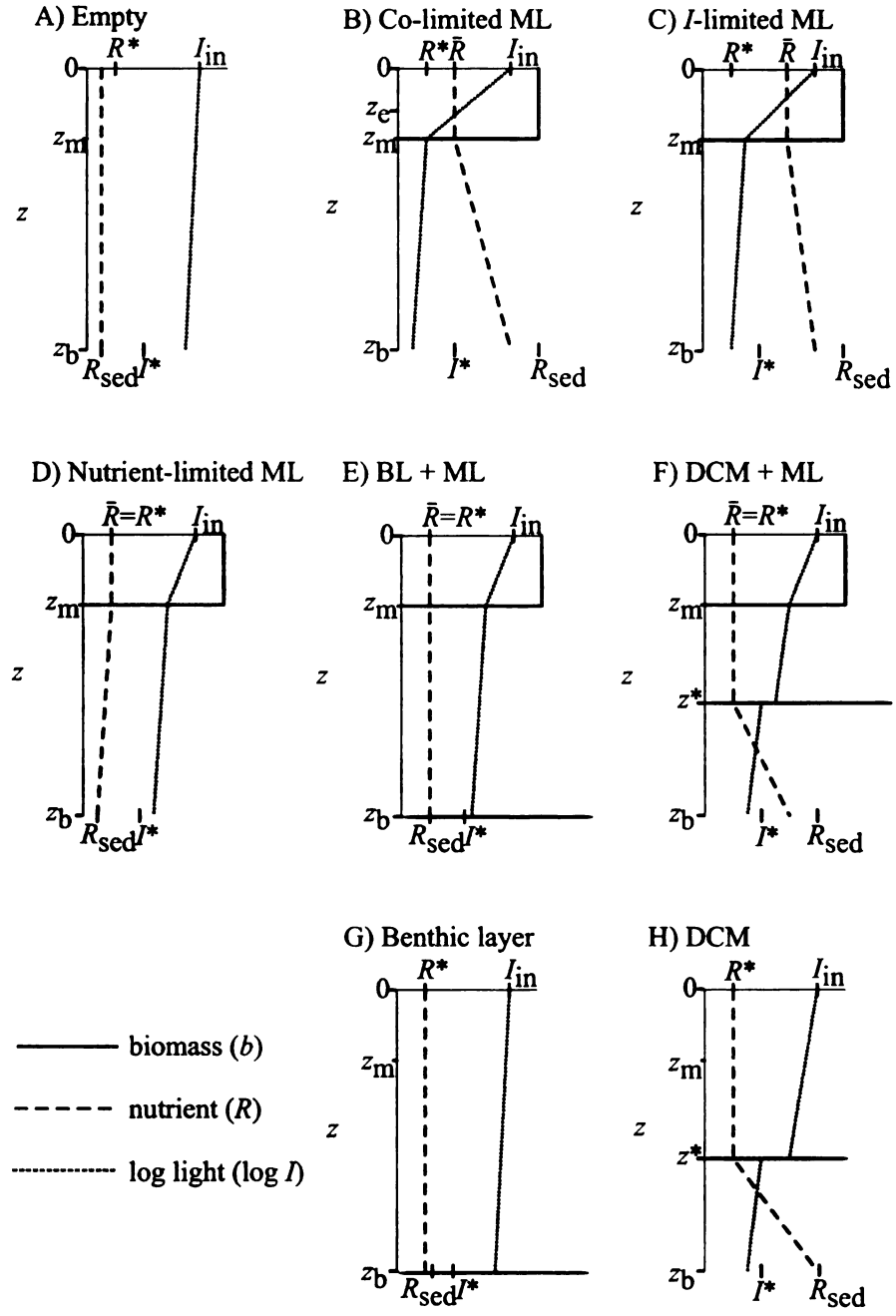

Figure 2.3: Equilibrium vertical profiles.

2.4.3 Transitions along environmental gradients

We now examine how the equilibrium vertical distribution, biomass, and resource limitation depend on environmental parameters. We focus on three environmental

parameters that are known to vary among water bodies or through time and that potentially affect phytoplankton communities: sediment nutrient concentration, R_{sed}; mixed layer nutrient input, R_{inML}; background light attenuation, a_{bg}; and mixed layer depth, z_{m}. Sediment nutrient concentration varies widely between lakes. Background light attenuation depends on the amount and composition of particulate and dissolved matter suspended in the water column. Mixed layer depth can vary both between and within bodies of water through time due to seasonal changes (Wetzel 1975). Note that other transitions are possible in addition to those that are described below.

Effect of sediment nutrient concentration. Nutrient enrichment in the form of sediment nutrient concentration causes phytoplankton to shift towards the surface. For example, in Fig. 2.4A, they shift from a BL+ML to a DCM+ML to a co-limited mixed layer to a completely light-limited mixed layer. Increasing R_{sed} pushes z^* and z_{e} towards the surface as the biomass becomes more light-limited. Total biomass increases until it is light-limited. Interestingly, the nutrient-limited mixed layer biomass is unaffected by increasing sediment nutrient concentration because the deep layer biomass uses it all for growth.

Effect of mixed layer nutrient input. Nutrient enrichment in the form of mixed layer nutrient input causes phytoplankton to shift towards the surface. For example, in Fig. 2.4A, they shift from a BL+ML to a DCM+ML to a co-limited mixed layer to a light-limited mixed layer. Increasing R_{inML} pushes z^* and z_{e} towards the surface as the biomass becomes more light limited. Total biomass steadily increases, but solely due to mixed layer biomass increasing: benthic layer biomass does not increase and DCM biomass actually slightly decreases with increasing R_{inML}.

Effect of background light attenuation. Increases in background light attenuation causes phytoplankton to shift towards the surface. For example, in Fig. 2.4B, the phytoplankton shift from a BL+ML to a DCM+ML to a co-limited mixed

layer to a light-limited mixed layer before eventually going extinct. Increasing a_{bg} pushes z^* and z_e towards the surface as the biomass becomes more light-limited. Increasing a_{bg} has no effect on completely nutrient-limited biomass (benthic layer or nutrient-limited mixed layer). However, for all other states, increasing a_{bg} decreases biomass.

Effect of mixed layer depth. Increases in mixed layer depth can cause phytoplankton to shift towards the surface due to entrainment once $z_m \geq z^*$. For example, in Fig. 2.4C, the phytoplankton shift from a DCM+ML to a co-limited mixed layer once the mixed layer entrains the DCM to a light-limited mixed layer and finally to an empty state when the mixed layer becomes too deep and the phytoplankton go extinct because of extreme light limitation. Increasing z_m has no effect on z^* for the DCM; however, z_e for the co-limited mixed layer becomes shallower with increasing mixed layer depth (although this is not universally true). Increasing mixed layer depth has negative, positive, or no effect on biomass, dependent on the state of the phytoplankton. Biomass in a BL, DCM, or nutrient-limited mixed layer (when a BL or DCM is present) is unaffected by increasing mixed layer depth. Biomass in a light-limited or nutrient-limited mixed layer (by itself) decreases with increasing mixed layer depth. Biomass in a co-limited mixed layer may increase or decrease with increasing mixed layer depth.

Figure 2.4. Effect of environmental parameter on biomass (top), state (middle), and vertical distribution (bottom). Top) Amount of biomass in benthic layer (BL), DCM, and mixed layer. Middle) State of the phytoplankton. Phytoplankton can be in a benthic layer + nutrient-limited mixed layer (BL+ML), DCM + nutrient-limited mixed layer (DCM+ML), co-limited mixed layer (Co-lim. ML), light-limited mixed layer (I-lim. ML), or extinct (Empty). Bottom) Dotted line is depth of colimitation if in the mixed layer, z_e, and solid line is depth of colimitation if in the deep layer, z^*. Gray shading indicates that biomass is present in the mixed layer. A) Effect of sediment phosphorus concentration, R_{sed}, on phytoplankton biomass and vertical distribution. Environmental parameters: $a_{bg} = 0.1$ m^{-1}; $z_m = 5$ m; $R_{inML} = 1$ mg P m^{-2} d^{-1}. B) Effect of R_{inML} on phytoplankton biomass and vertical distribution. Environmental parameters: $a_{bg} = 0.1$ m^{-1}; $z_m = 5$ m; $R_{sed} = 120$ μg P L^{-1}. C) Effect of a_{bg} on phytoplankton biomass and vertical distribution. Environmental parameters: $z_m = 5$ m; $R_{sed} = 40$ μg P L^{-1}; $R_{inML} = 1$ mg P m^{-2} d^{-1}. D) Effect of z_m on phytoplankton biomass and vertical distribution. Environmental parameters: $a_{bg} = 0.4$ m^{-1}; $R_{sed} = 40$ μg P L^{-1}; $R_{inML} = 1$ mg P m^{-2} d^{-1}.

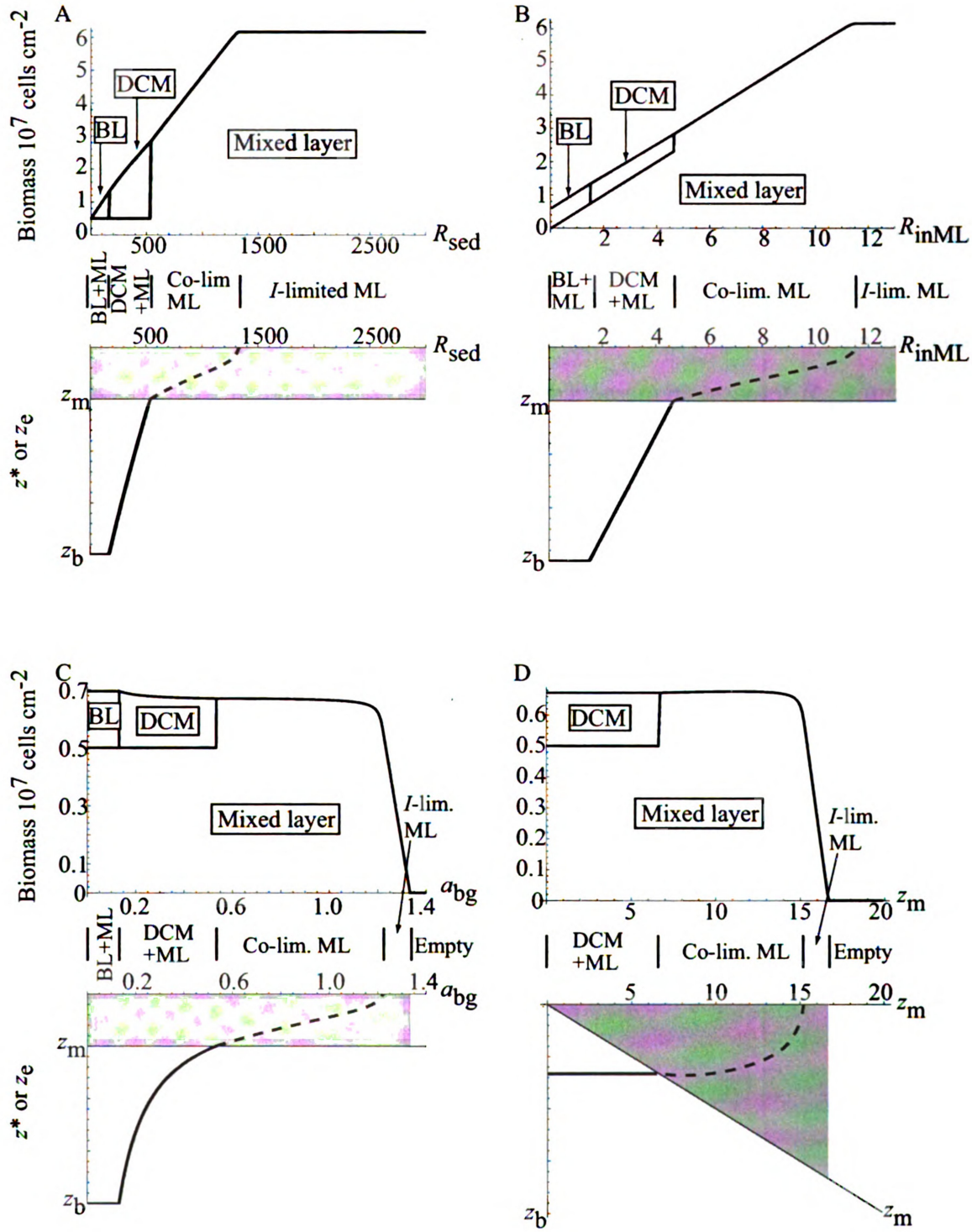

Figure 2.4: Effect of environmental parameter on biomass and vertical distribution.

Interactive effects of environmental parameters. The vertical distribution as a function of R_{sed} and R_{inML} is shown in Fig. 2.5. Increasing either of these parameters makes the phytoplankton more light-limited so that these parameters jointly determine vertical distribution. The difference between increasing either of these two parameters is subtle and not illustrated in Fig. 2.5 but can be seen by comparing Fig. 2.4A and Fig. 2.4B. When biomass is present in both layers, each exhibits asymmetric control over the nutrient sources so that only mixed layer biomass increases if R_{inML} increases and only deep layer biomass increases if R_{sed} increases.

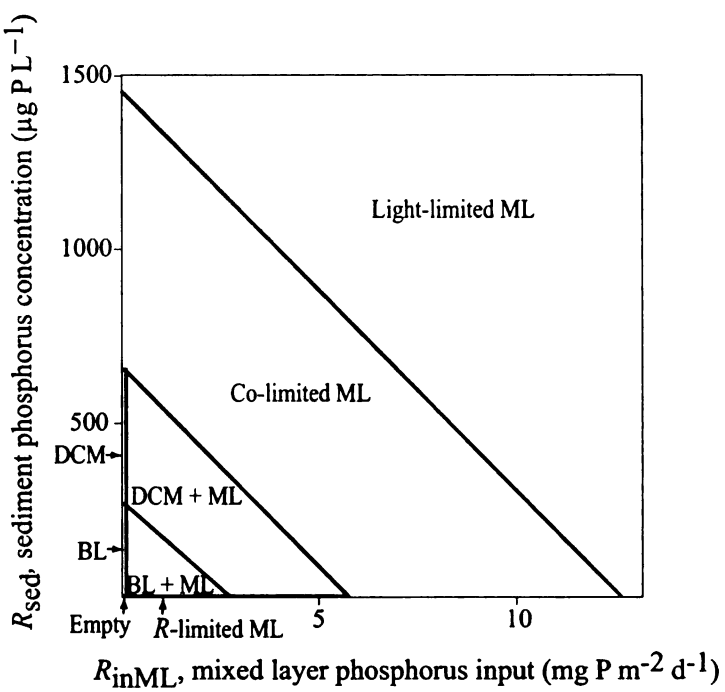

Figure 2.5: Two dimensional bifurcation plot of sediment phosphorus concentration, R_{sed}, and mixed layer nutrient input, R_{inML}. Note that the Benthic Layer and DCM regions are directly on the R_{sed} axis ($R_{\text{inML}} = 0$). Environmental parameters: $a_{\text{bg}} = 0.1\ \text{m}^{-1}$; $z_{\text{m}} = 5$ m.

The vertical distribution as a function of a_{bg} and z_{m} is shown in Fig. 2.6. Increasing either of these parameters makes the phytoplankton more light-limited as well, however, these parameters interact to determine vertical distribution. These parameters affect the light environment of the phytoplankton more, although mixed

layer depth can bring the biomass closer to nutrients at the bottom, and their effects can be less obvious. For example, some cases are unaffected by mixed layer depth (BL+ML to a DCM+ML) while others show non-unidirectional relationships (co-limited ML). All four environmental parameters may interact to determine vertical distribution. Overall, these four parameters, either individually or combined, shift the phytoplankton to more light-limited conditions if increased (results not shown).

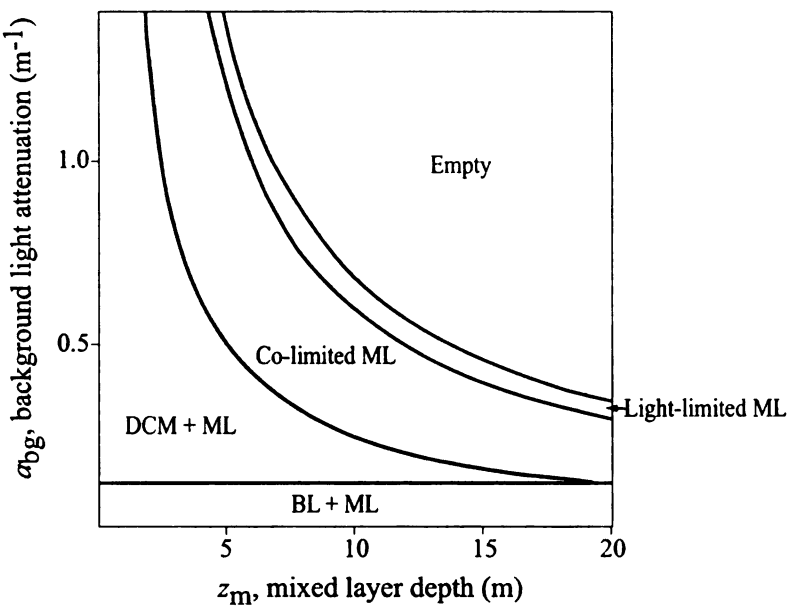

Figure 2.6: Two dimensional bifurcation plot of background light attenuation, a_{bg}, and mixed layer depth, z_m. Increases in both parameters can lead to extinction. Environmental parameters: $R_{sed} = 200\ \mu g\ P\ L^{-1}$; $R_{inML} = 0.1\ mg\ P\ m^{-2}\ d^{-1}$.

2.5 Discussion

Aquatic communities exhibit pronounced spatial patterns (Steele 1978). How competition structures the spatial distributions of organisms through feedbacks in abiotic and biotic components is important to understanding how biological heterogeneity is generated. We have shown how externally imposed heterogeneity in the form of resource gradients and mixing interacts with internally generated heterogeneity in the

form of competition, population dynamics, and movement to determine the spatial distribution of phytoplankton.

Our simplified model is like an x-ray that exposes the skeleton upon which the vertical distributions of phytoplankton are built. It also incorporates two important components of the phytoplankton environment required to replicate real patterns in aquatic systems. First, we add stratification, which creates spatially varying mixing, expands a thin layer to finite thickness in the mixed layer, and allows for different relative resource limitation within the mixed layer. Second, we add multiple nutrient sources, which can create multi-modal phytoplankton distributions.

The inclusion of stratification means that in our simplified model, phytoplankton can exist at a single point such as in a DCM or benthic layer, or can be homogeneously distributed throughout the mixed layer. In a DCM in a poorly-mixed water column, phytoplankton exist in a thin layer at their depth of equal limitation by nutrients and light, z^* (Klausmeier and Litchman 2001). However, when the depth of equal limitation occurs within the mixed layer, the thin layer is expanded to the thickness of the mixed layer and phytoplankton exist above and below the depth of equal limitation. Decreasing the mixed layer depth to zero in our model reveals a subtle mistake in the surface scum case of Klausmeier and Litchman (2001). They erroneously neglect the inevitable spatial gradient in light in a surface scum and conclude that a surface scum must be light-limited. Our current analysis shows this is not the case, because a surface scum may be co-limited over a range of R_{sed}. We also correct the formulas for biomass in this case (*see* page 63, Case 2 in Appendix).

One of the intriguing results of our study is the possibility that phytoplankton biomass could maintain source populations in both the mixed layer and deep layer simultaneously. Without nutrient input directly to the mixed layer, a phytoplankton population can grow in only one location. However, when there is nutrient input directly to the mixed layer, phytoplankton populations can grow in the mixed layer and

in the deep layer together. This bimodal distribution occurs not merely due to passive dispersal from a source habitat into a sink habitat, but instead because growing conditions are favorable in these two locations. Phytoplankton peak biomass in the mixed layer and deep layer is a common feature in many lakes (Fig. 2.1, J. Mellard unpub. data), which may be explained as the adaptive response of phytoplankton to multiple nutrient inputs to the water column. One alternative explanation is the coexistence of two species exhibiting a trade-off in their light and nutrient requirements that competitively divide the water column into separate niches (Yoshiyama et al. 2009); another alternative explanation is passive dispersal from a source to a sink habitat.

Other studies that have considered stratification have also found interesting results such as bistability of biomass between the mixed layer and deep layer (Yoshiyama and Nakajima 2002, Ryabov et al. 2009) and biomass straddling both layers simultaneously due to sinking or actual production in both layers (Huisman and Sommeijer 2002b, Hodges and Rudnick 2004 Beckmann and Hense 2007; also mentioned as a possibility in Ryabov et al. 2009). Our approach offers a third possibility and considers production in the mixed layer and/or deep layer but because the deep layer biomass exists in an infinitely thin layer, phytoplankton produced in that layer cannot be partially entrained in the mixed layer. Likely one of these results is more representative of reality, probably where biomass can straddle both layers with proportions from both layers dispersing across the boundary.

Although our results do not show bistability of biomass distributions, we do see that in some area of parameter space, a small change in a parameter can cause a major shift in phytoplankton vertical distribution. For example, in Fig. 2.4A and C, over a small range of R_{sed} and a_{bg} respectively, the DCM can shift many meters or the population can even change to a different vertical distribution state. Many bodies of water may exist in this range in parameter space since many have DCMs (Camacho

2006, Mellard et al., unpublished data). This could have important ramifications for the sensitivity of those bodies of water to environmental change.

The presence of a mixed layer adds complications that few studies have explored thoroughly (Beckmann and Hense 2007; but see Ryabov et al. 2009, Yoshiyama et al. 2009). The particular form of depth dependent mixing may influence results and previous studies have used many different forms ranging from no mixing in the deep layer (Huisman and Sommeijer 2002b) to a step function (Hodges and Rudnick 2004, Yoshiyama et al. 2009), to a smoothly varying thermocline (Yoshiyama et al. 2009, Ryabov et al. 2009) to a thermocline region with reduced diffusivities (Yoshiyama and Nakajima (2002). Future studies should examine the influence that the particular form of stratification has on results.

2.5.1 Assumptions, limitations, and extensions

In general, our inequalities guide the conditions under which our simplified model approximates the full model ($D(z) \gg v_{\max} z_{\mathrm{m}}$ and $D(z) \gg g z_{\mathrm{m}}^2$ for $0 \leq z \leq z_{\mathrm{m}}$ and $v_{\max}(z_{\mathrm{b}} - z_{\mathrm{m}}) \gg D(z)$ or $g(z_{\mathrm{b}} - z_{\mathrm{m}})^2 \gg D(z)$ for $z_{\mathrm{m}} < z \leq z_{\mathrm{b}}$). The ESS distribution is convergence stable (Klausmeier and Litchman 2001), and through either movement or growth the full model will converge on the simplified model when our inequalities for the deep layer hold.

If the mixed layer is well-mixed according to our inequalities, our simplified model approximates the full model well. If there is no mixed layer, then we have potential conditions for a surface bloom (*see* Model predictions in next section of discussion), essentially a completely poorly-mixed water column ($z_m = 0$). In between these two scenarios, the simplified model may not do a good job of approximating the full model.

Many phytoplankton groups such as cryptophytes, dinoflagellates, green algae, and chrysophytes have flagella and are actively motile. Other phytoplankton groups

such as cyanobacteria and diatoms regulate their depth through physiological control of their buoyancy (*see* review in Cullen and MacIntyre 1998 and Waite et al. 1997 for diatoms in particular). Our model applies broadly to all of these groups of phytoplankton.

However, not all phytoplankton can taxis along the gradient in growth rate because their taxis speed is too slow or mixing is too great. Some diatoms are well-mixed in the surface layer so $D(z) \gg v_{\max} z_{\mathrm{m}}$ and $D(z) \gg g z_{\mathrm{m}}^2$ for $0 \leq z \leq z_{\mathrm{m}}$ and it would seem our model would hold under these conditions. However, criteria for the deep layer must also be met so that $v_{\max}(z_{\mathrm{b}} - z_{\mathrm{m}}) \gg D(z)$ or $g(z_{\mathrm{b}} - z_{\mathrm{m}})^2 \gg D(z)$ for $z_{\mathrm{m}} < z \leq z_{\mathrm{b}}$. Some diatoms and other species may not be able to meet these criteria in the deep layer if mixing there is strong (big $D(z)$) or the water column is not deep (small $z_{\mathrm{b}} - z_{\mathrm{m}}$).

Deep water columns allow another way for even neutrally buoyant species to reach the ESS by making it easier to satisfy the second condition for our approximation, $g(z_{\mathrm{b}} - z_{\mathrm{m}})^2 \gg D(z)$. In this case, our model also does a reasonable job of approximating positively or negatively buoyant species with low but realistic speeds (J. Mellard, unpublished simulations). However, our simplified model can deviate significantly from the full model (results not shown) for positively or negatively buoyant species with faster speeds (> 0.2 m d^{-1}) or in shallower water columns (such as 20 m). Finally, buoyancy does not affect our results if z_{e} is in mixed layer and we follow our assumption of perfect mixing and sinking does not affect our results in the case of a benthic layer.

The assumption of a well-mixed layer can be broken in several ways. If $D(z)$ for $0 \leq z \leq z_{\mathrm{m}}$ is small, then the mixed layer may not be considered well-mixed. If z_{m} is large then this allows another way for the mixed layer to not be completely mixed, particularly if $v_{\max}$ is large or for species that are significantly positively or negatively buoyant. For example, in the case of $D(z) = 100$ m^2 d^{-1} for $0 \leq z \leq z_{\mathrm{m}}$, a $z_{\mathrm{m}} = 4$

m, and a positively buoyant species with velocities of 6 m d^{-1}, the inequality where our simplified model approximates the full model breaks down and not only can there be non-uniform biomass in the mixed layer but addition of the high buoyancy can make the phytoplankton switch vertical distribution states completely in comparison to the state of a neutrally buoyant species.

The main cases in which our simplified model will not apply are when the mixed layer is intermediate between well- and poorly-mixed and when the deep layer thickness ($z_b - z_m$) is small and phytoplankton can not regulate their depth. These cases will require numerical solution of the full model, possibly with the addition of sinking or buoyancy (as in Huisman and Sommeijer 2002b, Huisman et al. 2004, Ryabov et al. 2009).

2.5.2 Model predictions

Increasing sediment nutrient concentration, R_{sed}, decreases the DCM depth and increases all biomass until it becomes light-limited (Fig. 2.4A). This prediction is in accordance with the trophic status hypothesis of Moll and Stoermer (1982) that nutrient-rich lakes will support a larger, shallower DCM. If we consider R_{sed} to be representative of trophic status, a comparison of the DCMs in relatively nutrient-rich Lake Michigan and nutrient-poor Lake Superior supports both our predictions and the trophic status hypothesis (Moll and Stoermer 1982).

Increasing mixed layer nutrient input, R_{inML}, decreases DCM depth and increases mixed layer biomass, while having little effect on deep layer biomass (Fig. 2.4B). In Sawtooth Valley, Idaho lakes, experiments and simulations showed that fertilization in the form of surface nutrient input increases mixed layer biomass but had little effect on DCM biomass (Gross et al. 1997). Additionally, in Lake Geneva, a reduction in phosphorus inputs to the surface due to human activity has led to a deepening of the depth of DCM and annual nutrient depleted zone (Anneville and Leboulanger 2001).

Both of these studies support our predictions, contrary to other models which predict a tradeoff between mixed layer and deep layer biomass (Christensen et al. 1995).

Increasing background light attenuation, a_{bg}, generally decreases DCM depth and total biomass, especially the mixed layer biomass (Figs. 2.4C). Unfortunately, few empirical studies examine how background attenuation is related to vertical distribution and biomass, rather using total attenuation as the light-related environmental parameter. Total attenuation does however predict how the depth of the DCM varies both among and within the five Laurentian Great Lakes (Barbiero and Tuchman 2001). In a comparison of two Finnish lakes, the dark water lake with high color values and shallow Secchi depth had a shallower depth distribution of phytoplankton than the clear water lake with low color values and deep Secchi depth (Holopainen et al. 2003). The negative effect of a_{bg} on mixed layer biomass is supported by experimental manipulation of background light attenuation in field enclosures (Diehl et al. 2002).

Mixed layer depth, z_m, can have a negative, positive, or no effect on biomass over some range of mixing depths dependent on the resource limitation state and vertical distribution of the phytoplankton (Figs. 2.4D). Less physically realistic models predict a unimodal relationship of mixed layer biomass with mixed layer depth (Huisman and Weissing 1995; Diehl 2002). Unfortunately, direct comparison of predictions from these other models with ours is hampered by additional processes such as nutrient input (Huisman and Weissing 1995) and sinking (Diehl 2002) that are directly proportional to mixed layer depth in their models.

While many environmental parameters vary widely between bodies of water, mixed layer depth also exhibits large variation seasonally within a body of water. Seasonal variation in mixed layer depth plays a major role in determining the seasonal cycle in vertical distribution and can affect the importance of deep layer biomass (Lindholm 1992). Surprisingly, few studies have systematically examined effects of mixed layer

depth on phytoplankton spatial and physiological structure. Mixed layer biomass showed a unimodal relationship with mixed layer depth across lakes (Kunz and Diehl 2003) and within field enclosures (Diehl et al. 2002) which agrees with our prediction of state-dependent effects of z_m on B_{ML} (Figs. 2.4D). Both of these studies also support our prediction of a shift from nutrient limitation to light limitation with increasing mixed layer depth.

We also predict the location of the DCM to be at the transition from nutrient limitation to light limitation, which is supported by data from Lake Tahoe (Coon et al. 1987). With increased nutrient input, biomass can reach very high levels in a light-limited mixed layer (J. Mellard, unpublished results). Surface blooms often contain the most biomass throughout the season in a lake, which may support our prediction that decreasing z_m to zero in water columns with high nutrient levels can create extremely high biomass surface layers (Paerl 1988).

2.5.3 Relevance

The fundamental relationships of phytoplankton with nutrients, light, and mixing revealed in our study may also guide lake management solutions. For example, in management of nutrient loading, not only the concentrations, but the locations of input to the water column are important. Overall, the best way to reduce algal biomass is probably to reduce all nutrient inputs (R_{sed}, R_{inML}), but reducing inputs to the mixed layer (R_{inML}) may be the most effective for decreasing biomass, given our results. Some hypereutrophic lakes may require very large reductions in phosphorus loading which may or may not help depending on the severity of phosphorus limitation for the phytoplankton as well as the potential for sediment phosphorus release (Marsden 1989). If this is the situation, artificial mixing that increases mixing depth (z_m) may be the best option (Lorenzen and Mitchell 1973, Visser et al. 1996), which we predict will reduce biomass if it enhances light limitation.

Climate change affects the heat budget and other physical processes of a lake which, in turn, determine stratification and mixed layer depth. In particular, climate change may affect mixed layer depth (Magnuson et al. 1997; Schindler 1997), which we predict to have state-dependent effects on phytoplankton vertical distribution and biomass (*see* Figs. 2.4D). Climate change also alters precipitation, hence the hydrological regime on the surrounding landscape that affects nutrient inputs and water clarity. Anthropogenically driven atmospheric nutrient deposition is also increasing, even in pristine areas (Hartmann et al. 2008; Neff et al. 2008). Climate induced changes in stratification and nutrient budgets have already affected phytoplankton community biomass and composition in some lakes (O'Reilly et al. 2003; Verburg et al. 2003; Jöhnk et al. 2008). However, climate change effects on vertical distribution have so far gone unreported. An important task is to dissect how climate and other anthropogenically induced changes will be channeled through a number of environmental drivers to determine phytoplankton vertical distribution and production (Karlsson et al. 2009). Our model provides a spatially explicit framework to explore how multiple feedback loops between biotic and abiotic factors in the aquatic ecosystem will respond to human-induced environmental change.

2.6 Appendix

Simplified model

In the following, we first write down $\bar{g}_{\mathrm{ML}}$ when growth in the surface layer is limited by light, limited by nutrients, or co-limited by nutrients and light for later convenience. Next we show that four cases out of the twelve logically possible combinations of biomass in the mixed and deep layers are theoretically infeasible, leaving eight possible cases (Table 2.3). Then we solve for the steady states of these cases, and evaluate their stability.

Growth in the surface layer

Growth in the surface layer $\bar{g}_{\mathrm{ML}}$ is written as

$$\bar{g}_{\mathrm{ML}} = \frac{1}{z_{\mathrm{m}}} \int_0^{z_{\mathrm{m}}} \min\left(f_I(I(z)), f_R(\bar{R}_{\mathrm{ML}})\right) dz. \tag{A1}$$

When $f_R(\bar{R}_{\mathrm{ML}}) \geq f_I(I_{\mathrm{in}})$, growth is limited by light only, and $\bar{g}_{\mathrm{ML}}$ is:

$$\bar{g}_{\mathrm{ML}} = \frac{1}{z_{\mathrm{m}}} \int_0^{z_{\mathrm{m}}} f_I(I(z)) dz. \tag{A2}$$

When we use a Michaelis-Menten formulation $f_I(I) = rI/\left(I + K_I\right)$, the integral can be computed following Monsi and Saeki (1953) and Huisman and Weissing (1994):

$$\bar{g}_{\mathrm{ML}} = \frac{r}{a_{\mathrm{bg}} z_{\mathrm{m}} + aB_{\mathrm{ML}}} \log\left[\frac{K_I + I_{\mathrm{in}}}{K_I + I_{\mathrm{in}} e^{-\left(a_{\mathrm{bg}} z_{\mathrm{m}} + aB_{\mathrm{ML}}\right)}}\right]. \tag{A3}$$

When $f_R(\bar{R}_{\mathrm{ML}}) \leq f_I(I(z_{\mathrm{m}}))$, growth is limited by nutrients only, and the integral is trivially computed:

$$\bar{g}_{\mathrm{ML}} = f_R(\bar{R}_{\mathrm{ML}}). \tag{A4}$$

When $f_I(I(z_\mathrm{m})) < f_R(\bar{R}_\mathrm{ML}) < f_I(I_\mathrm{in})$, growth is co-limited by nutrients and light. Because $f_I(I(z)) - f_R(\bar{R}_\mathrm{ML})$ decreases monotonically for $0 \leq z \leq z_\mathrm{m}$, there is a unique co-limitation depth $0 \leq z_\mathrm{e} \leq z_\mathrm{m}$ that satisfies:

$$f_R(\bar{R}_\mathrm{ML}) = f_I(I(z_\mathrm{e})), \tag{A5}$$

and the integral splits into a nutrient-limited and a light-limited part:

$$\bar{g}_\mathrm{ML} = \frac{1}{z_\mathrm{m}} \left[\int_0^{z_\mathrm{e}} f_R(\bar{R}_\mathrm{ML}) dz + \int_{z_\mathrm{e}}^{z_\mathrm{m}} f_I(I(z)) dz \right]. \tag{A6}$$

Each integral of (Eq. A6) is computed following (Eq. A3) and (Eq. A4):

$$\bar{g}_\mathrm{ML} = \frac{z_\mathrm{e}}{z_\mathrm{m}} f_R(\bar{R}_\mathrm{ML}) + \frac{r}{a_\mathrm{bg} z_\mathrm{m} + a B_\mathrm{ML}} \log \left[\frac{K_I + I_\mathrm{in} e^{-\left(a_\mathrm{bg} z_\mathrm{e} + a B_\mathrm{ML} z_\mathrm{e}/z_\mathrm{m}\right)}}{K_I + I_\mathrm{in} e^{-\left(a_\mathrm{bg} z_\mathrm{m} + a B_\mathrm{ML}\right)}} \right]. \tag{A7}$$

To summarize, $\bar{g}_\mathrm{ML}$ is expressed by (Eq. A3) when $f_R(\bar{R}_\mathrm{ML}) \geq f_I(I_\mathrm{in})$, by (Eq. A4) when $f_R(\bar{R}_\mathrm{ML}) \leq f_I(I_\mathrm{in})$, and by (Eq. A7) when $f_I(I(z_\mathrm{m})) < f_R(\bar{R}_\mathrm{ML}) < f_I(I_\mathrm{in})$. The co-limitation depth z_e is obtained from (Eq. A5).

Four infeasible cases

Under light limitation, $\partial g/\partial I = df_I/dI > 0$ while g is independent of nutrients ($\partial g/\partial R = 0$) from our assumption. Light decreases with depth $dI/dz < 0$, and nutrients are constant in the surface layer $dR/dz = 0$. Differentiating g with respect to z we have

$$\frac{dg}{dz} = \frac{\partial g}{\partial I}\frac{dI}{dz} + \frac{\partial g}{\partial R}\frac{dR}{dz}. \tag{A8}$$

Thus $dg/dz < 0$ under light limitation. Likewise, $dg/dz = 0$ under nutrient limitation in the surface layer. As we saw before, there is a unique co-limitation depth z_e when growth is co-limited by nutrients and light in the surface layer, and below z_e, growth is limited by light. Therefore the following inequality is satisfied under co-limitation or light limitation:

$$g(z) > g(z_m) \text{ for } 0 \leq z < z_m. \tag{A9}$$

Suppose there is positive biomass in the surface layer, $B_{ML} > 0$, whose growth is limited by light or co-limited by nutrients and light, and $g(z_m) - m \geq 0$. Because of (Eq. A9) it is obvious that net growth in the surface layer satisfies

$$\frac{1}{z_m} \int_0^{z_m} (g(z) - m)\, dz > 0. \tag{A10}$$

This contradicts the first equality of (Eq. 2.13). Therefore $g(z_m) - m < 0$ when $B_{ML} > 0$ and the growth is limited by light or co-limited. Because $g(z_m) - m < 0$, $I(z_m) < I^*$. Therefore $g(z) - m < 0$ for $z_m < z \leq z_b$. This prevents the second equality of (Eq. 2.13) from being satisfied anywhere in the deep layer, and hence B_{DL} should be 0.

To conclude, if $B_{ML} > 0$ and the growth is limited by light or co-limited by nutrients and light, $B_{DL} = 0$ at steady state. This excludes four cases, (DCM)+(light-limited ML), (DCM)+(co-limited ML), (benthic layer)+(co-limited ML), and (benthic layer)+(light-limited ML), from steady state distributions.

Eight possible cases

Case 1: Empty

Knowns: $B_{ML} = 0$, $B_{DL} = 0$

Unknowns: $\bar{R}_{\mathrm{ML}}$

Equations to solve:

Because $B_{\mathrm{ML}} = B_{\mathrm{DL}} = 0$, we have only one equation derived from (Eq. 2.21) to solve for one unknown $\bar{R}_{\mathrm{ML}}$:

$$R_{\mathrm{inML}} + \frac{D_{\mathrm{DL}}\left(R_{\mathrm{sed}} - \bar{R}_{\mathrm{ML}}\right)}{z_{\mathrm{b}} + 1/h - z_{\mathrm{m}}} = 0, \tag{A11}$$

and obtain

$$\bar{R}_{\mathrm{ML}} = R_{\mathrm{sed}} + \frac{\left(z_{\mathrm{b}} + 1/h - z_{\mathrm{m}}\right) R_{\mathrm{inML}}}{D_{\mathrm{DL}}}. \tag{A12}$$

From (Eq. 2.26) light profile is expressed by

$$I(z) = I_{\mathrm{in}} e^{-a_{\mathrm{bg}} z}. \tag{A13}$$

Consistency/stability criteria:

It is easy to see that $\bar{g}_{\mathrm{ML}} \geq g(z)$ for $z_{\mathrm{m}} < z \leq z_{\mathrm{b}}$. Therefore the case "empty" is stable when $\bar{g}_{\mathrm{ML}} - m \leq 0$. From (Eq. A3), (Eq. A4), and (Eq. A7), this condition is summarized by:

$$\begin{cases} \frac{r}{a_{\mathrm{bg}} z_{\mathrm{m}}} \log\left(\frac{K_I + I_{\mathrm{in}}}{K_I + I_{\mathrm{in}} e^{-a_{\mathrm{bg}} z_{\mathrm{m}}}}\right) - m \leq 0 \\ \text{when } f_R(\bar{R}_{\mathrm{ML}}) \geq f_I(I_{\mathrm{in}}), \\ \frac{z_{\mathrm{e}}}{z_{\mathrm{m}}} f_R(\bar{R}_{\mathrm{ML}}) + \frac{r}{a_{\mathrm{bg}} z_{\mathrm{m}}} \log\left(\frac{K_I + I_{\mathrm{in}} e^{-a_{\mathrm{bg}} z_{\mathrm{e}}}}{K_I + I_{\mathrm{in}} e^{-a_{\mathrm{bg}} z_{\mathrm{m}}}}\right) - m \leq 0 \\ \text{when } f_I(I(z_{\mathrm{m}})) < f_R(\bar{R}_{\mathrm{ML}}) < f_I(I_{\mathrm{in}}), \\ f_R(\bar{R}_{\mathrm{ML}}) - m \leq 0 \\ \text{when } f_R(\bar{R}_{\mathrm{ML}}) \leq f_I(I(z_{\mathrm{m}})), \end{cases} \tag{A14}$$

where z_e is obtained from (Eq. A5). The frontier of the first inequality of (Eq. A14),

$$\frac{r}{a_{bg} z_m} \log\left(\frac{K_I + I_{in}}{K_I + I_{in} e^{-a_{bg} z_m}}\right) - m = 0, \tag{A15}$$

separates empty and light-limited ML regions; the second,

$$\frac{z_e}{z_m} f_R(\bar{R}_{ML}) + \frac{r}{a_{bg} z_m} \log\left(\frac{K_I + I_{in} e^{-a_{bg} z_e}}{K_I + I_{in} e^{-a_{bg} z_m}}\right) - m = 0, \tag{A16}$$

separates empty and co-limited ML regions. The third inequality of (Eq. A14) implies $\bar{R}_{ML} \leq R^*$ and the frontier,

$$R_{sed} + \frac{(z_b + 1/h - z_m)\, R_{inML}}{D_{DL}} = R^*, \tag{A17}$$

separates the empty and the benthic layer or DCM or nutrient-limited ML or some possible combination of these cases.

Case 2: Co-limited mixed layer

Knowns: $B_{DL} = 0$

Unknowns: B_{ML}, z_e, $\bar{R}_{ML}$

Equations to solve:

Because $B_{ML} > 0$ and $B_{DL} = 0$ we have equalities from (Eq. 2.13) and (Eq. 2.21) to solve for $\bar{R}_{ML}$ and B_{ML}:

$$-\frac{m(1-\varepsilon) B_{ML}}{Y} + R_{inML} + \frac{D_{DL}(R_{sed} - \bar{R}_{ML})}{z_b + 1/h - z_m} = 0 \tag{A18}$$

$$(\bar{g}_{ML} - m =) \frac{1}{z_m}\left[\int_0^{z_m} \min(f_I(I(z)), f_R(\bar{R}_{ML}))dz\right] - m = 0, \tag{A19}$$

where the light profile is from (Eq. 2.26):

$$I(z) = \begin{cases} I_{\text{in}} e^{-\left(a_{\text{bg}} z + a B_{\text{ML}} z / z_{\text{m}}\right)} & \text{for } 0 \le z \le z_{\text{m}} \\ I_{\text{in}} e^{-\left(a_{\text{bg}} z + a B_{\text{ML}}\right)} & \text{for } z_{\text{m}} < z \le z_{\text{b}} \end{cases} . \tag{A20}$$

Specifically when growth is co-limited by nutrients and light, $\bar{g}_{\text{ML}}$ is expressed by (Eq. A7), and the equality (Eq. A19) is rewritten by

$$\frac{z_{\text{e}}}{z_{\text{m}}} f_R(\bar{R}_{\text{ML}}) + \frac{r}{a_{\text{bg}} z_{\text{m}} + a B_{\text{ML}}} \log \left[\frac{K_I + I_{\text{in}} e^{-\left(a_{\text{bg}} z_{\text{e}} + a B_{\text{ML}} z_{\text{e}} / z_{\text{m}}\right)}}{K_I + I_{\text{in}} e^{-\left(a_{\text{bg}} z_{\text{m}} + a B_{\text{ML}}\right)}} \right] - m = 0, \tag{A21}$$

where z_{e} is obtained from (Eq. A5). Equations (Eq. A18) and (Eq. A21) are solved numerically for unknowns B_{ML} and $\bar{R}_{\text{ML}}$ with z_{e} from (Eq. A5).

Consistency/stability criteria:

Stability is already ensured because $I(z) < I(z_{\text{m}}) < I^*$ for $z_{\text{m}} < z \le z_{\text{b}}$ (see "Four impossible cases" section for the proof). Existence of positive steady state requires positive biomass $B_{\text{ML}} > 0$ and equal limitation depth within the surface layer $0 < z_{\text{e}} < z_{\text{m}}$. The frontier of the first inequality is obtained by setting $B_{\text{ML}} = 0$ in (Eq. A18), (Eq. A21), and (Eq. A5), which is identical to the second inequality of (Eq. A16). This separates co-limited ML and empty regions. One frontier of the second inequality is obtained by setting $z_{\text{e}} = 0$ in (Eq. A18), (Eq. A21), and (Eq.

A5):

$$\begin{cases} -\frac{m(1-\varepsilon)B_{\mathrm{ML}}}{Y} + R_{\mathrm{inML}} + \frac{D_{\mathrm{DL}}(R_{\mathrm{sed}}-\bar{R}_{\mathrm{ML}})}{z_{\mathrm{b}}+1/h-z_{\mathrm{m}}} = 0 \\ \frac{r}{a_{\mathrm{bg}}z_{\mathrm{m}}+aB_{\mathrm{ML}}} \log\left[\frac{K_I+I_{\mathrm{in}}}{K_I+I_{\mathrm{in}}e^{-\left(a_{\mathrm{bg}}z_{\mathrm{m}}+aB_{\mathrm{ML}}\right)}}\right] - m = 0 \\ f_I(I_{\mathrm{in}}) - f_R(\bar{R}_{\mathrm{ML}}) = 0 \end{cases} . \quad \text{(A22)}$$

When we use Michaelis-Menten formulations for f_I and f_R, we obtain an equality algebraically from (Eq. A22). This frontier separates co-limited and light-limited ML regions. The other one is obtained by setting $z_{\mathrm{e}} = z_{\mathrm{m}}$ in (Eq. A18), (Eq. A21), and (Eq. A5):

$$\begin{cases} -\frac{m(1-\varepsilon)B_{\mathrm{ML}}}{Y} + R_{\mathrm{inML}} + \frac{D_{\mathrm{DL}}(R_{\mathrm{sed}}-\bar{R}_{\mathrm{ML}})}{z_{\mathrm{b}}+1/h-z_{\mathrm{m}}} = 0 \\ f_R(\bar{R}_{\mathrm{ML}}) - m = 0 \\ f_I\left(I_{\mathrm{in}}e^{-\left(a_{\mathrm{bg}}z_{\mathrm{m}}+aB_{\mathrm{ML}}\right)}\right) - f_R(\bar{R}_{\mathrm{ML}}) = 0 \end{cases} . \quad \text{(A23)}$$

From the second equality of (Eq. A23), $\bar{R}_{\mathrm{ML}} = R^*$. From the second and the third equalities, we have

$$I_{\mathrm{in}}e^{-\left(a_{\mathrm{bg}}z_{\mathrm{m}}+aB_{\mathrm{ML}}\right)} = I^*, \quad \text{(A24)}$$

which yields

$$B_{\mathrm{ML}} = \frac{\log\left(I_{\mathrm{in}}/I^*\right) - a_{\mathrm{bg}}z_{\mathrm{m}}}{a}. \quad \text{(A25)}$$

Substituting $\bar{R}_{\mathrm{ML}} = R^*$ and (Eq. A25) in the first equality of (Eq. A23) we obtain

$$\frac{YD_{\mathrm{DL}}\left(R_{\mathrm{sed}} - R^*\right)}{m\left(1-\varepsilon\right)\left(z_{\mathrm{b}} + 1/h - z_{\mathrm{m}}\right)} - \frac{\log\left(I_{\mathrm{in}}/I^*\right) - a_{\mathrm{bg}} z_{\mathrm{m}}}{a} + \frac{YR_{\mathrm{inML}}}{m\left(1-\varepsilon\right)} = 0. \qquad \text{(A26)}$$

When $R_{\mathrm{inML}} = 0$, (Eq. A26) is identical with (Eq. A62), and separates co-limited ML and DCM regions.

Case 3: Light-limited mixed layer

Knowns: $B_{\mathrm{DL}} = 0$

Unknowns: B_{ML}, $\bar{R}_{\mathrm{ML}}$

Equations to solve.

$B_{\mathrm{ML}} > 0$ and $B_{\mathrm{DL}} = 0$ in this case, thus the same equalities (Eq. A18) and (Eq. A19) with the light profile (Eq. A20) hold as in the co-limited ML case. Under light limitation for growth, $\bar{g}_{\mathrm{ML}}$ is expressed by (Eq. A3), and (Eq. A19) is rewritten by

$$\frac{r}{a_{\mathrm{bg}} z_{\mathrm{m}} + aB_{\mathrm{ML}}} \log\left[\frac{K_I + I_{\mathrm{in}}}{K_I + I_{\mathrm{in}} e^{-\left(a_{\mathrm{bg}} z_{\mathrm{m}} + aB_{\mathrm{ML}}\right)}}\right] - m = 0. \qquad \text{(A27)}$$

Equalities (Eq. A18) and (Eq. A27) are solved numerically for the two unknowns $\bar{R}_{\mathrm{ML}}$ and B_{ML}.

Consistency/stability criteria:

Stability is ensured because $I(z) < I(z_{\mathrm{m}}) < I^*$ for $z_{\mathrm{m}} < z \leq z_{\mathrm{b}}$. The existence of a positive steady state requires $B_{\mathrm{ML}} > 0$ and $f_I(I_{\mathrm{in}}) < f_R(\bar{R}_{\mathrm{ML}})$. The frontier of the first inequality is obtained by setting $B_{\mathrm{ML}} = 0$ in (Eq. A18) and (Eq. A27), which is identical with (Eq. A15). The frontier of the second inequality is obtained by setting $f_I(I_{\mathrm{in}}) - f_R(\bar{R}_{\mathrm{ML}}) = 0$, which is identical with what is obtained from (Eq. A22).

Case 4: Nutrient-limited mixed layer

Knowns: $B_{\mathrm{DL}} = 0$, $\bar{R}_{\mathrm{ML}} = R^*$

Unknowns: B_{ML}

Equations to solve:

The same equalities (Eq. A18) and (Eq. A19) with light profile (Eq. A20) hold because $B_{\mathrm{ML}} > 0$ and $B_{\mathrm{DL}} = 0$ in this case. Under nutrient limitation for growth, $\bar{g}_{\mathrm{ML}}$ is expressed by (Eq. A4), and (Eq. A19) is,

$$f_R(\bar{R}_{\mathrm{ML}}) - m = 0, \tag{A28}$$

which means $\bar{R}_{\mathrm{ML}} = R^*$. Substituting $\bar{R}_{\mathrm{ML}} = R^*$ in (Eq. A18), we obtain

$$-\frac{m\,(1-\varepsilon)\,B_{\mathrm{ML}}}{Y} + R_{\mathrm{inML}} + \frac{D_{\mathrm{DL}}\,(R_{\mathrm{sed}} - R^*)}{z_{\mathrm{b}} + 1/h - z_{\mathrm{m}}} = 0. \tag{A29}$$

Rearranging (Eq. A29) we have B_{ML}:

$$B_{\mathrm{ML}} = \frac{Y R_{\mathrm{inML}}}{m\,(1-\varepsilon)} + \frac{Y D_{\mathrm{DL}}\,(R_{\mathrm{sed}} - R^*)}{m\,(1-\varepsilon)\,(z_{\mathrm{b}} + 1/h - z_{\mathrm{m}})}. \tag{A30}$$

Consistency/stability criteria:

The existence of a positive steady state requires $B_{\mathrm{ML}} > 0$ and $f_I(I(z_{\mathrm{m}})) > f(\bar{R}_{\mathrm{ML}})$ $(= m)$. The latter inequality implies $I(z_{\mathrm{m}}) > I^*$. The frontier of the first inequality is obtained from (Eq. A30), which is identical with (Eq. A17). The frontier of the second inequality is rewritten as:

$$I_{\mathrm{in}} e^{-\left(a_{\mathrm{bg}} z_{\mathrm{m}} + a B_{\mathrm{ML}}\right)} = I^*. \tag{A31}$$

Substituting B_{ML} with (Eq. A30) in (Eq. A31), some rearrangement gives the same equality as (Eq. A26).

Stability requires $g(z) - m \leq 0$ for $z_m < z \leq z_b$. When $B_{DL} = 0$ and $R_{sed} > \bar{R}_{ML}$, $dR/dz > 0$ from (Eq. 2.19). Because $\bar{R}_{ML} = R^*$ here, we have $R(z) > R^*$ for $z_m < z \leq z_b$ in this case. With $I(z_m) > I^*$, there is $\delta > 0$ such that $g(z_m + \delta) - m > 0$. Therefore a nutrient-limited ML is unstable when $R_{sed} > R^*$ and is stable when $R_{sed} \leq R^*$. Considering the conditions for existence $B_{ML} > 0$ and stability $R_{sed} \leq R^*$, some rearrangement of (Eq. A30) gives an inequality $R_{inML} > 0$ that must be satisfied.

Case 5: Benthic layer and Nutrient-limited mixed layer

Knowns: $\bar{R}_{ML} = R^*$

Unknowns: B_{ML}, B_{DL}

Equations to solve:

Growth in the surface layer is limited by nutrients, that is, $\bar{R}_{ML} = R^*$. Because $B_{ML} > 0$, $B_{DL} > 0$, and $\bar{R}_{ML} = R^*$, we have equalities from (Eq. 2.21) and (Eq. 2.24):

$$-\frac{m(1-\varepsilon)B_{ML}}{Y} + R_{inML} = 0, \tag{A32}$$

$$-\frac{m(1-\varepsilon)B_{DL}}{Y} + hD_{DL}(R_{sed} - R^*) = 0, \tag{A33}$$

and obtain,

$$B_{ML} = \frac{YR_{inML}}{m(1-\varepsilon)}, \tag{A34}$$

$$B_{DL} = \frac{hYD_{DL}(R_{sed} - R^*)}{m(1-\varepsilon)}. \tag{A35}$$

The light profile is expressed by (Eq. 2.26).

Consistency/stability criteria:

Stability is ensured because $R(z) = R^*$ for $0 \leq z \leq z_b$. The existence of a positive

steady state requires $B_{\mathrm{ML}} > 0$, $B_{\mathrm{DL}} > 0$, and $I(z_{\mathrm{b}}) \geq I^*$. These first two conditions imply $R_{\mathrm{inML}} > 0$ and $R_{\mathrm{sed}} > R^*$, respectively. The frontiers $R_{\mathrm{inML}} = 0$ separates (benthic layer + nutrient-limited ML) and benthic layer regions, and $R_{\mathrm{sed}} = R^*$, (benthic layer + nutrient-limited ML) and nutrient-limited ML regions. Substituting B_{ML} and B_{DL} in (Eq. 2.26) with (Eq. A34) and (Eq. A35), the last condition $I(z_{\mathrm{b}}) \geq I^*$ is rewritten as:

$$I_{\mathrm{in}} e^{-\left[a_{\mathrm{bg}} z_{\mathrm{b}} + \frac{aYR_{\mathrm{inML}}}{m(1-\varepsilon)} + \frac{ahYD_{\mathrm{DL}}(R_{\mathrm{sed}} - R^*)}{m(1-\varepsilon)}\right]} \geq I^*, \tag{A36}$$

which is rearranged to get:

$$\frac{hYD_{\mathrm{DL}}\left(R_{\mathrm{sed}} - R^*\right)}{m\left(1-\varepsilon\right)} - \frac{\log\left(I_{\mathrm{in}}/I^*\right) - a_{\mathrm{bg}} z_{\mathrm{b}}}{a} + \frac{YR_{\mathrm{inML}}}{m\left(1-\varepsilon\right)} \leq 0. \tag{A37}$$

The frontier of (Eq. A37) separates the (benthic layer + nutrient-limited ML) and (DCM + nutrient-limited ML) regions.

Case 6: DCM and Nutrient-limited mixed layer

Knowns: $\bar{R}_{\mathrm{ML}} = R^*$

Unknowns: B_{ML}, B_{DL}, z^*

Equations to solve:

Because $B_{\mathrm{ML}} > 0$, $B_{\mathrm{DL}} > 0$, and $\bar{R}_{\mathrm{ML}} = R^*$, we obtain equalities (Eq. A32) and

$$-\frac{m\left(1-\varepsilon\right)B_{\mathrm{DL}}}{Y} + \frac{D_{\mathrm{DL}}\left(R_{\mathrm{sed}} - R^*\right)}{z_{\mathrm{b}} + 1/h - z^*} = 0, \tag{A38}$$

from (Eq. 2.21) and (Eq. 2.24). Light profile is expressed by (Eq. 2.26). At z^*,

growth is co-limited by nutrients and light, thus $I(z^{*+}) = I^*$:

$$I_{\text{in}} e^{-\left(a_{\text{bg}} z^* + aB_{\text{ML}} + aB_{\text{DL}}\right)} = I^*. \tag{A39}$$

From (Eq. A32) we obtain B_{ML}, which is expressed by (Eq. A34). Equalities (Eq. A38) and (Eq. A39) are simultaneously solved for B_{DL} and z^*.

Consistency/stability criteria:

DCM and nutrient-limited ML is stable because $R(z) = R^*$ for $0 \leq z < z^*$ and $I(z) \leq I^*$ for $z^* \leq z \leq z_{\text{b}}$. The existence of a positive steady state requires: $B_{\text{ML}} > 0$, $B_{\text{DL}} > 0$, and $z_{\text{m}} < z^* < z_{\text{b}}$. The first condition is satisfied when $R_{\text{inML}} > 0$. Rearranging (Eq. A38), we get:

$$B_{\text{DL}} = \frac{YD_{\text{DL}}\left(R_{\text{sed}} - R^*\right)}{m\left(1-\varepsilon\right)\left(z_{\text{b}} + 1/h - z^*\right)}. \tag{A40}$$

Substituting B_{ML} from (Eq. A34), (Eq. A39) is rearranged and we get:

$$B_{\text{DL}} = \frac{\log\left(I_{\text{in}}/I^*\right) - a_{\text{bg}} z^*}{a} - \frac{YR_{\text{inML}}}{m\left(1-\varepsilon\right)}. \tag{A41}$$

From (Eq. A40) and (Eq. A41) we have an equality:

$$\frac{YD_{\text{DL}}\left(R_{\text{sed}} - R^*\right)}{m\left(1-\varepsilon\right)\left(z_{\text{b}} + 1/h - z^*\right)} = \frac{\log\left(I_{\text{in}}/I^*\right) - a_{\text{bg}} z^*}{a} - \frac{YR_{\text{inML}}}{m\left(1-\varepsilon\right)}, \tag{A42}$$

which is solved for z^*. The one frontier of the condition $z_{\text{m}} < z^* < z_{\text{b}}$ is obtained by substituting $z^* = z_{\text{m}}$ in (Eq. A42):

$$\frac{YD_{\text{DL}}\left(R_{\text{sed}} - R^*\right)}{m\left(1-\varepsilon\right)\left(z_{\text{b}} + 1/h - z_{\text{m}}\right)} - \frac{\log\left(I_{\text{in}}/I^*\right) - a_{\text{bg}} z_{\text{m}}}{a} + \frac{YR_{\text{inML}}}{m\left(1-\varepsilon\right)} = 0, \tag{A43}$$

which is identical with (Eq. A26) and separates (DCM + nutrient-limited ML) and

co-limited ML regions. The other one is obtained by substituting $z^* = z_b$:

$$\frac{hYD_{DL}\left(R_{sed} - R^*\right)}{m\left(1-\varepsilon\right)} - \frac{\log\left(I_{in}/I^*\right) - a_{bg}z_b}{a} + \frac{YR_{inML}}{m\left(1-\varepsilon\right)} = 0, \tag{A44}$$

which is identical with the frontier of (Eq. A37), and separates the (DCM + nutrient-limited ML) and (benthic layer + nutrient-limited ML) regions.

Case 7: Benthic Layer (BL)

Knowns: $B_{ML} = 0$

Unknowns: B_{DL}, $\bar{R}_{ML}$

Equations to solve:

When $B_{ML} = 0$ and $z^* = z_b$, the following equalities are derived from (Eq. 2.21) and (Eq. 2.24):

$$\begin{aligned} R_{inML} + \frac{D_{DL}\left(R^* - \bar{R}_{ML}\right)}{z_b - z_m} &= 0, \\ -\frac{m\left(1-\varepsilon\right)B_{DL}}{Y} + hD_{DL}\left(R_{sed} - R^*\right) - \frac{D_{DL}\left(R^* - \bar{R}_{ML}\right)}{z_b - z_m} &= 0, \end{aligned} \tag{A45}$$

and we obtain two unknowns:

$$\bar{R}_{ML} = R^* + \frac{\left(z_b - z_m\right)R_{inML}}{D_{DL}}, \tag{A46}$$

$$B_{DL} = \frac{hYD_{DL}\left(R_{sed} - R^*\right)}{m\left(1-\varepsilon\right)} + \frac{YR_{inML}}{m\left(1-\varepsilon\right)}. \tag{A47}$$

From (Eq. 2.26), the light profile is,

$$I(z) = \begin{cases} I_{in}e^{-a_{bg}z} & \text{for } 0 \le z < z_b \\ I_{in}e^{-\left(a_{bg}z + aB_{DL}\right)} & \text{for } z = z_b \end{cases}. \tag{A48}$$

Consistency/stability criteria:

First we consider the existence of the positive steady state. From (Eq. A47), $B_{\mathrm{DL}} > 0$ when

$$hD_{\mathrm{DL}}\left(R_{\mathrm{sed}} - R^*\right) + R_{\mathrm{inML}} > 0. \tag{A49}$$

Net growth $g(z_{\mathrm{b}}) - m = 0$ when

$$I(z_{\mathrm{b}}) = I_{\mathrm{in}} e^{-\left(a_{\mathrm{bg}} z_{\mathrm{b}} + aB_{\mathrm{DL}}\right)} \geq I^*. \tag{A50}$$

The two above inequalities (Eq. A49) and (Eq. A50) ensure the existence of a positive steady state.

Next we consider the stability criteria. Net growth should be negative or 0 everywhere for the stability. When $R_{\mathrm{inML}} = 0$, $g(z) - m = 0$ because $R(z) = R^*$ for $0 \leq z \leq z_{\mathrm{b}}$, and hence benthic layer is stable. When $R_{\mathrm{inML}} > 0$, the benthic layer is unstable because $\bar{R}_{\mathrm{ML}} > R^*$ from (Eq. A46) and $I(z) > I^*$ from (Eq. A50).

To summarize, the stability of the benthic layer requires $R_{\mathrm{inML}} = 0$; in this case, the inequality (Eq. A49) is simplified, and the parameter region where the deep layer is stable is expressed by:

$$\begin{cases} R_{\mathrm{sed}} - R^* > 0 \\ I_{\mathrm{in}} e^{-\left(a_{\mathrm{bg}} z_{\mathrm{b}} + aB_{\mathrm{DL}}\right)} \geq I^* \end{cases}. \tag{A51}$$

The frontier of the first inequality, $R_{\mathrm{sed}} = R^*$, separates the benthic layer and empty regions, which is identical with (Eq. A17) when $R_{\mathrm{inML}} = 0$. Substituting B_{DL} with

(Eq. A47), the frontier of the second inequality of (Eq. A51) is written as,

$$\frac{hYD_{\mathrm{DL}}\left(R_{\mathrm{sed}}-R^{*}\right)}{m\left(1-\varepsilon\right)}-\frac{\log\left(I_{\mathrm{in}}/I^{*}\right)-a_{\mathrm{bg}}z_{\mathrm{b}}}{a}=0, \tag{A52}$$

which separates the benthic layer and DCM regions.

Case 8: DCM

Knowns: $B_{\mathrm{ML}}=0$

Unknowns: B_{DL}, z^{*}, $\bar{R}_{\mathrm{ML}}$

Equations to solve:

When $B_{\mathrm{ML}}=0$, the following equalities are obtained from (Eq. 2.21) and (Eq. 2.24):

$$R_{\mathrm{inML}}+\frac{D_{\mathrm{DL}}\left(R^{*}-\bar{R}_{\mathrm{ML}}\right)}{z^{*}-z_{\mathrm{m}}}=0, \tag{A53}$$

$$-\frac{m\left(1-\varepsilon\right)B_{\mathrm{DL}}}{Y}+\frac{D_{\mathrm{DL}}\left(R_{\mathrm{sed}}-R^{*}\right)}{z_{\mathrm{b}}+1/h-z^{*}}-\frac{D_{\mathrm{DL}}\left(R^{*}-\bar{R}_{\mathrm{ML}}\right)}{z^{*}-z_{\mathrm{m}}}=0. \tag{A54}$$

From (Eq. 2.26), the light profile can be expressed by

$$I(z)=\begin{cases} I_{\mathrm{in}}e^{-a_{\mathrm{bg}}z} & \text{for } 0\leq z<z^{*} \\ I_{\mathrm{in}}e^{-\left(a_{\mathrm{bg}}z+aB_{\mathrm{DL}}\right)} & \text{for } z^{*}\leq z\leq z_{\mathrm{b}} \end{cases}. \tag{A55}$$

A stable DCM must be co-limited by nutrients and light. Therefore $I(z^{*+})=I^{*}$, that is,

$$I_{\mathrm{in}}e^{-\left(a_{\mathrm{bg}}z^{*}+aB_{\mathrm{DL}}\right)}=I^{*}. \tag{A56}$$

Solving (Eq. A53), (Eq. A54), and (Eq. A56), we obtain three unknowns, $\bar{R}_{\mathrm{ML}}$,

B_{DL}, and z^*.

Consistency/stability criteria:

As with the case of a benthic layer, a DCM is unstable when $R_{\mathrm{inML}} > 0$ because $\bar{R}_{\mathrm{ML}} > R^*$ from (Eq. A53) and $I(z) > I^*$ for $0 \leq z < z^*$ from (Eq. A56). So we consider $R_{\mathrm{inML}} = 0$. In this case, $\bar{R}_{\mathrm{ML}} = R^*$, and rearranging (Eq. A54) we have

$$B_{\mathrm{DL}} = \frac{Y D_{\mathrm{DL}} \left(R_{\mathrm{sed}} - R^*\right)}{m\,(1-\varepsilon)\left(z_{\mathrm{b}} + 1/h - z^*\right)}, \tag{A57}$$

and rearranging (Eq. A56) we have

$$B_{\mathrm{DL}} = \frac{\log\left(I_{\mathrm{in}}/I^*\right) - a_{\mathrm{bg}} z^*}{a}. \tag{A58}$$

From (Eq. A57) and (Eq. A58) an equality is obtained:

$$\frac{Y D_{\mathrm{DL}} \left(R_{\mathrm{sed}} - R^*\right)}{m\,(1-\varepsilon)\left(z_{\mathrm{b}} + 1/h - z^*\right)} = \frac{\log\left(I_{\mathrm{in}}/I^*\right) - a_{\mathrm{bg}} z^*}{a}, \tag{A59}$$

which is solved algebraically for z^* (Klausmeier and Litchman 2001). The obtained z^* should satisfy

$$z_{\mathrm{m}} < z^* < z_{\mathrm{b}}. \tag{A60}$$

From (Eq. A57), the existence of a positive steady state requires

$$R_{\mathrm{sed}} > R^*. \tag{A61}$$

$R_{\mathrm{inML}} = 0$ and inequalities (Eq. A60) and (Eq. A61) define the parameter region where the DCM is stable.

One frontier of (Eq. A60), $z^* = z_{\mathrm{m}}$, is expressed by substituting z^* in (Eq. A59)

with z_{m}:

$$\frac{YD_{\mathrm{DL}}\left(R_{\mathrm{sed}}-R^{*}\right)}{m\left(1-\varepsilon\right)\left(z_{\mathrm{b}}+1/h-z_{\mathrm{m}}\right)}-\frac{\log\left(I_{\mathrm{in}}/I^{*}\right)-a_{\mathrm{bg}}z_{\mathrm{m}}}{a}=0, \tag{A62}$$

which separates DCM and co-limited ML regions, and the other one, $z^{*}=z_{\mathrm{b}}$,

$$\frac{hYD_{\mathrm{DL}}\left(R_{\mathrm{sed}}-R^{*}\right)}{m\left(1-\varepsilon\right)}-\frac{\log\left(I_{\mathrm{in}}/I^{*}\right)-a_{\mathrm{bg}}z_{\mathrm{b}}}{a}=0, \tag{A63}$$

separates the DCM and benthic layer regions. Note that this frontier is identical with (Eq. A52). The frontier of (Eq. A61), $R_{\mathrm{sed}}=R^{*}$, separates the DCM and empty regions.

Chapter 3

Experimental test of phytoplankton competition for nutrients and light in poorly-mixed water columns

Jarad P. Mellard

with

Kohei Yoshiyama, Elena Litchman, and Christopher A. Klausmeier

3.1 Abstract

Despite the importance of the vertical distribution of phytoplankton for primary production and energy transfer to higher trophic levels, our mechanistic understanding of the phenomenon is poor. Recent theory of the vertical distribution of phytoplankton considers how interacting niche construction processes such as resource depletion, behavior, and population dynamics contribute to spatial heterogeneity in the aquatic

environment. To test this theory, we used a motile phytoplankton species (*Chlamydomonas reinhardtii*) growing in poorly-mixed water columns with opposing resource gradients of nutrients and light to examine how intraspecific competition determines the vertical distribution of phytoplankton. Under these conditions, theory predicts that a species should aggregate at a single depth, an evolutionary stable strategy (ESS). This depth of aggregation, or biomass maximum, should change through time due to depletion of available resources. In addition, the depth of the ESS aggregation should be deeper under low amounts of nutrient loading and shallower under higher amounts of nutrient loading. We tested these theoretical predictions in our experimental water columns. Supporting predictions, we routinely observed a single biomass maximum, where much of the population was aggregated, and the equilibrium depth of the biomass maximum was at the surface under higher nutrient loading. However, at equilibrium, low nutrient loading led to a non-distinct biomass maximum with the population distributed over most of the water column instead of the distinct subsurface peak predicted by theory. Also supporting predictions, total biomass across water columns was positively related to nutrient supply. Further supporting predictions, we also found evidence of light limitation for a surface biomass maximum and nutrient limitation for a deep biomass maximum. In addition, the resource environment was strongly modified by the behavioral movement, self-shading, nutrient uptake, and growth of the phytoplankton. The light level leaving the bottom of the water column, I_{out}, declined through time as the phytoplankton grew and was negatively related to nutrient loading. Nutrients were strongly depleted where biomass was present by the end of the experiment. This experimental study shows that the vertical distribution of phytoplankton may be driven by intraspecific resource competition in space.

3.2 Introduction

What determines the abundance and spatial distribution of organisms is one of the main questions in ecology (Brown 1984). External controls in the form of resources and stresses distributed in space along with organism-specific preferences and tolerances are commonly suspected to determine spatial distributions (MacArthur 1972). However, it has long been recognized that there are feedbacks on the environment and often the environment is modified by the activities of organisms themselves (Levins 1979). In self-organizing systems, spatial patterns can form through interactions internal to the system without intervention by external influence (Klausmeier 1999, van de Koppel et al. 2008). Studies are needed that explicitly model and measure how feedbacks between the strategies of organisms and their biotic and abiotic environments determine spatial patterns (Laland et al. 1999, Hastings et al. 2007).

Our approach to examining spatial distributions of organisms fuses externally imposed heterogeneity with self-organizing dynamics. A verbal model of how external and internal heterogeneity interact is: 1) Resource gradients represent external environmental heterogeneity. 2) Organisms sense these resource gradients and select habitats based on perceived quality. 3) The organisms' growth results in population dynamics. 4) Population dynamics create feedbacks on the resource environment. 5) The organisms undergo further strategic movement based on the feedbacks in the resource environment that all the other organisms have created.

Phytoplankton are ideal for examining these interacting processes. Phytoplankton require nutrients and light to grow and these essential resources usually form opposing gradients in the vertical dimension in the aquatic environment (Reynolds 1984). These gradients in resources are actually set or enhanced by the phytoplankton themselves due to nutrient uptake and self-shading (Klausmeier and Litchman 2001). The hypotheses of what determines the vertical distribution of phytoplankton remain

largely untested (but see Carney et al. 1988) and few studies have attempted to recreate vertical distributions under controlled settings based on existing hypotheses (but see Jaeger et al. 2008).

Vertical distributions of phytoplankton are strongly dependent on the physics operating in a body of water (Huisman et al. 1999*c*, Jaeger et al. 2008). In a completely well-mixed water column, phytoplankton are homogenized and form no patterns in vertical distribution. However, the environment is not always well mixed, in which case we can expect pronounced patterns. Multiple distinct vertical distributions are possible in poorly-mixed systems including a benthic layer, where phytoplankton form a layer directly on the sediment surface, a deep chlorophyll maximum (DCM), where phytoplankton form a layer in a poorly-mixed portion of the water column away from the boundaries, and a surface layer, where phytoplankton form a layer at the surface of the water. Several hypotheses have been proposed to explain the formation of DCMs, such as near-inertial internal wave shear (Franks 1995), sinking in a density stratified water column (Condie and Bormans 1997), depth dependent grazing by zooplankton or mixotrophs (Tittel et al. 2003), diel vertical migration of algae (Sommer and Gliwicz 1986, Gasol et al. 1991), behavioral responses to sensory cues (Gervais 1998, Clegg et al. 2007), and preferential movement to and growth at an optimal depth in opposing resource gradients (Fee 1976, Klausmeier and Litchman 2001). We focus on this last hypothesis, how movement and growth in opposing resource gradients can determine phytoplankton vertical distributions, because theory (Klausmeier and Litchman 2001) has made testable predictions related to this hypothesis that are amenable to experimentation.

Motile algae in poorly-mixed water columns can be thought of as playing a game in the opposing resource gradients of nutrients and light (Klausmeier and Litchman 2001). Motile algae are common and represent important components of phytoplankton communities in freshwater and marine environments (Reynolds 1984, Cullen and

MacIntyre 1998). Using a spatially-explicit dynamical model, Klausmeier and Litchman (2001) show that motile phytoplankton can form a thin layer in poorly-mixed water columns as is also observed in the field (Fee 1976, Gasol et al. 1991, Gervais 1998, Mellard et al. Chapter 4). They show that their full dynamical model can be approximated by a game-theoretical model that has the advantage of providing analytical results for greater insight. The game-theoretical model considers motile algae to form an infinitely thin layer at their depth of co-limitation. This strategic depth, z^*, is a convergence stable evolutionarily stable strategy (ESS) and prevents growth elsewhere in the water column.

The model makes specific predictions about the vertical distribution of algae (Klausmeier and Litchman 2001): 1) Phytoplankton can form a thin layer, 2) the depth of the layer depends on environmental conditions, specifically it should be deeper under low-nutrient conditions and shallower under high-nutrient conditions, 3) biomass should be positively associated with nutrient supply over the range of nutrient supply, from adequate to saturating, 4) phytoplankton in a surface layer should be co-limited (Mellard et al. Chapter 2) or light-limited, whereas phytoplankton in a benthic layer should be nutrient-limited, and those in a DCM co-limited by nutrients and light. We evaluated these predictions with the aid of a dynamic model and experimental plankton towers focusing on whether algae aggregate and whether aggregation patterns depend on environmental conditions.

3.3 Theory

We expanded on previously published theoretical work (Klausmeier and Litchman 2001) by examining dynamics of the full model used to verify the more fully explored game-theoretic model. Because transient dynamics were not explored in Klausmeier and Litchman (2001) or elsewhere, we present some of these results here because

they are directly applicable to results from our experiment. The full model includes spatially-explicit equations for biomass, b, nutrients, R, and light, I in a one-dimensional water column where z is depth with the surface at $z = 0$ and the bottom at $z = z_b$. See Appendix for a full description of the model.

Model predictions

Under the conditions we are examining, simulations predict algae to aggregate and form a thin layer, hence the use of the game-theoretic model proposed by Klausmeier and Litchman (2001) should be valid. However, because the game-theoretic model assumes the system approaches a stable equilibrium, some of the predictions may not be valid for the time scale of our experiment (50 days). The game-theoretic model also assumes an infinite swimming speed that should not be valid for any species we use in our experiments. Therefore, we present predictions from the full dynamical model, which have not been presented before, as well as predictions from the game-theoretic model proposed by Klausmeier and Litchman (2001).

Simulations suggest the following transient dynamics. Algae that start in a uniform distribution should behaviorally aggregate at the surface by the end of day 1 (Figure 3.1 bottom left plots). They should grow exponentially initially (Figure 3.1 top left plots) before reaching carrying capacity which will happen sooner in low-nutrient towers (Figure 3.1a) than in mid-level nutrient towers (Figure 3.1b) or high-nutrient towers (Figure 3.1c). In low and mid-level nutrient towers, algae should move down to acquire more nutrients once they are depleted at the surface. In low-nutrient towers, algae should remain at the bottom of the water column to take up the little nutrients available if enough light penetrates there (Figure 3.1a bottom right plot). In mid-level nutrient towers, algae should form a layer somewhere between the surface and the bottom in a DCM where nutrient and light supply are balanced by the uptake and self-shading of the algae (Figure 3.1b bottom right plot). High nutrient towers results in higher biomass, so algae face intense light competition due to

plentiful nutrients and should remain at the surface (Figure 3.1c bottom right plot).

Figure 3.1. Predicted total biomass (top left), depth distribution of biomass through time (bottom left) and equilibrium (day 50) distribution of biomass, nutrients, and light (bottom right) for a) low-nutrient supply (R_{in} =5 μg P L^{-1}), b) mid-level nutrient supply (R_{in} =50 μg P L^{-1}), and c) high-nutrient supply (R_{in} =5000 μg P L^{-1}). The top left plot of each part shows biomass integrated over the entire water column. In the bottom left plot of each part, biomass density is shaded so that higher biomass is in darker shades. The solid line on that plot shows the average depth of the biomass and the dashed line shows the location of the biomass maximum. In the bottom right plot of each part, the equilibrium (day 50) biomass, nutrients, and light are all scaled to their maximum to fit on one plot but units above each plot show absolute quantities. The I^* value on those plots shows break-even light level and is relativized to the maximum light level as well.

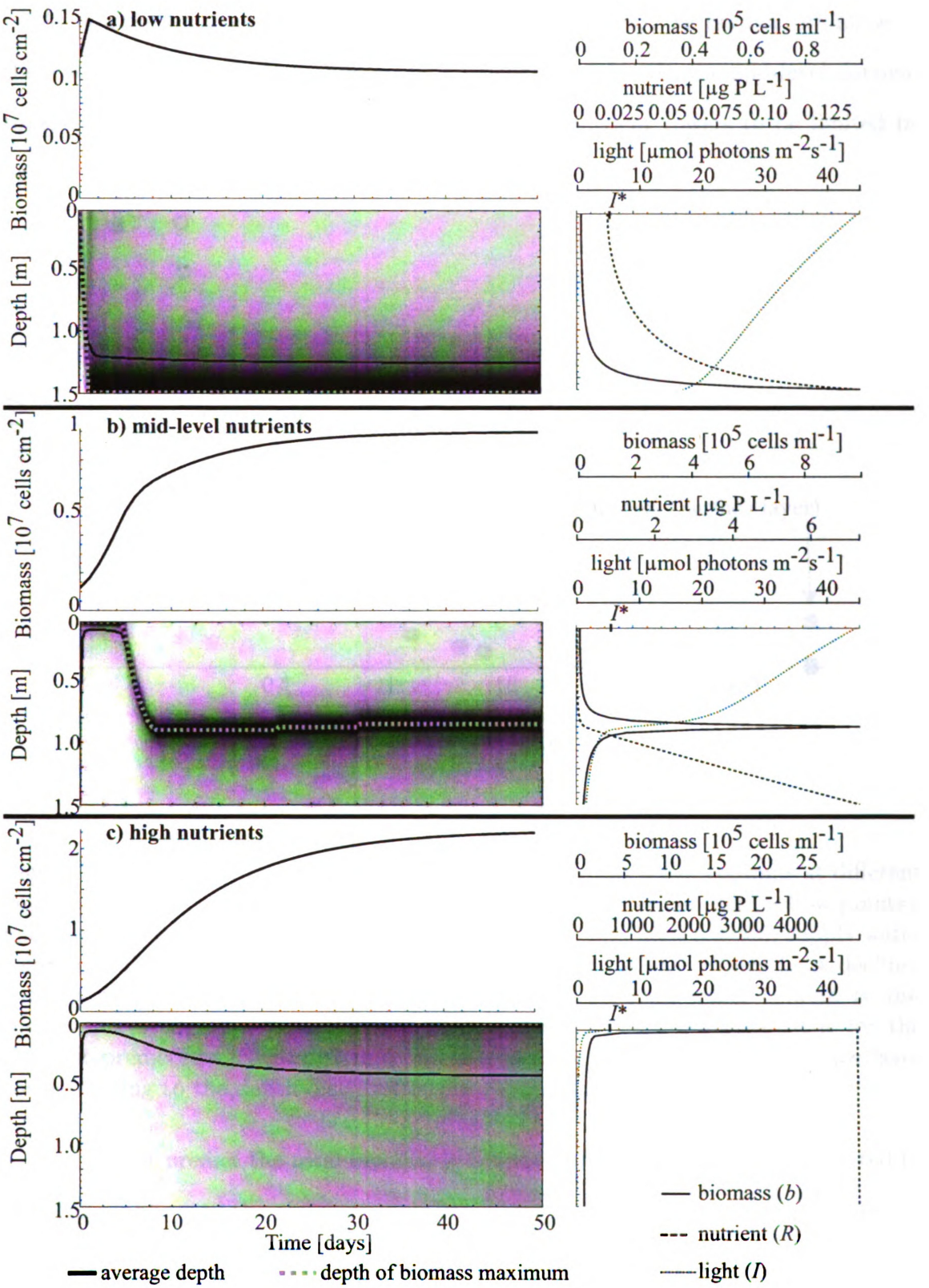

Figure 3.1: Predicted total and depth distribution of biomass through time.

At equilibrium (predicted to be reached after 50 days), we predict the algae in the low-nutrient towers to be limited by nutrients, the algae in the mid-level nutrient towers to be co-limited, and the algae in the high-nutrient towers to be limited by light (Figure 3.2).

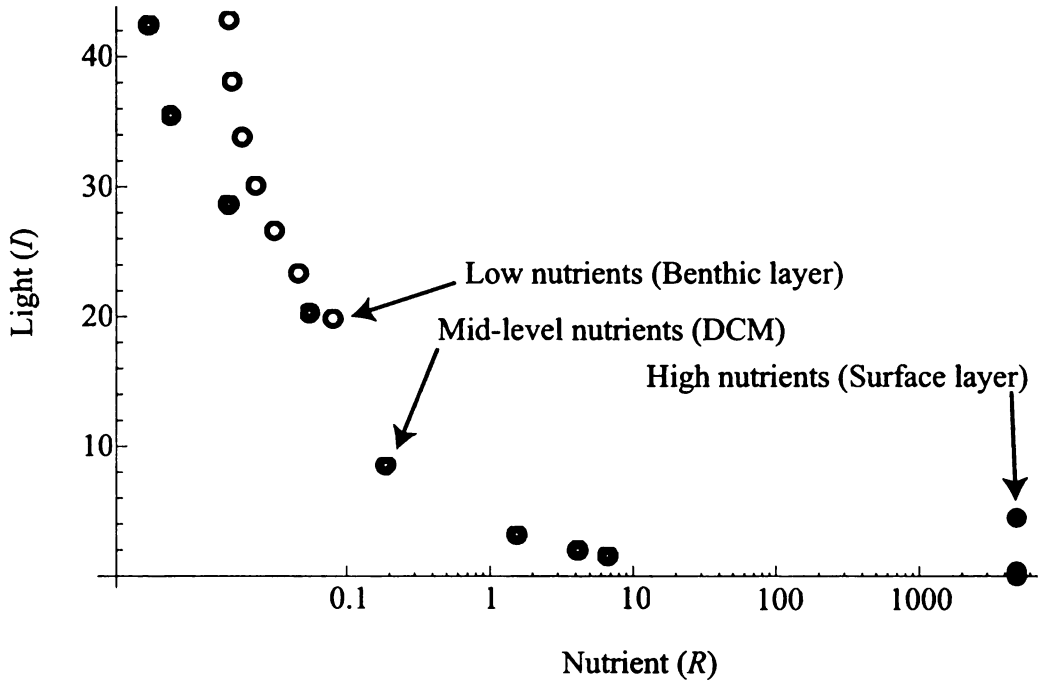

Figure 3.2: Points are resource conditions within different water columns at different depths. Resource conditions for a low-nutrient supply water column (hollow points), mid-level nutrient supply water column (gray donuts), and high-nutrient supply water column (solid points, some on top of one another) are shown. Since light declines with depth, the point with the highest light value for each water column is also the shallowest depth. Note that the arrows show the resource conditions for the different predicted vertical distributions of a benthic layer, DCM, and surface layer corresponding to the depth distributions in Figure 3.1.

We further predict the total biomass in a water column to be positively related to nutrient supply until the algae are completely light limited (Figure 3.3a). In addition, we predict the vertical position of the thin layer to be shallower under higher nutrient conditions (Figure 3.3b).

We designed an experiment to evaluate whether these predictions are upheld in

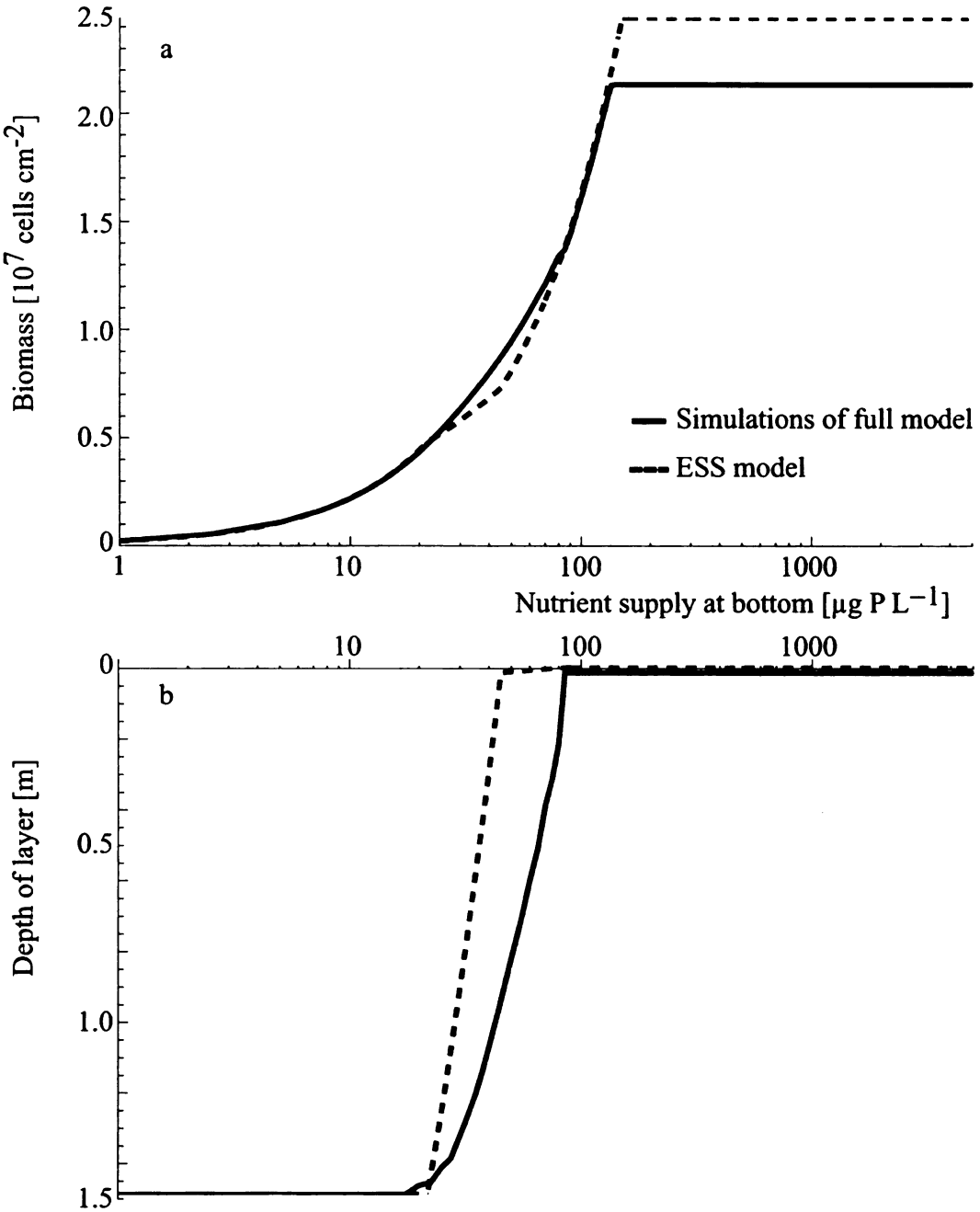

Figure 3.3: Predicted integrated biomass (a) depth of algal layer and (b) depth of the algal layer as a function of nutrient concentration at the bottom. Both (a) and (b) have a solid line representing simulations from the full model averaged over days 30-50 and a dashed line representing the equilibrium biomass (a) and z^* depth (b) predicted by the ESS model.

water columns under controlled settings. We manipulated one factor, nutrient supply, while holding all other factors constant.

3.4 Experiment methods

Experimental setup

We used cylindrical plankton towers to examine spatial distributions of phytoplankton (Picture in Appendix). Tower dimensions were 1.5 m height, 0.2 m diameter and constructed from clear cast acrylic tubes (Total Plastics, Kalamazoo, MI). Towers had ports along the vertical dimension with silicone stoppers that were punctured with needle syringes to take samples or inject nutrients. Towers were covered with heavy duty black plastic sheeting to maintain a unidirectional light source and increase light attenuation. Towers were illuminated 24 hours a day to maintain the light gradient with a single cool 42 watt fluorescent light (Technical Consumer Products, Aurora, Ohio) above each tower. In order to have only one limiting nutrient, phosphorus, towers were filled with autoclaved WC medium (Guillard 1975) without phosphorus but with 5X all other ingredients, including bicarbonate in order to eliminate carbon limitation. Towers were inoculated with cultured *Chlamydomonas reinhardtii* 2935 (Carolina Biological Supply), a flagellated green alga commonly found in temperate freshwater lakes (Reynolds 1984). Towers were then mixed by stirring the whole column vigorously. After inoculation, we injected concentrated phosphorus (K_2HPO_4) at 10 depths in each tower to create a nutrient gradient initially in concentrations corresponding to the experiment treatments (next paragraph). We confirmed that the algae were homogenously mixed and the nutrient gradient was present initially by withdrawing samples within an hour after injecting the phosphorus. A clear plastic sheeting (saran wrap) was placed loosely over the top of each tower during the experiment to reduce probability of contaminants and invaders but still allow gas

exchange.

Experiment treatments

Our towers represented an environmental gradient in nutrient loading, with increasing phosphorus concentrations injected at the bottom (deepest port). Nutrient concentrations of 5, 10, 50, 100, 250, 500, 1000, and 5000 μg P L^{-1} were injected at the bottom of towers 1 through 8, respectively. During each sampling, some volume was removed from each tower. In order to keep the water level relatively constant as well as maintain a constant nutrient supply into the system, we injected nutrients back into the system. After most sampling days, we set up a gravity fed nutrient addition system that slowly injected approximately 250 mL of concentrated phosphorus WC medium into the bottom port of each tower. This slow injection system took approximately 12 hours to complete each time. The days we injected nutrients are indicated by arrows on Figure 3.4.

Sampling

Two main sampling schemes were employed. For the first 15 days of the experiment, 17 relatively evenly spaced ports were sampled for biological analysis and for days 16 through 50, 21 relatively evenly spaced ports were sampled for biological analysis. We increased our spatial resolution by adding these four other ports. For the first four days of the experiment, seven relatively evenly spaced ports were sampled for nutrient analysis and for days five through 50, eight relatively evenly spaced ports were sampled for nutrient analysis. We sampled every three to four days for the first 25 days of the experiment and every three to seven days thereafter. We ended the experiment after 50 days because we observed no further distinct changes in spatial distribution of algae, biomass was declining in most towers, and our model predicted towers should have reached equilibrium by then. We refer to the the last 20 days of the experiment as at equilibrium, since spatial distributions appeared to have reached steady state.

Samples were taken from each port using 22-gauge 3-inch hypodermic needles (Air-Tite Products Co, Inc., Virginia Beach, VA) in 10 mL B-D syringes (Becton Dickinson & co., Franklin Lakes, NJ), and placed in liquid scintillation vials for phytoplankton enumeration or filtered through 0.45 μm nylon, 25 mm syringe filters (Fisher Scientific, Hampton, NH) and placed in 10 mL centrifuge tubes (Corning Incorporated, Corning, NY) for nutrient analysis. Cell densities were measured on CASY cell counter Model TT (Schärfe-System, Reutlingen, Germany) using a 4-30 μm cell diameter range and preserved afterwards using Lugols solution. Cells were also examined under an inverted scope to check for signs that they were alive and possible morphological changes. Dissolved phosphorus was measured using the orthophosphate method on Lachat Instruments Quick Chem 8500 (Lachat Instruments a Hach Co Brand, Loveland, CO). At the end of the experiment we measured the C:N:P of particulate matter, chlorophyll *a*, and temperature at the same eight ports in the tower where dissolved nutrients were measured. Particulate carbon and nitrogen were measured by filtering samples on 25 mm Whatman GF/F pre-combusted glass fiber filters (Whatman plc, Springfield Mill, UK) before combusting them in a Costech Elemental Combustion System CHNS-O (Costech Analytical Technologies, Inc., Valencia, CA). Particulate phosphorus was measured by filtering samples on 25 mm Whatman GF/B acid-washed glass fiber filters, performing persulfate digestion on the filters, and then analyzed colorimetrically on a Shimadzu spectrophotometer UV-240PC (Shimadzu Scientific Instruments, Columbia, MD) at 880 nm. Chlorophyll *a* was measured by filtering onto a 25 mm Whatman GF/B filter, which was extracted with ethanol and measured fluorometrically (Welschmeyer 1994). We also measured pH at two points in each tower to make sure there was not a vertical gradient in pH. Light was measured at the surface and bottom of the water columns before the experiment started, at the bottom of the water columns throughout the experiment, and through the water columns at the end of the experiment. Light was measured using

a LI-COR Quantum/Radiometer/Photometer model LI-185B (LI-COR Biosciences, Lincoln, NE).

Data analysis

To summarize the vertical distributions, we fit three functions to the vertical profiles of biomass and used information criteria to distinguish which function fit best (see Appendix). The three functions were: a constant ($b(z) = c$), a line ($b(z) = nz+c$), and an exponential plus a constant ($b(z) = ne^{-sz} + c$). We chose these functions because our data looked representative of these functions and comparing the line function and the exponential plus a constant function allowed us to distinguish if a thin layer was present or not. The exponential part of the exponential plus a constant function describes the biomass in the thin layer. There was never a peak at depth so the exponential function is pinned at the surface. We used ΔAIC_C to determine the best function (Burnham and Anderson 2002). If the exponential plus a constant function did not fit best or found a biomass minimum at the surface then we characterized the profile to have no surface layer present. When no surface layer was present, layer biomass and width for that profile were not calculated. Surface layer biomass was calculated by integrating $b(z) = ne^{-sz}$ over the depth of the tower, however, note that only the top few centimeters really contributed to the surface layer biomass due to the exponential decay in the equation. Background biomass was calculated as cz_b from the best fit function, where z_b is tower depth. When a surface layer was present, total biomass was calculated as the sum of surface layer biomass and background biomass. The characteristic layer thickness was calculated as $1/s$. When a surface layer was not present, the line function always fit better than the constant so total biomass was calculated using the line function and integrated using the trapezoid rule.

Linear regression was conducted on equilibrium biomass and log biomass versus log nutrient supply because biomass appeared to show heteroscedasticity. How-

ever, we present the untransformed biomass data because we present the model predicted biomass untransformed as well. Relationships were also checked for significant quadratic terms but none were found. Linear regressions were also conducted on log light at the bottom, and all chlorophyll, nutrient, and stoichiometric response variables with log nutrient supply as the independent continuous variable for all towers. ANCOVAs were conducted on all chlorophyll, nutrient, and stoichiometric response variables with log nutrient supply as the independent continuous variable and surface versus deep as the independent categorical variable for towers that had a surface layer present at the end of the experiment (treatments 100-5000 μg P L^{-1}). Statistical analyses were performed in *Mathematica* v7 (Wolfram Research, Inc., Champaign, IL) and *R* v2.10 (The R Foundation for Statistical Computing, Vienna, Austria).

3.5 Experiment results

All towers showed initial behavioral aggregation of the algae in response to resource gradients, where algae went from a uniform distribution on day 0 to aggregating at the surface by day 1 (Figure 3.4 shows representative results). Once aggregated (Figure 3.4 top left plots), algae depleted nutrients locally through growth and moved down if nutrients were limiting (Figure 3.4a,b bottom left plots). At the end of the experiment, algae in the lowest nutrient treatment were relatively evenly distributed with a biomass minimum at the surface (Figure 3.4a bottom right plot). Sufficient light penetrated to the bottom so that $I_{\text{out}} > I^*$. Nutrients were in low abundance throughout the water column (Figure 3.4a bottom right plot). In the mid-level nutrient treatment, biomass was spread throughout the water column (Figure 3.4b bottom right plot). In the highest nutrient treatment, algae exhibited a biomass maximum at the surface (Figure 3.4c bottom right plot). Light was depleted and below I^* beneath the surface maximum. Nutrients were depleted at the surface and in high abundance

at depth.

Figure 3.4. Observed total biomass (top left), depth distribution of biomass through time (bottom left) and equilibrium (day 50) distribution of biomass, nutrients, and light (bottom right) for a) low-nutrient supply (R_{in} =5 μg P L^{-1}), b) mid-level nutrient supply (R_{in} =50 μg P L^{-1}), and c) high-nutrient supply (R_{in} =5000 μg P L^{-1}). The top left plot of each part shows biomass integrated over the entire water column. In the bottom left plot of each part, biomass density is shaded so that higher biomass is in darker shades. The solid line on that plot shows the average depth of the biomass and the dashed line shows the location of the biomass maximum. The small arrows along the bottom of that plot indicates the days that phosphorus was injected at the bottom of the towers. In the bottom right plot of each part, biomass, nutrients, and light are all scaled to their maximum to fit on one plot but units above each plot show absolute quantities. The I^* value on those plots shows break-even light level and is relativized to the maximum light level as well.

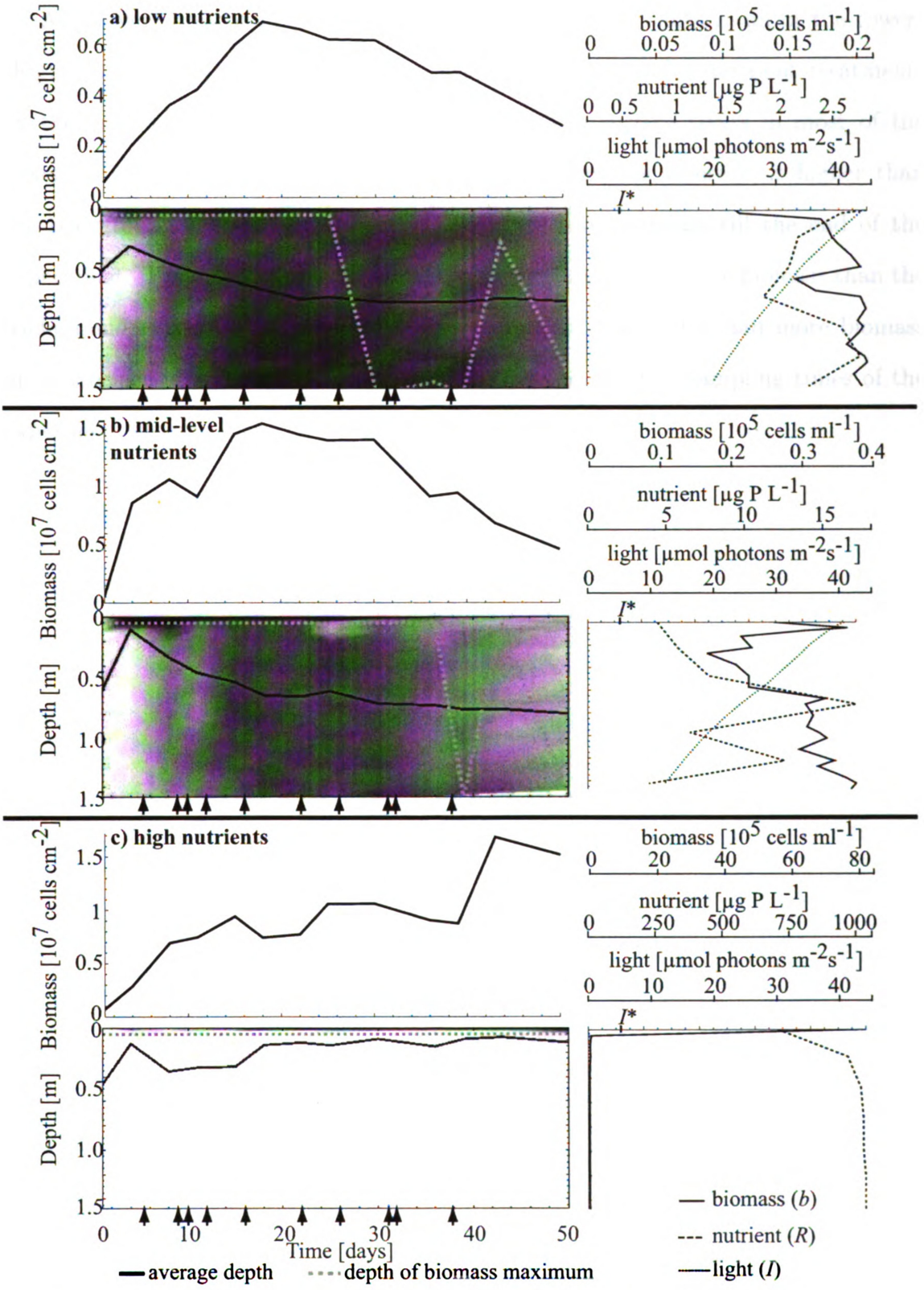

Figure 3.4: Observed total and depth distribution of biomass through time.

Algae were present in a distinct surface layer at most times in all of the towers (Figure 3.5a-h). However, the surface layer disappeared in low-nutrient treatments by the end of the experiment (Figure 3.5a-c). The surface layers in most of the towers (Figure 3.5b-d,f,g) show an early peak in biomass where it is higher than the background followed by a decline in surface layer biomass till the end of the experiment. Two of the towers never had a surface layer with more biomass than the background (Figure 3.5a,e) and the highest nutrient tower only had more biomass in the surface layer than the background during the last two sampling times of the experiment (Figure 3.5h).

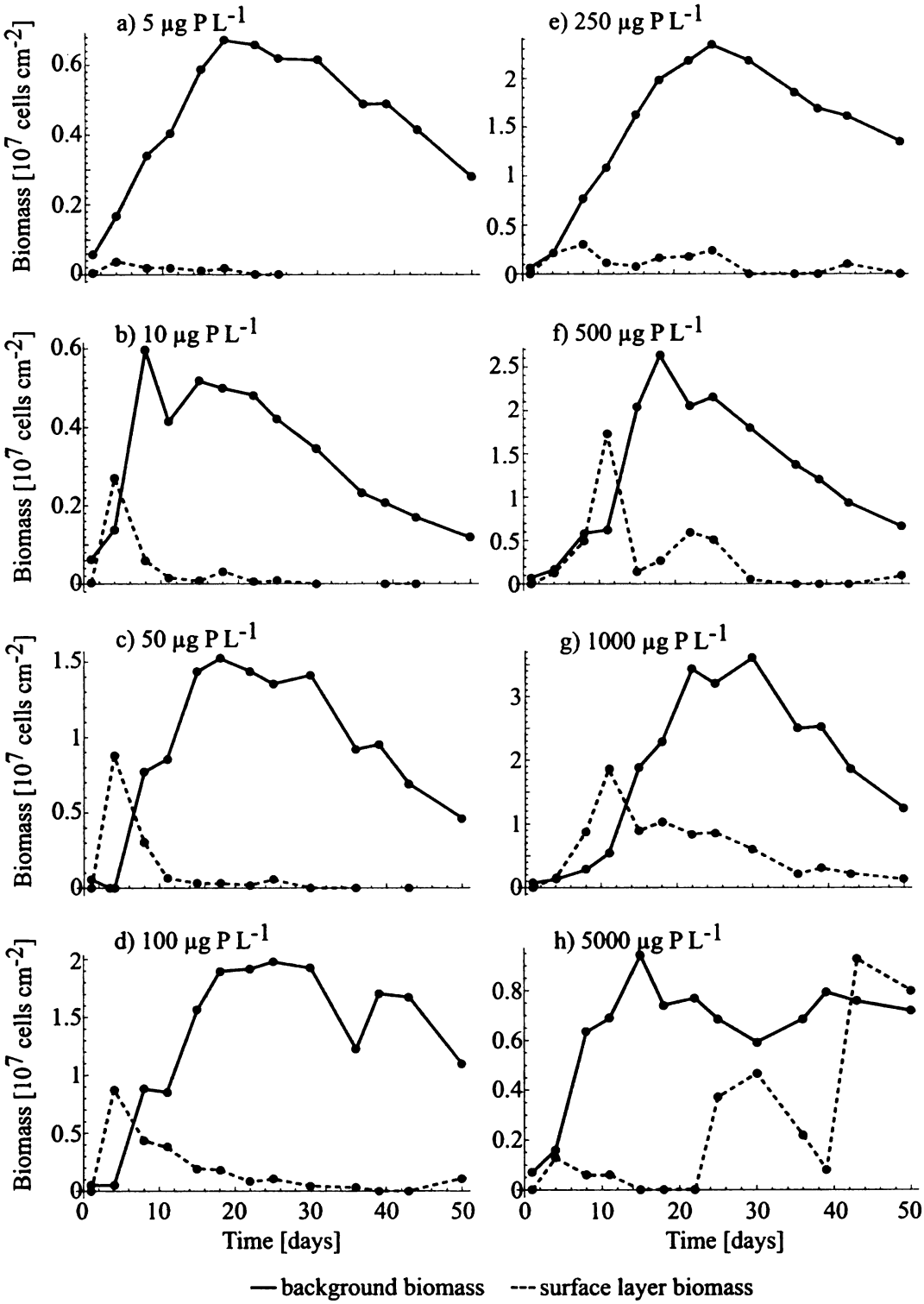

Figure 3.5: Amount of biomass in surface layer (if present) and background through time for all eight treatments (a is lowest nutrients increasing to h, the highest nutrients).

Concerning the limiting resource, by day 50, the algae at all depths in the lowest and mid-level nutrient towers were relatively more nutrient limited than the highest nutrient tower (Figure 3.6 and note that nutrient axis is on log scale). The algae at all depths in the highest nutrient tower appear to be primarily limited by light as evidenced by their extremely low light levels at all depths (see also Figure 3.4c bottom left plot).

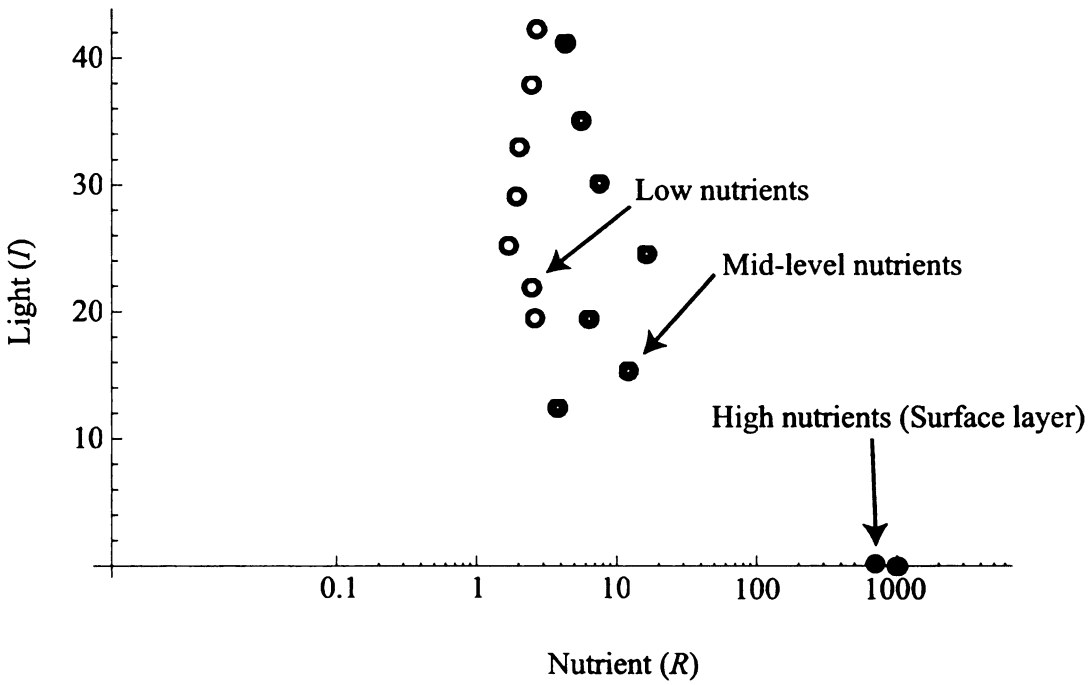

Figure 3.6: Data points are resource conditions within different water columns at different depths. Resource conditions for a low-nutrient supply tower (hollow points), mid-level nutrient supply tower (gray donuts), and high-nutrient supply tower (solid points, some on top of one another) are shown corresponding to nutrient treatments R_{in} =5, 50 and 5000 μg P L^{-1} respectively. Since light declines with depth, the data point with the highest light value for each tower is also the shallowest depth. Note that the arrows point out the different treatments corresponding to the depth distributions in Figure 3.4.

Total biomass averaged over the last 20 days of the experiment was positively related to nutrient supply (Figure 3.7a) with a near significant linear relationship between biomass and log nutrient supply ($P = 0.06$) and a significant linear relationship between log biomass and log nutrient supply (not shown, $P < 0.05$). The

depth of the biomass maximum was negatively related to nutrient supply, i.e. deeper under low-nutrient loading and shallower under higher nutrient loading (Figure 3.7b). The biomass maximum was always at the surface for the five highest nutrient supply towers.

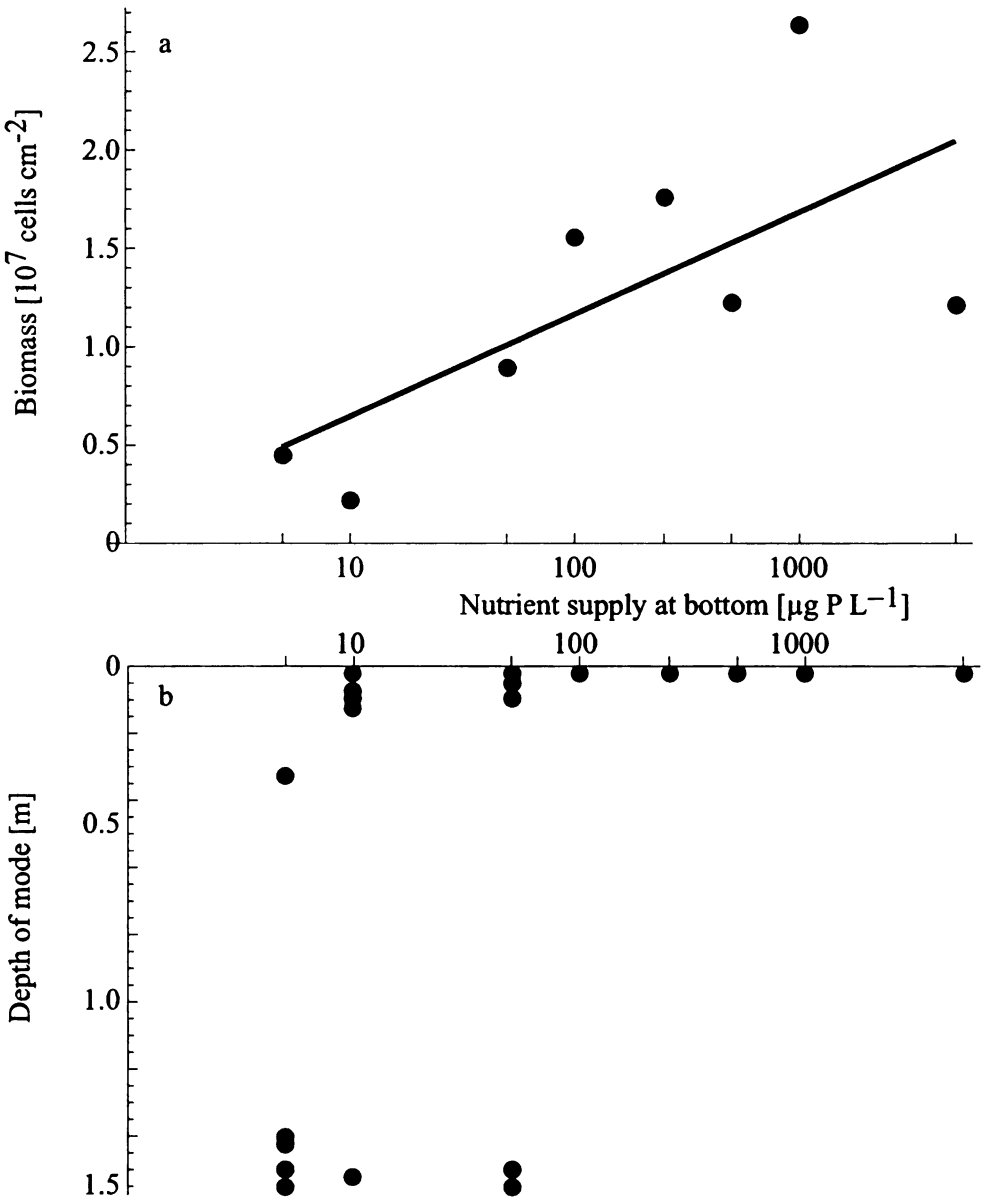

Figure 3.7: Effect of nutrient treatment on equilibrium biomass and depth distribution. a) Observed integrated biomass averaged over days 30-50 as a function of nutrient treatment. Shown is the almost significant linear relationship between biomass and log nutrient supply (slope= 22503, $t = 2.28$, $P = 0.06$) and not shown is the significant linear relationship between log biomass and log nutrient supply (slope= 0.26, $t = 2.77$, $P < 0.05$). b) Observed modal depths for days 30-50 as a function of nutrient treatment. Note that points for the nutrient treatments of 5, 10, and 50 μg P L^{-1} have been offset 0.025 m for clarity while the points for nutrient treatments of 100, 250, 500, 1000, 5000 μg P L^{-1} all fall directly on top of one another and have not been offset.

Algae were present throughout the water column, without a distinct aggregation at the end of the experiment in low to mid-level nutrient towers (R_{in} =5–50 μg P L^{-1}). The portion of the biomass in the layer, where present, shows an increasing trend with nutrient treatment (Figure 3.8). Although the surface layer was very pronounced when present, only in the highest nutrient treatment was there more biomass in the layer than in the background at the end of the experiment (Figure 3.8).

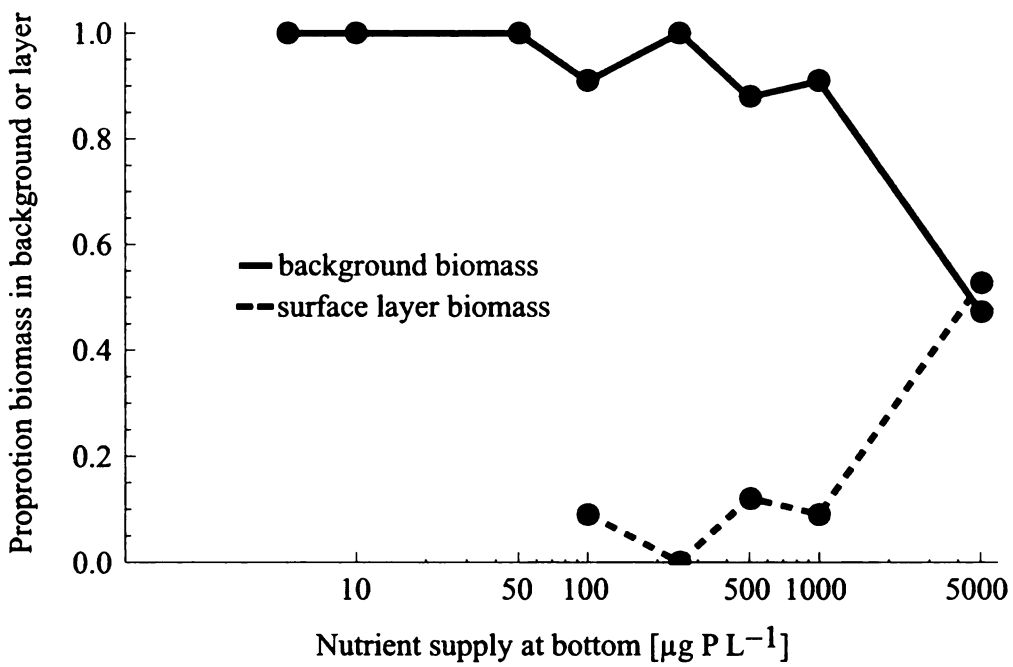

Figure 3.8: Proportion of biomass in the surface layer and the background at the end of the experiment versus nutrient treatment.

The thickness of the layer (if present) peaked early in the experiment and then declined and disappeared in low to mid-level nutrient towers (Figure 3.9a-c), while generally declining in the higher nutrient towers (Figure 3.9d-h).

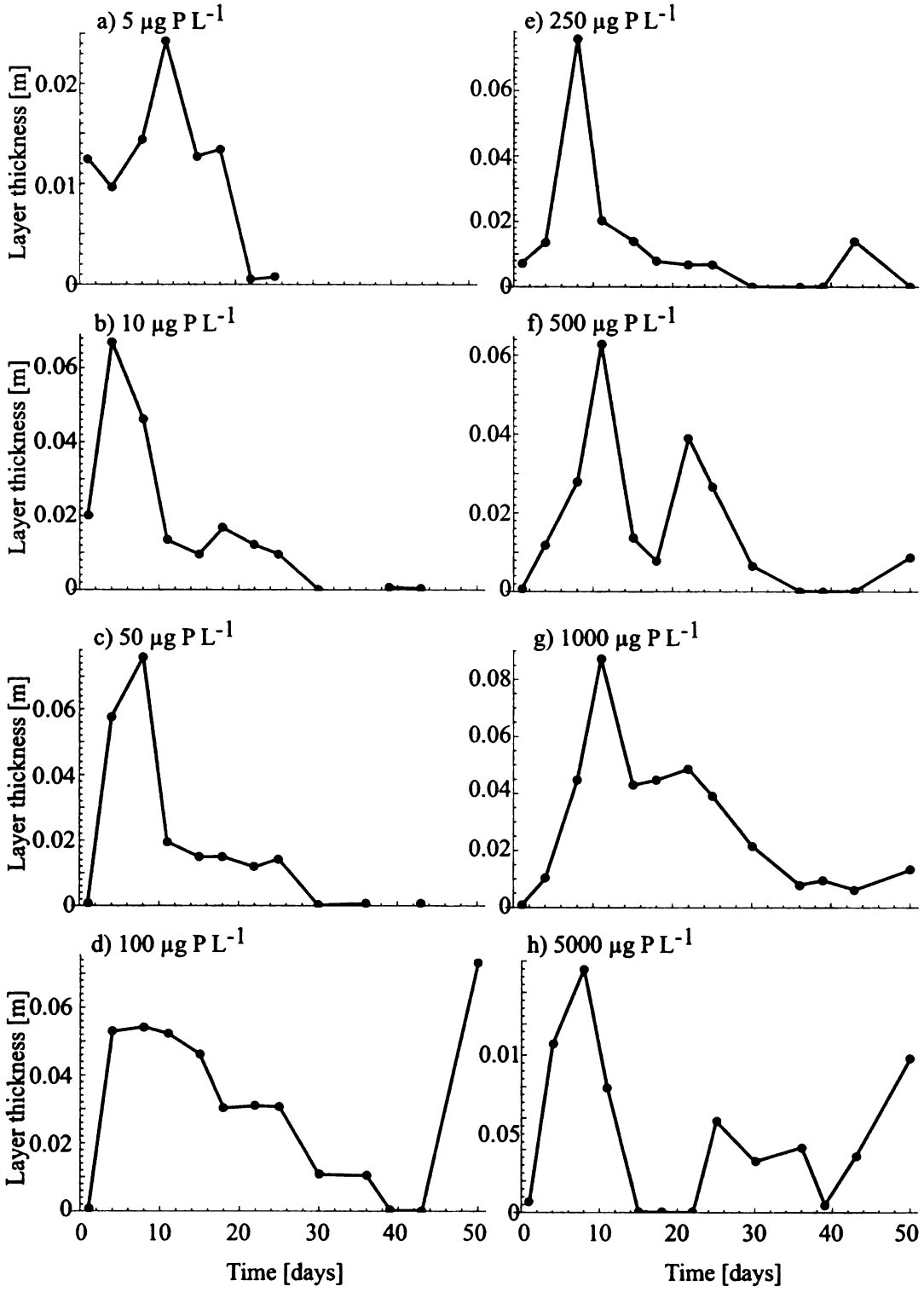

Figure 3.9: Characteristic layer thickness for all treatments and times. Points are only plotted if a surface layer was calculated to exist.

The light level at the bottom of the water column, I_{out}, declined through time in all treatments (not shown). At the end of the experiment, I_{out} was lower in the higher nutrient treatments (Figure 3.10) with a significant linear relationship between log I_{out} and log nutrient treatment ($P < 0.01$). At the end of experiment, chlorophyll concentration exhibited subsurface maxima in the three lowest nutrient treatment towers, although the subsurface maxima were not well-defined peaks. Conversely, the five highest nutrient treatment towers exhibited surface maxima for chlorophyll concentration (Appendix Figure A2a-h). In this way, chlorophyll mimics the biomass distributions (Appendix Figure A1). Log chlorophyll concentration was positively related to nutrient supply of the experimental treatments ($P < 0.001$, not shown).

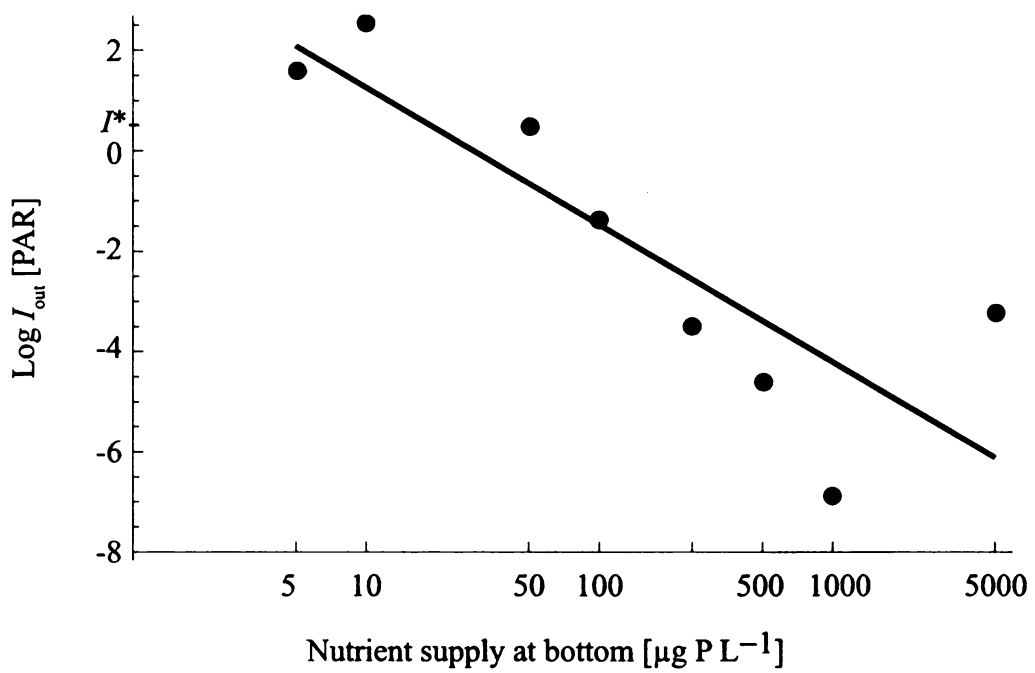

Figure 3.10: At the end of the experiment, the light level leaving the bottom of the water column, I_{out}, is shown as a function of nutrient treatment. There was a significant linear relationship between log I_{out} and log nutrient treatment (slope= -1.18, $t = -3.88$, $P < 0.01$).

3.5.1 Physiology

Although theory assumes constant physiology, we measured considerable physiological variation in our experiment. Chlorophyll concentrations per cell were positively related to nutrient supply of the experimental treatments ($P < 0.001$, Figure 3.11a). Carbon per cell was not related to nutrient supply (results not shown). However, the chlorophyll-to-carbon ratio was positively related to nutrient supply ($P < 0.001$, Figure 3.11b). The nonlimiting nutrient, nitrogen per cell was not related to nutrient supply (results not shown). In towers where peaks occurred (high-nutrient supply towers), cellular phosphorus quota was positively related to nutrient supply across all towers ($P < 0.001$, results not shown) and nutrient supply had a larger effect on deep biomass (different slopes, $P < 0.001$, Figure 3.11d). To distinguish the effects of nutrients on surface layer populations versus deep populations, we divided the data into two categories: surface layer and deep. The s is for surface layer data points and d is for deep data points in Figure 3.11d-f, and in those figures, we are focusing only on towers with a distinct layer.

Particulate C:N ratio was negatively related to nutrient supply ($P < 0.005$, Figure 3.11c). Particulate C:P ratio was also negatively related to nutrient supply across all towers ($P < 0.001$, results not shown) and the surface biomass had a higher C:P than the deeper biomass in the higher nutrient treatment towers (different intercepts, $P < 0.001$, Figure 3.11e). Particulate N:P ratio was negatively related to nutrient supply across all towers ($P < 0.001$, results not shown) and the surface biomass had a higher N:P than the deeper biomass in the higher nutrient treatment towers (different intercepts, $P < 0.001$, Figure 3.11f).

Figure 3.11. Chlorophyll *a*, nutrient, and stoichiometric quantities at the end of the experiment as a function of nutrient supply. Plots a-c show the regression lines from all treatments and sampling depths. Plots d-f show the regression lines from ANCOVAs conducted only on treatments with a surface layer present at the end of the experiment. The solid line is for the d=deep data points and the dashed line is for the s=surface data points. Only significant relations are shown and if the ANCOVA was significant for a variable, those results are shown rather than the linear regression results for all treatments. a) Chlorophyll *a* per cell is positively related to log nutrient treatment (N=60, $slope = 3.77 \times 10^{-7}$, $t = 11.21$, $P < 0.001$, as is chlorophyll, not shown, N=60, $slope = 1.34$, $t = 9.25$, $P < 0.001$). b) Chlorophyll *a* to carbon ratio (Chl:C) is positively related to log nutrient treatment (N=60, $slope = 3.95 \times 10^{-3}$, $t = 12.45$, $P < 0.001$). c) Carbon:nitrogen ratio of particulate matter is negatively related to log nutrient treatment (N=60, $slope = -0.69$, $t = -3.01$, $P < 0.005$). d) Phosphorus cellular quota is positively related to log nutrient treatment but the slopes differs between the deep (N=33, $slope = 2.04 \times 10^{-6}$, $t = 16.747$, $P < 0.001$) and surface data points (N=4, $slope = 1.74 \times 10^{-6}$, $t = 12.52$, $P < 0.001$). e) Carbon:phosphorus ratio of particulate matter is negatively related to log nutrient treatment but the intercept differs between the deep (N=33, $intercept = 169.76$, $t = 8.269$, $P < 0.001$) and surface data points (N=4, $intercept = 192.39$, $t = 25.117$, $P < 0.001$). f) Nitrogen:phosphorus ratio of particulate matter is negatively related to log nutrient treatment but the intercept differs between the deep (N=33, $intercept = 145.50$, $t = 20.53$, $P < 0.001$) and surface data points (N=4, $intercept = 164.91$, $t = 25.117$, $P < 0.001$).

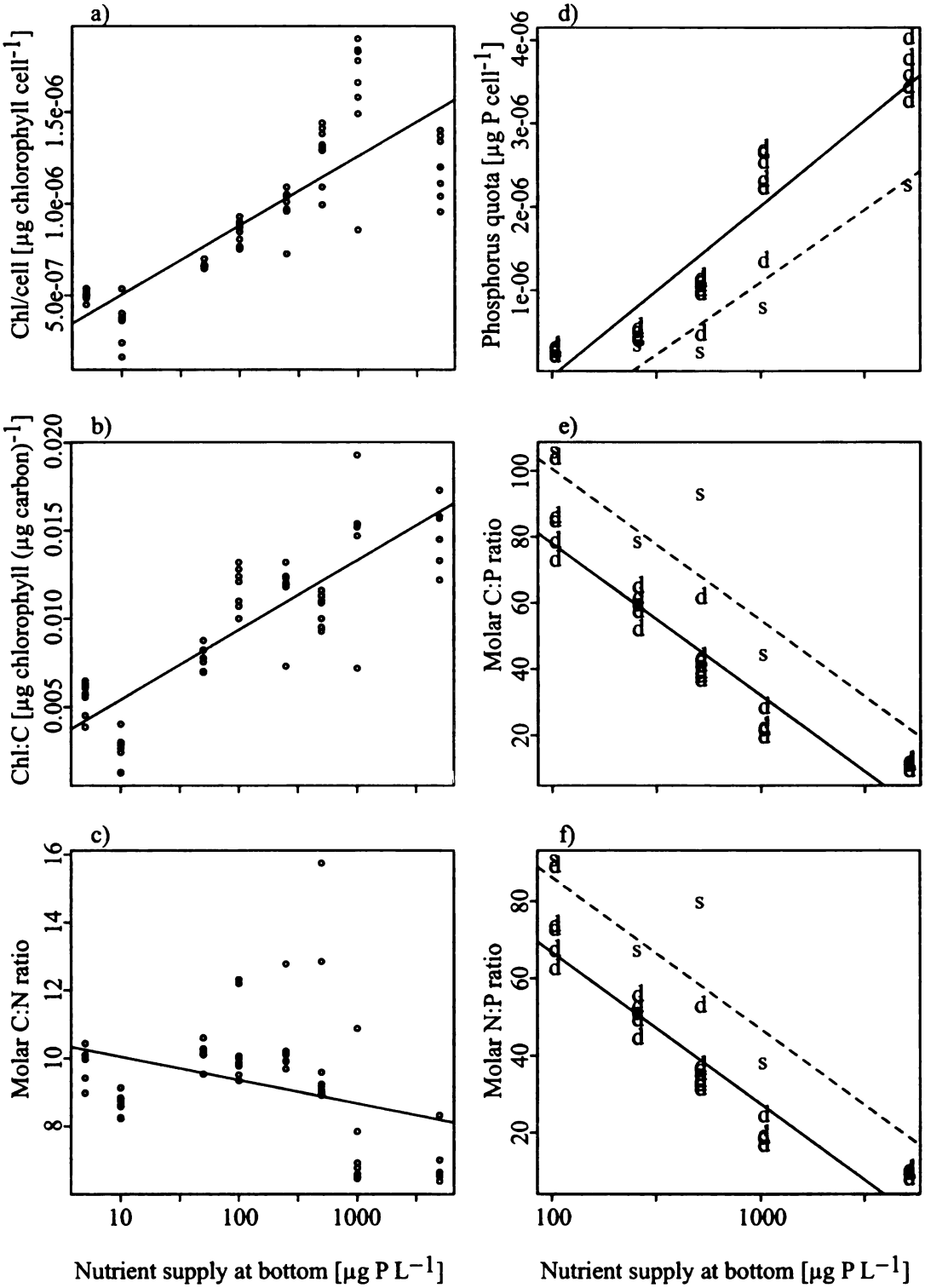

Figure 3.11: Chlorophyll *a*, nutrient, and stoichiometric quantities.

3.6 Discussion

We examined how externally imposed heterogeneity and biological self-organization interact to determine phytoplankton spatial distributions. We explained how the spatial distribution and abundance of a species may be driven by feedbacks between resource gradients, behavioral movement, and population dynamics. We have shown how intraspecific competition can drive the vertical distribution of phytoplankton in poorly mixed environments.

Other studies have shown how particular processes may influence vertical distributions. Carney et al. (1988) convincingly showed with field studies how interspecific resource competition for nutrients and light can structure vertical distributions of phytoplankton. Several studies have used experimental water columns to examine other processes that have been hypothesized to explain the vertical distribution of phytoplankton such as diel vertical migrations (Arvola et al. 1991), sedimentation losses (Pannard et al. 2007), and mixing (Jaeger et al. 2008).

Our goal was to examine if model predictions are supported by our experimental test of how competition determines the vertical distribution of phytoplankton. We focused on qualitative patterns due to uncertainty in several of the model parameters. The first prediction we considered was that algae will form a thin layer (Klausmeier and Litchman 2001). This prediction was supported for the surface layer case, as in high-nutrient treatments, we observed surface aggregations (Figure 3.5). Additionally, algae were aggregated in a thin surface layer in most treatments over the whole duration of the experiment and in low and mid-level nutrient treatments over most of the duration of the experiment. However, the prediction that algae will form a thin layer was not supported for the DCM or benthic layer case.

The second prediction was that the depth of the thin layer should be deeper under low-nutrient conditions and shallower under high-nutrient conditions. Support for this

prediction was mixed (Figure 3.7b), as the equilibrium depths of the biomass maxima were deeper in the low-nutrient treatments than the high-nutrient treatments. The five highest nutrient treatments all had surface biomass maxima, but, in the three lowest nutrient treatments, there was no clear relationship between equilibrium depth of the biomass maximum and nutrient supply.

The third prediction was that over a range of nutrient concentrations, the total biomass should be positively associated with nutrient concentrations at the bottom of the water column. This prediction was supported (Figure 3.7a), as equilibrium total biomass was higher in the higher nutrient treatments. While it may seem obvious that more biomass should grow at higher nutrient levels, in our experimental water columns, nutrient supply and algal biomass can be spatially separated.

The fourth prediction was that a surface layer should occur under high-nutrient supply conditions and be co- or light limited, a benthic layer should occur under low-nutrient supply conditions and be nutrient limited, and a DCM should occur under mid-level nutrient supply conditions and be colimited. This prediction was somewhat supported (Figure 3.6). In the lowest nutrient tower, algae at all depths appear to be primarily limited by nutrients because the points representing resource conditions are at low levels of nutrients while all at relatively high light levels. The algae at all depths in the highest nutrient tower appear to be primarily limited by light because the points representing resource conditions are at low levels of light while all depths were at relatively high-nutrient levels. In Figure 3.4, biomass maxima were near the bottom in the lowest nutrient treatment and at the surface in the highest nutrient treatment so we see some support for our model-driven hypotheses. The towers appear to be arrayed along a nutrient limited to light limited gradient but none are exactly at the point of colimitation which is predicted by ESS theory for a DCM. Perhaps this is the reason we did not observe a strong, persistent DCM in this study.

What limited growth overall? Our experiment may show scale-dependent limi-

tation. At the local level, nutrients were present in measurable concentrations indicating that nutrients were never limiting. However, algae did move down in the lowest nutrient treatments presumably to acquire more nutrients because they were nutrient-limited. At the whole ecosystem level, more nutrients would always cause more growth based on i) within an ecosystem- biomass was still increasing at day 50 in the highest nutrient treatment (Figure 3.4c) and ii) across ecosystems- biomass exhibited a non-saturating relationship with nutrient treatment (Figure 3.7a). Light was limiting at least locally in high-nutrient treatments based on vertical distributions of biomass across towers and light levels below break-even levels toward the bottom (Figure 3.10).

Klausmeier and Litchman (2001) also make other predictions regarding the resource conditions within the water column for a DCM. They predict that nutrients should be at the break-even level, R^*, above the thin layer and linearly increase below it and that light immediately below the thin layer should be at the break-even level I^*. While direct support for this prediction is equivocal because we never observed a well-defined DCM, light was below I^* for the highest nutrient treatment (Figure 3.4c). However, this theoretical I^* value is derived from parameters that have large confidence intervals (e.g. light half saturation constant, K_I) and uncertainty in their estimate (e.g. mortality, m) and assume constant physiology. Mortality was at least the amount of media we withdrew to sample relative to the total volume of media in a tower, however, mortality could be at least the levels commonly assumed in the literature (0.1 d^{-1}) but this is a difficult parameter to measure (Crumpton and Wetzel 1982). In addition, mortality likely changed over the course of the experiment, as the biomass in most of the towers eventually declined. The cause of this mortality is unknown but can be a common phenomenon in experiments (Fogg and Thake 1987).

Some results not related to previous predictions may be unanticipated. In Figure 3.5, the biomass in the surface layer was greater than the background in some towers

but these towers are not all high-nutrient towers as one might expect, nor are they all low-nutrient towers. Furthermore, those towers that had higher biomass in the surface layer than the background reached that transition at different times in the experiment. In the lower nutrient towers (Figure 3.5b-d), the transition to high biomass in the surface layer happened around day four but in higher nutrient towers (Figure 3.5f,g), the transition occurred later, around day 12, and in the highest nutrient tower (Figure 3.5h), the transition did not occur until around day 45.

Interestingly, the proportion of biomass in a distinct surface layer appears positively related to nutrient treatment (Figure 3.8). This could be due to the greater amount of biomass having a stronger effect on the resource environment and therefore creating a sharper fitness gradient. All towers showed a spike in layer thickness early in the experiment before generally thinning (Figure 3.9). It is interesting that layers concentrated before they disappeared in the lower nutrient towers (Figure 3.9a-c), rather than thickening due to the population spreading out because the layer location has depleted resources. Consistently, the thinnest layer occurred in the highest nutrient tower, perhaps because the light gradient was so sharp in that tower that algae were tightly packed in the layer in an attempt to get enough light to persist (Figure 3.9h).

At the beginning of the experiment, we imposed strong vertical heterogeneity. Nevertheless, algae could live and grow at any location in every tower, i.e. this species had a very large fundamental niche. However, through growth, aggregation, and intraspecific competition by depletion of resources, algae reduced the locations where they could grow in each tower, i.e. they created a realized niche confined in space (for example Figure 3.4c). These niche construction processes shape the environment for future generations of the algae in each tower (Laland et al. 1999, Hastings et al. 2007).

Overall, there is mixed agreement between predictions from the full dynamic model

and experimental results (compare Figures 3.1-3.3 with Figures 3.4,3.6,3.7). We focused on qualitative support for predictions and it appears that most of the predictions were upheld. Surface layers formed under predicted nutrient replete conditions and appeared to be relatively more light limited. However, our predictions related to a sub-surface layer formation (DCM or benthic layer) were not all fully supported because we never observed a clearly defined sub-surface layer in any of the treatments.

There are several potential reasons we never observed a well-defined sub-surface layer (i.e. a DCM): 1) Algae could not detect the resource gradients sufficiently to respond. We expect this kind of layer to form at low to mid-level nutrient supply. Under these conditions, algae quickly consume these nutrients and once the surface is no longer the best place in the water column, they move down. However, the nutrient gradient is small and may not be detectable to the algae at this point. The algae are then left to wander on a fitness landscape that is relatively flat. There is some field evidence that the genus we chose for our experiments, *Chlamydomonas*, does not always show distinct vertical distributions even when other genera in the water column do (Spaulding et al. 1994). 2) Because the range of nutrient levels over which we predict a DCM to be the equilibrium strategy is narrow (Figure 3.7b), we may have missed that range in parameter space with our treatments. 3) Algae are actively migrating on a diurnal cycle or at random, as predicted to be a good strategy in opposing resource gradients (Cullen and MacIntyre 1998). 4) Algae are adjusting their light harvesting machinery with depth instead of moving to different light conditions. There definitely is some variation in chlorophyll per cell with depth in the towers (Figure A3a) but for towers where a surface layer was present, the surface did not have a different slope or intercept than the deep points in the relationship with nutrient supply.

The models we employed consider constant stoichiometry. However, the physiological and stoichiometry data indicate differences in cellular pigments and nutrients

between treatments and in some cases, with depth. The chlorophyll *a* per cell was higher in higher nutrient towers (Figure 3.11a), which might be due to greater phosphorus availability if chlorophyll production was nutrient limited in towers but might support the prediction that light competition is very important under high-nutrient conditions so cells are making more chlorophyll. The chlorophyll *a*:carbon ratio mimics this relationship so might also support this prediction (Figure 3.11b). Our values of 0.001-0.019 are within range of Chl:C reported by others in the field and lab (Sharp et al. 1980, Eppley et al. 1988, Fennel and Boss 2003).

The C:N decrease with increasing nutrient supply (Figure 3.11c) is somewhat puzzling given that neither particulate carbon per cell nor particulate nitrogen per cell was related to nutrient supply. However, the relationship is weak ($R^2 = 0.12$) and the C:N may be driven by the higher chlorophyll per cell in higher nutrient towers because chlorophyll is known to have a significant nitrogen component (Sterner and Elser 2002). Cellular phosphorus quota was greater in the deeper portion of the water column than the surface for higher nutrient treatments (Figure 3.11d) which would make sense if cells deeper in the water column are nutrient replete. The C:P and the N:P ratios were greater in the surface and declined with increasing nutrient supply for the high-nutrient treatments (Figure 3.11e,f). Increasing phosphorus supply could decrease these ratios because cells have more phosphorus (Figure 3.11c) and carbon per cell and nitrogen per cell were not related to nutrient treatment.

Our physiological and stoichiometric data shows that chlorophyll per cell varies across nutrient treatments and phosphorus quota varies across nutrient treatments and with depth. This complexity should be incorporated in future models. Models that consider how chlorophyll and biomass with depth may not be perfectly correlated have been developed (Fennel and Boss 2003) but predictions should be explored across large environmental gradients, such as gradients in nutrient loading. Models with variable stoichiometry (Grover 2009, Jaeger et al. 2010) have just scratched the

surface of possible ramifications for spatial distributions and our experimental results indicates that more attention should be given to this area. However, modeling variable stoichiometry in space can be challenging and we will have to rely on increasingly complex model development (Grover 2009).

More experiments should be conducted to test recent theory on stratified water columns and multiple species competition. For example, inclusion of spatially varying mixing can test theoretical predictions of the vertical distribution of phytoplankton in stratified water columns (Mellard et al. Chapter 2). Experiments with multiple species can test theoretical predictions of interspecific competition for nutrients and light in spatially complex environments (Yoshiyama et al. 2009).

Although our experimental water columns are not a perfect replica of a lake or other body of water, our results have implications for field data. We have shown that, at least for surface layers, layer formation can be driven by plentiful nutrient supply with motile algae moving to locations where conditions are best for growth. We have shown this is due to the relative importance of nutrients and light under different nutrient supplies and the influence of the algal population itself, through nutrient uptake and self-shading. These results illustrate the plausibility of a mechanism for surface bloom formation in bodies of water when nutrients are supplied only from below: blooms can occur from nutrients diffusing from the bottom rather than surface runoff or direct addition to the epilimnion. Some of the model predictions were upheld, which may make it more likely that extensions of the model will be useful in future analyses.

On the other hand, our towers may have real limitations as scale models of poorly-mixed water columns and definitely have limited relevance for describing processes in whole aquatic ecosystems (Carpenter 1996). Our towers may not be representative of water columns in lakes for example because of their dimensions. Although we attempted to scale down the physics (depth, light) in the experiment and model using

dimensional analysis, the organisms were not scaled down. This means that even if the 1.5 m towers can represent a 15 m water column, the biology of the organism in the tower is unchanged and so the height of our towers could be too short to represent the resource gradients that span many meters in water columns of lakes. Therefore, just because competition in opposing nutrient and light gradients did not lead to a clearly defined DCM does not mean that these processes cannot drive patterns in real water columns of lakes. Field experiments are needed for further examination of these processes.

In conclusion, the experiment qualitatively supports our conceptual and mathematical models for spatial distributions of phytoplankton. We have shown that phytoplankton exhibit a fast behavioral response to resource gradients. Phytoplankton grow at the depth they have selected, developing strong aggregations, and creating a niche in resource space through impacts on their environment. Phytoplankton may then modify their behavioral strategies as a consequence of these feedbacks and the strategies of the other phytoplankton cells in the water column.

3.7 Appendix

3.7.1 Model

The full model includes spatially-explicit equations for biomass, b, nutrients, R, and light, I in a one-dimensional water column where z is depth with the surface at $z = 0$ and the bottom at $z = z_b$.

Change in biomass at depth z is the balance of growth, death, and passive and active movement.

$$\frac{\partial b}{\partial t} = \min(f_I(I(z,t)), f_R(R(z,t))) - m)b + D\frac{\partial^2 b}{\partial z^2} + \frac{\partial}{\partial z}\left[v\left(\frac{\partial g}{\partial z}\right)b\right] \qquad \text{(A1)}$$

Phytoplankton do not leave or enter the water column, so boundary conditions are:

$$\left[D\frac{\partial b}{\partial z} + v\left(\frac{\partial g}{\partial z}\right)b\right]\Bigg|_{z=0,z_b} = 0 \qquad \text{(A2)}$$

Nutrients R are taken up by phytoplankton with a yield Y of biomass per unit nutrient consumed, are mixed with eddy diffusion coefficient D, and are recycled from dead phytoplankton with proportion ε.

$$\frac{\partial R}{\partial t} = -\frac{b}{Y}\min(f_I(I(z,t)), f_R(R(z,t))) + D\frac{\partial^2 R}{\partial z^2} + \varepsilon m\frac{b}{Y} \qquad \text{(A3)}$$

Nutrients have no surface flux but diffuse into the water column from the sediments where they have fixed concentration R_{in} at a rate proportional to the concentration difference across the interface. The permeability of the interface is described by h.

$$\left.\frac{\partial R}{\partial z}\right|_{z=0} = 0 \quad \text{and} \quad \left.\frac{\partial R}{\partial z}\right|_{z=z_b} = h(R_{in} - R(z_b)) \qquad \text{(A4)}$$

Light follows Lambert-Beer's law, decreasing due to attenuation from biomass and background turbidity (Kirk 1975*a*). The attenuation coefficient due to biomass is a

and due to background is a_{bg}.

$$I(z,t) = I_{\text{in}} e^{-\left(a_{\text{bg}} z + \int_0^z ab(Z,t)dZ\right)} \tag{A5}$$

Functions $f_I(I)$ and $f_R(R)$ are the potential growth rates as a function of the resource I or R when that resource is limiting. We use the Michaelis-Menten form for the functions in our numerical solutions, $f_I(I) = rI/(I + K_I)$ and $f_R(R) = rR/(R + K_R)$ where r is the maximum growth rate and K_I and K_R are half-saturation constants for light and nutrients, respectively. Our qualitative results, however, should hold for other bounded, strictly increasing functions. Biomass is lost at density independent rate m, which encompasses all sources of mortality. Net growth at depth z is only possible if both I is greater than the break even light level, $I^* = f_I^{-1}(m)$ and R is greater than the break even nutrient concentration, $R^* = f_R^{-1}(m)$ (Tilman 1982). A turbulent eddy diffusion coefficient D describes passive movement. Active movement is described by a taxis term (Okubo 1980). Phytoplankton behavior is governed by simple rules. They move up if conditions immediately above are better than immediately below, move down if conditions immediately below are better than immediately above, and do not move if conditions are worse immediately above and below. To describe this behavior, we let phytoplankton movement depend on the gradient in growth rate, $\partial g/\partial z$, with velocity $v\left(\frac{\partial g}{\partial z}\right)$. We assume v to be an odd decreasing function that approaches v_{max} as $\partial g/\partial z$ approaches negative infinity (positive v is upward), approaches $-v_{\text{max}}$ as $\partial g/\partial z$ approaches positive infinity, and $v(0) = 0$. The specific equation we use for v is $v = v_{\text{max}} \cdot \frac{\partial g}{\partial z} / \left(\frac{\partial g}{\partial z} + K_{\text{swim}}\right)$.

Model analysis and parameterization

We simulated the full model with VODE (Brown et al. 1989) following Huisman and Sommeijer (2002). To capture the same spatial resolution that we could measure in the experiment, we set the number of bins to be the same as the number of

sampling ports in the experimental towers ($nz = 60$). In addition, we employed the Monsi-Saeki formulation (Monsi and Saeki 1953) for light limited growth within each bin. We simulated the model over the same time course as the experiment (50 days) with initial conditions approximating the same quantity and vertical distribution of biomass (homogenized) and nutrients (linear gradient) as the initial conditions in the experiment. We assume phosphorus to be the limiting nutrient in the model.

Parameters were measured independent of the experiment or back calculated from the experiment (Table 3.1). The incoming light at the surface, I_{in}, was measured as the photosynthetically active radiation, PAR, just beneath the surface in a tower filled with water before the experiment began. The values for a and a_{bg} were determined by regressions of light on integrated biomass values for all towers and sampling times. Specifically, I_{in} was set to 43 and $\log\left(\frac{I_{\text{in}}}{I_{\text{out}}}\right)$ was regressed on integrated biomass. The slope of this regression is a, the algal attenuation coefficient. The y-intercept divided by z_{b} is a_{bg}, the background light attenuation. The nutrient concentration at the sediments, R_{in}, was the dissolved phosphorus concentration injected at the bottom of the towers. The sediment-water column permeability, h, was calculated from the equations of nutrient flux using the highest nutrient tower and a regression for the portion of the experiment when a surface layer of algae was well-formed. The water column depth, z_{b}, was measured before and during the experiment. Prior to the experiment, the maximum growth rate, r, and the phosphorus half-saturation constant, K_R, was determined for the strain of *Chlamydomonas* used in the experiment by fitting a growth-phosphorus curve to growth rates in different phosphorus treatments (C. Steiner pers. comm.). Prior to the experiment, the light half-saturation constant, K_I, were determined for the strain of *Chlamydomonas* used in the experiment by fitting a growth-irradiance curve to growth rates in different irradiance treatments (A. Schwaderer pers. comm.). The mortality rate, m, was calculated to be the average proportion of total media removed from the experiment in a day (=0.0009 in Table

3.1). The cellular phosphorus quota, q, was calculated from particulate phosphorus measurements at the end of the experiment by averaging this quota value across all towers and sampling depths. The maximum swimming speed, V_{swim}, was taken from Reynolds (1984) and represents an estimate of a theoretical maximum for all species. The swimming speed half-saturation constant, K_{swim}, was set to a value that gave reasonable vertical distributions and smoothly running numerical simulations. The diffusion coefficient, D, was estimated, based on previous tower experiments using a passive tracer, to be the diffusion level required to homogenize the dye over measured time periods.

Table 3.1: Parameter values unless noted otherwise.

Parameter [units]	Value	Range (* = 95% CIs)	Source
$R_{in}[\mu g\ P\ L^{-1}]$	treatment	5-5000	DP injecting at bottom of tower
$h[m^{-1}]$	0.25	$0.19 - 0.30$ *	Experiment
$I_{in}[\mu mol\ photons\ m^{-2}s^{-1}]$	43	37-43	Experiment
$a_{bg}[m^{-1}]$	0.476	$0 - 0.96$ *	Experiment
$z_b[m]$	1.5	$1.45 - 1.5$	Experiment
$D[m^2d^{-1}]$	1	$1 - 10$	Dye experiment
$r[d^{-1}]$	1.7	$1.55 - 1.80$ *	Physiological experiments (1)
$m[d^{-1}]$	0.1	$0.0009 - 0.1$	Experiment withdrawal and literature
$K_R[\mu g\ P\ L^{-1}]$	1.4	$0.68 - 2.10$ *	Physiological experiments (1)
$K_I[\mu mol\ photons\ m^{-2}s^{-1}]$	85	$3.35 - 168$ *	Physiological experiments (2)
$Y[cells\ mL^{-1}\left[\mu g\ P\ L^{-1}\right]^{-1}]$	8.93×10^{-4}	$1.16 \times 10^{-5} - 7.19 \times 10^{-4}$ *	Experiment
$a[m^{-1}\left[cells\ mL^{-1}\right]^{-1}]$	2.84×10^{-5}	$2.13 - 3.54 \times 10^{-5}$ *	Experiment
$K_{swim}[m\ d^{-1}]$	3		Experiment estimate
$v_{max}[m\ d^{-1}]$	10	$10 - 100$	Literature (3)

Sources.- (1) C. Steiner pers. comm. (2) A. Schwaderer pers. comm. (3) Reynolds 1984.

3.7.2 Appendix figures

Figure 3.12. Biomass profiles for all towers at two time points: day 1 and day 50. Each profile has the best fit function using information criteria. Note that for the three lowest nutrient supply towers (a, b, c) on day 50 the best function was the line function. However, for all other towers on day 50, the exponential function was the best function, indicating the presence of a surface layer. On day 1, the exponential function was the best for all towers.

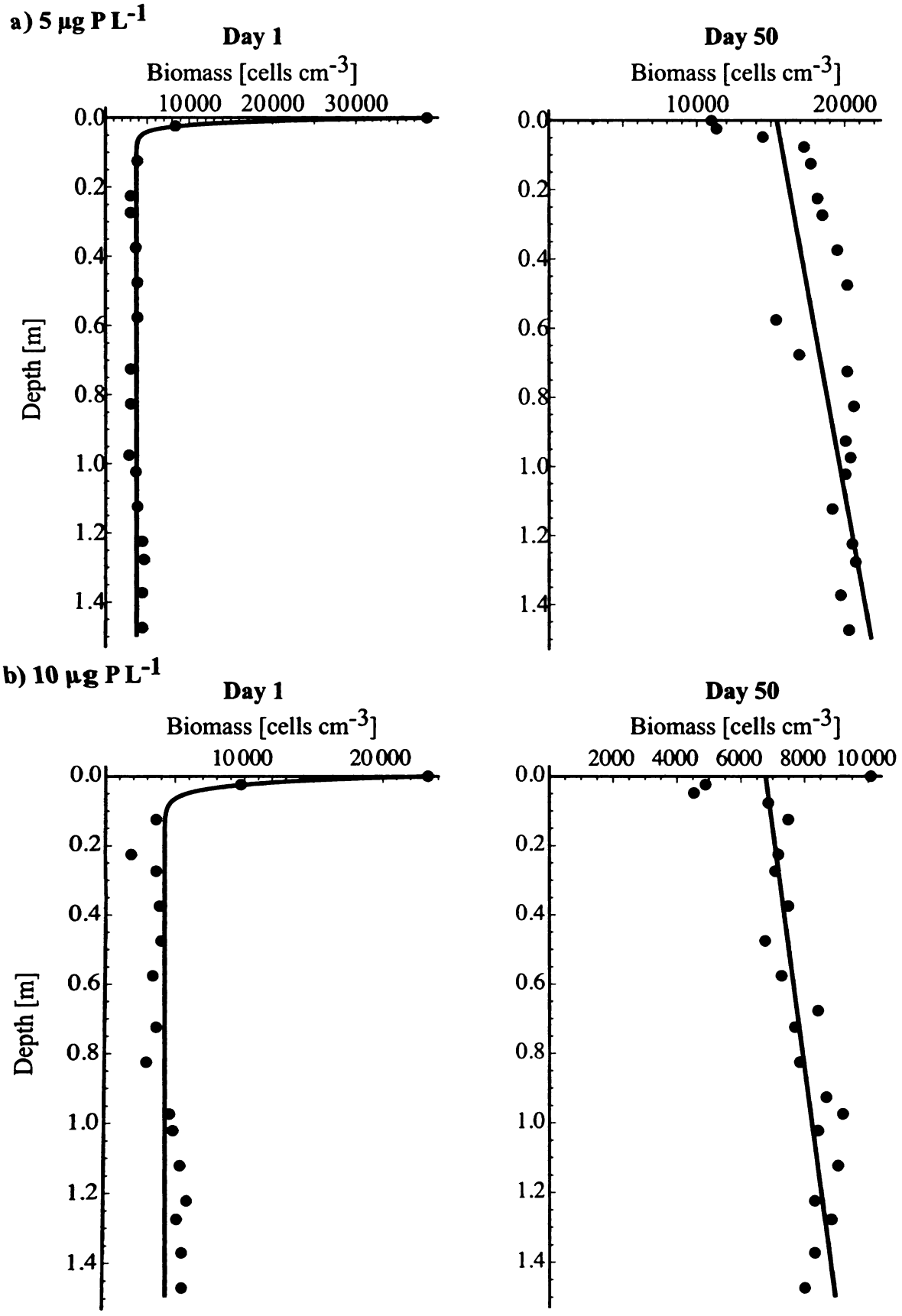

Figure 3.12: Biomass profiles for all towers at two time points: day 1 and day 50.

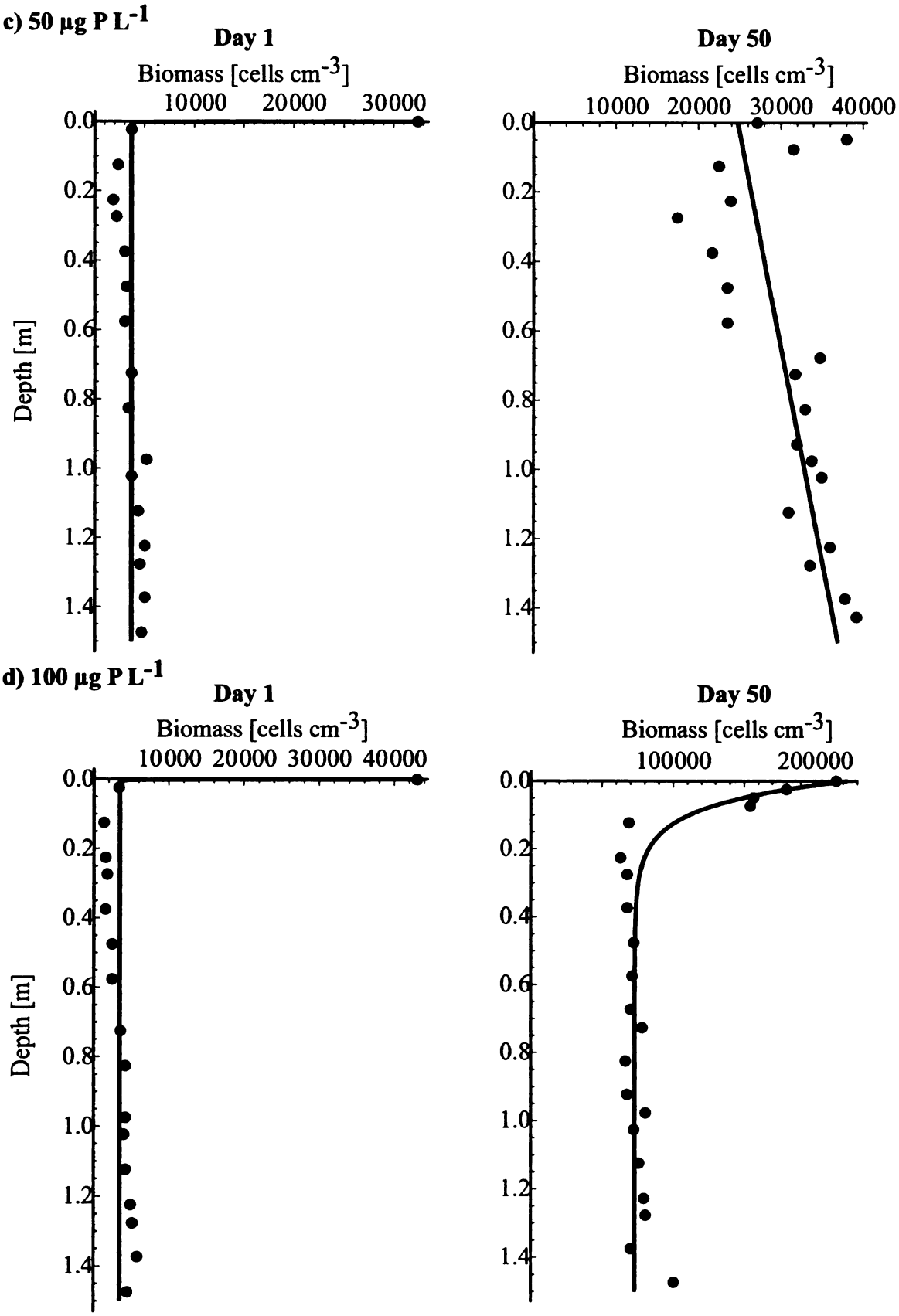

Figure 3.12 continued

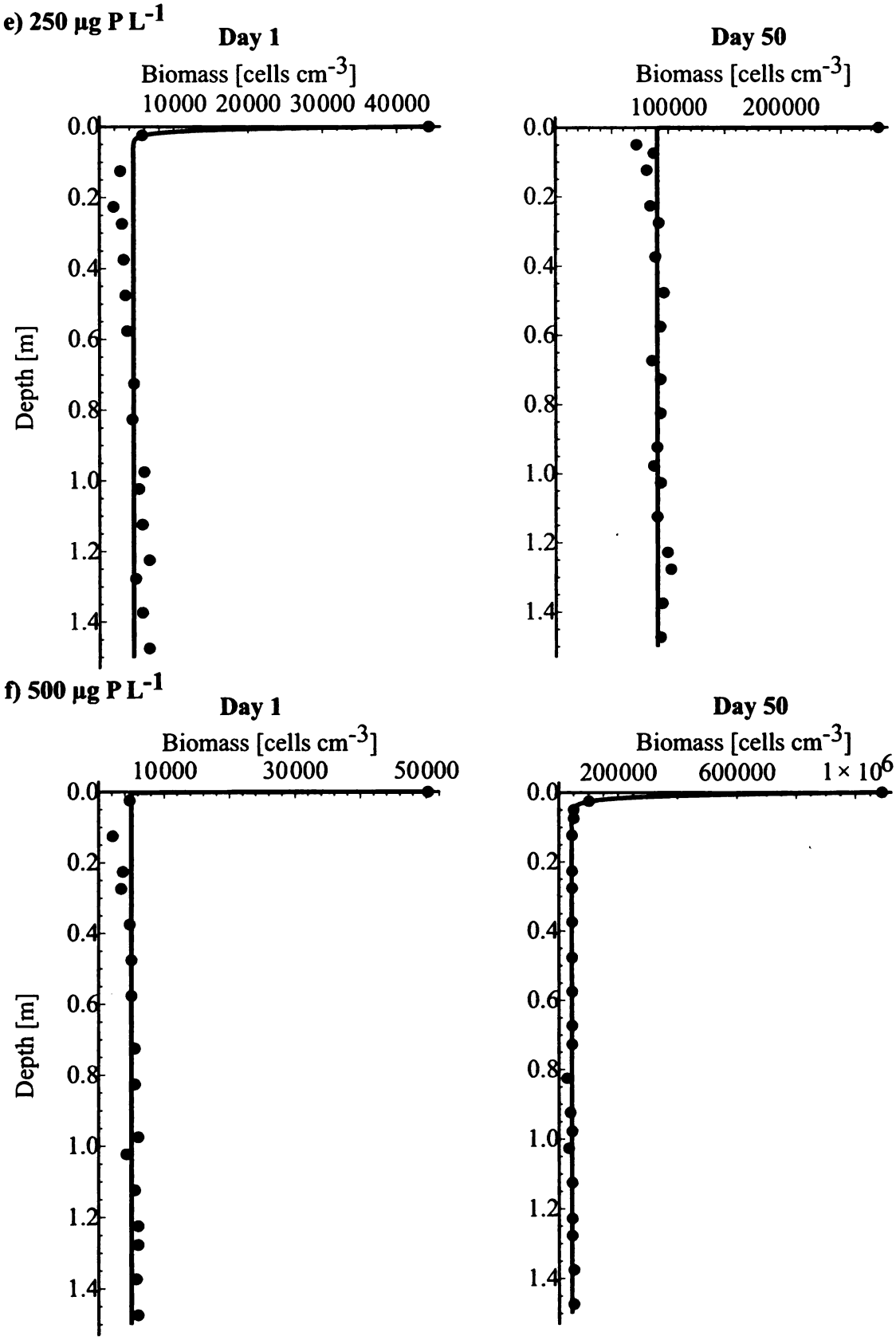

Figure 3.12 continued

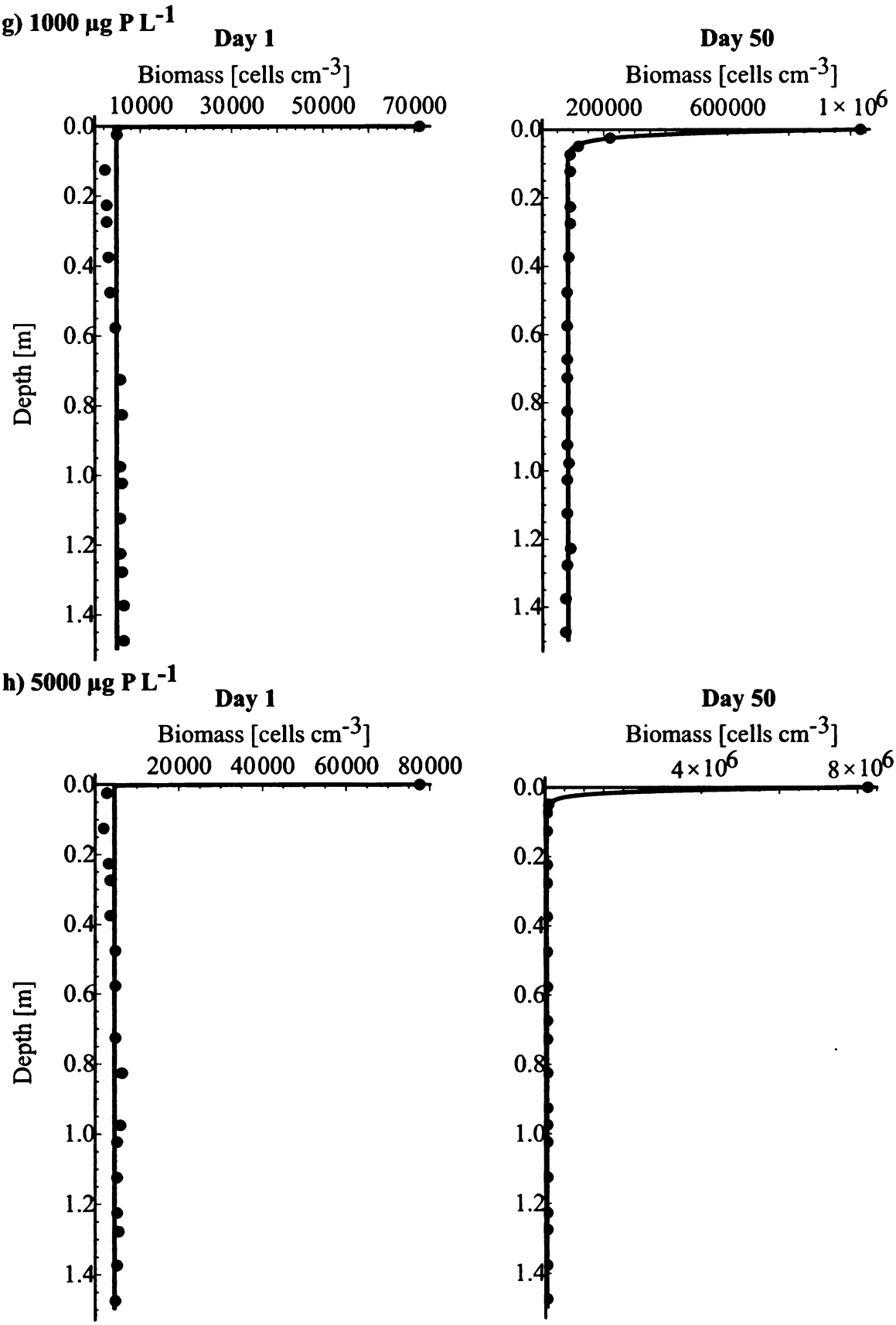

Figure 3.12 continued

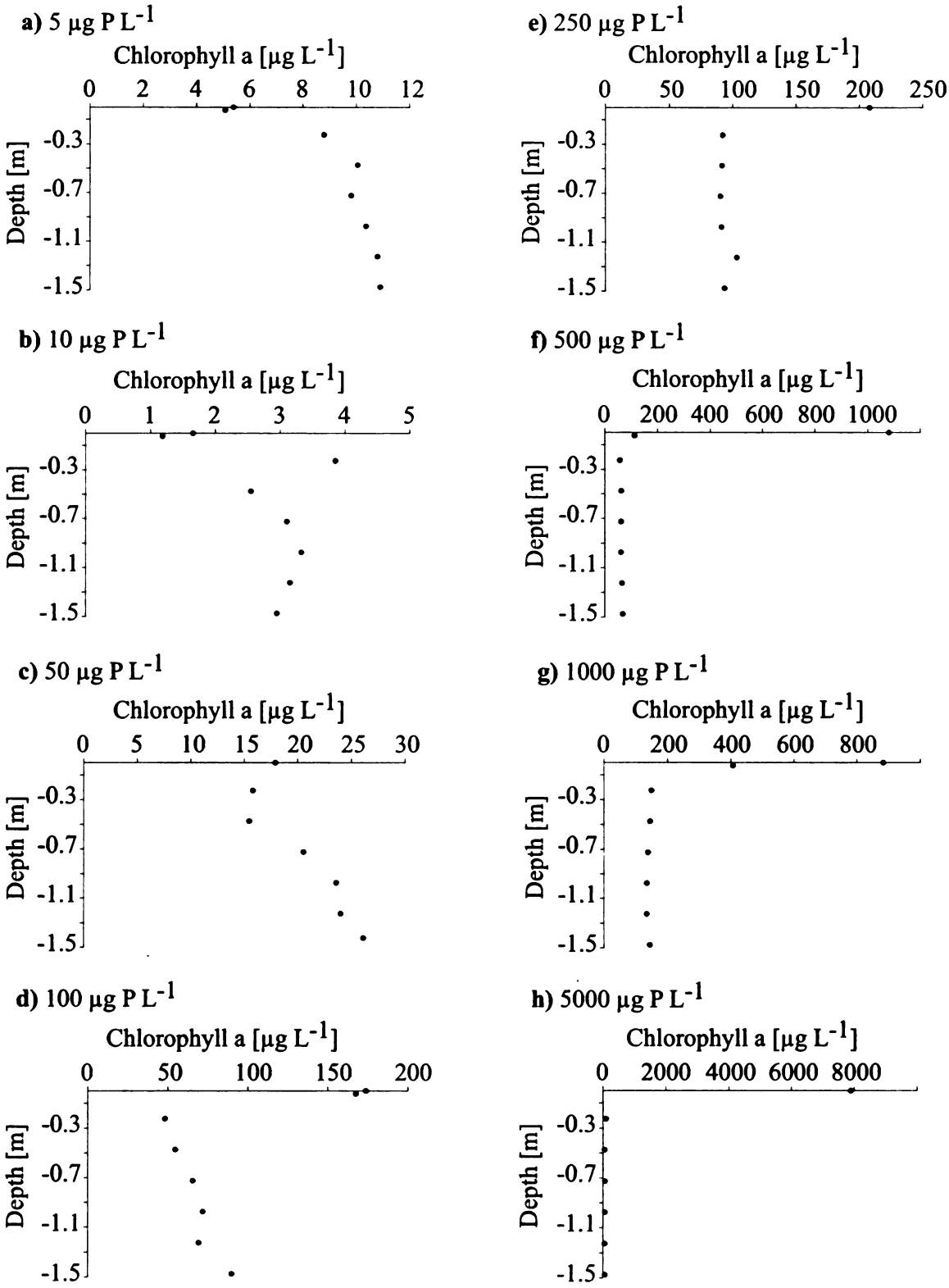

Figure 3.13: Profiles of chlorophyll *a* at the end of the experiment for all towers.

Figure 3.14: Picture 1: Picture of experimental plankton towers.

Chapter 4

Community-wide phytoplankton vertical distribution in stratified temperate lakes

Jarad P. Mellard

with

Mary A. Evans, Don R. Schoolmaster Jr., Kohei Yoshiyama, Elena Litchman, and Christopher A. Klausmeier

4.1 Abstract

Understanding spatial heterogeneity in ecological communities is a perennial task for ecologists. Spatial patterns for some aquatic organisms are poorly known and the factors that determine them even less known. In particular, a plethora of phytoplankton spatial distributions in the vertical dimension occur in nature. Both phytoplankton total abundnce and community composition show patterns in the vertical dimension. What drives patterns in vertical distributions of phytoplankton? The goals of our

study were first, to examine variation in phytoplankton community structure in lakes, in particular phytoplankton vertical distributions, and second, to evaluate recent theoretical predictions across broad environmental gradients. Theoretical predictions come from several models that predict the depth where algae should aggregate, what limits their growth, amount of biomass in different locations of the water column, and conditions for coexistence of multiple species within a lake. To test these predictions and document variation in community structure with depth and across lakes, we conducted a survey of 30 lakes in western Michigan (USA) throughout the stratified season. Lake survey results showed that for lakes with single sub-surface phytoplankton biomass peaks, the vertical position of the peak was shallower at greater background light attenuation and turbulent mixing but deeper in deeper water columns, as predicted by theory. Biomass in the deep layer increased with total phosphorus near the bottom and biomass in the mixed layer increased with total phosphorus in the mixed layer, as predicted by theory. Vertical distributions of phytoplankton were typically composed of multiple peaks of biomass. The number of peaks was related to the amount of physical space available for peaks to form and the sharpness of the nutrient and light gradients. Each peak in a lake exists at different nutrient and light levels, which are negatively related to one another. Species compositions of phytoplankton communities were structured in space, not only across broad environmental gradients between lakes but also structured along the vertical axis within lakes. Communities were more similar within than between lakes. Community similarity within lakes likely arises due to different resources acting in opposition: light attenuation acts to make communities more similar but the sharpness of the nutrient gradient acts to make communities more dissimilar. Vertical niches could be filled by many different taxonomic groups and species and was not consistent across lakes. Taxonomic groups were related to environmental variables across lakes but some showed additional relationships with local resource conditions within lakes that makes predicting community

structure across lakes and with depth challenging. Species dominance changed along the vertical dimension as well, particularly in deeper lakes. This study quantitatively describes a variety of vertical distributions of phytoplankton communities occurring across environmental gradients, characterizes them and their environments, and explicitly links the patterns to underlying mechanisms such as competition for multiple resources, grazing, and physical mixing processes.

4.2 Introduction

Ecological communities exhibit pronounced spatial patterns. Populations are distributed variably in space, often relative to underlying spatial heterogeneity in resources. The boundaries of a population in space and the abundance patterns within those boundaries, may be set by tolerances to stressors and requirements for resources (MacArthur 1972) as well as self-modification of the environment (Levins 1979). Species with different tolerances and requirements may competitively sort themselves in space along these resource gradients as well as modify the environment for others. Species sorting can create community-level patterns with resulting composition and diversity impacted by the spatial heterogeneity in resources (Levin 1976, Stevens and Carson 2002).

Planktonic communities are responsible for much of the world's primary production and influence major biogeochemical cycles, ecosystem function, and fisheries (Falkowski et al. 1998). Plankton live in a fluid environment, subject to water motion. Biological, chemical, and physical processes operating in bodies of water create spatial heterogeneity (Reynolds 1984). Spatial heterogeneity adds to the problem of understanding already complex ecological systems (Skellam 1951, MacArthur 1972, Steele 1974, Levin 1994). In the aquatic environment, vertical spatial heterogeneity comes in many forms, including: patchiness of populations (biological), turbulent mixing gradients and light (physical), and nutrient gradients (chemical).

Phytoplankton vertical distributions can be extremely patchy. Fee (1976) showed that primary production can vary at least three fold within a couple meters span in the water column. Assuming primary production is proportional to chlorophyll *a*, primary production within several meters in the water column may vary more than 25-fold in some lakes. Field et al. (1998) show that such a difference in primary production is roughly equivalent to the difference between a desert and a tropical

rainforest!

Phytoplankton exhibit contrasting vertical distributions both between bodies of water and through time within a body of water. They can be in high abundance in the mixed layer or in pronounced surface blooms (Paerl 1988). Frequently phytoplankton form a peak in abundance called a deep chlorophyll maximum, DCM, in the deep poorly-mixed layer (Fee 1976). A DCM may be the global maximum of chlorophyll *a*, or a local maximum, and it may have a single well-defined narrow peak, or a broad hump (Camacho 2006). Part of the intrigue of DCMs is that they are found far from the surface, away from the source of light and yet can be responsible for much of the primary production within a lake (Fee 1976). If enough light reaches the bottom, algae can also reach high abundances in a benthic layer, accessing nutrients entering the water column from the sediments (Sand-Jensen and Borum 1991).

Vertical physical and chemical gradients further structure the environment of the phytoplankton. Fluid mixing and turbulence in lakes are effects of multiple interacting physical processes (wind shear, convective cooling, internal waves, seiches, Langmuir circulation, inflow, etc. (Wetzel 1975). Often, the result of these processes is temperature-driven density stratification, which can be characterized by the following variables: turbulent (vertical) eddy diffusivity, D, and depth of the mixed layer, z_{m}. These variables are the exact parameters in many models (Chapter 2, Huisman and Weissing 1994, Klausmeier and Litchman 2001, Diehl et al. 2002, Huisman et al. 2004) and can be used to summarize the physical conditions in lakes. Essential resources such as nutrients and light are distributed heterogeneously and usually form opposing gradients, creating a dilemma for algae. Nutrients generally enter the water column from the sediments but may also be supplied through horizontal advective sources such as surface runoff or riverine inputs. Nutrient concentrations (Tilman 1982, Watson et al. 1997) and nutrient ratios (Smith 1982, Tilman 1982), as well as nutrient-to-light ratios (Smith 1986, Carney et al. 1988, Reynolds 1998), have been

shown to be important in determining phytoplankton community structure. Light is attenuated exponentially with depth due to abiotic and biotic absorbance and scattering according to Lambert-Beer's law (Kirk 1975*b*).

These complex biological and environmental gradients create a challenge for ecologists. For example, in this spatially complex environment, multiple resources interact with behavioral movement of the algae, modification of the environment due to nutrient uptake and self-shading, and strategic adjustment due to the modified environment to determine vertical patchiness of populations that drives spatial heterogeneity. Fee (1976) showed that there is often a significant phytoplankton population in a single peak at or below the thermocline that can have important consequences for the ecosystem processes operating throughout the water column, and called for systematic investigations of the algal populations below the thermoclines in other lakes.

Vertical distributions of populations compose the community structure of the water column. Populations interact with each other through many of the same mechanisms that individuals interact, and through interspecific competition, to determine community-wide patterns in phytoplankton vertical distribution. The result of these processes is spatial heterogeneity within the community, which may explain the coexistence of many species of phytoplankton (Hutchinson 1961). Recently, Longhi and Beisner (2009) looked at how various environmental factors affect vertical distribution of phytoplankton across lakes and regions. They found the global chlorophyll maximum to occur shallower in lakes with greater temperature variability, higher total phosphorus in the mixed layer, and increasing light attenuation by dissolved organic matter, (i.e., "color"). They also show that groups of phytoplankton with different pigment compositions are distributed differently in the water column both by their mean depth and their variation in depth. Perhaps the best evidence for community spatial variation due to resource competition comes from Lake Tahoe. Through the use of field patterns, transplant experiments, and measurements of demographic pro-

cesses and kinetics, Carney et al. (1988) convincingly showed that two species of diatoms partitioned habitat in the vertical dimension. In addition, a more recent study has shown that, in limnocorrals, low levels of mixing in combination with deep water columns allowed for vertical niche separation of different taxonomic groups of algae (Jaeger et al. 2008).

Although these studies aid in our understanding of patterns of phytoplankton vertical and community structure across environments, we contend that there is still a lack of knowledge of how communities respond to, use, and divide the vertical dimension. Explicit tests of predictions from prior theory and measurements of parameters for models of vertical distributions of phytoplankton are still missing. Also missing are quantitative classifications of vertical distributions, along with fine scale measures of turbulence, nutrients, and light. Detailed community analyses of species composition and diversity along the vertical dimension among diverse bodies of water are necessary to test theoretical predictions. This study aims to remedy some of these deficiencies in understanding determinants of vertical distributions of phytoplankton. Anthropogenic stresses and predictions of widespread aquatic community reorganization due to climate change (Schindler 1997) make it vital to measure and understand the ecosystem- and community-level processes operating in bodies of water.

4.2.1 Predictions from previous theory:

I. Ecosystem (bulk properties of the community)

We have extended dynamic models of phytoplankton growing in well-mixed environments (Huisman and Weissing 1994) and poorly mixed environments with opposing resource gradients (Klausmeier and Litchman 2001) to include spatially-varying mixing conditions and multiple nutrient sources (Chapter 2). Our model predicts the equilibrium spatial distribution of the phytoplankton as well as what limits their growth. Eight distinct cases of phytoplankton vertical structure are possible. Popu-

lations here are considered to represent the bulk properties of the community. Our model also predicts how the vertical distribution and biomass in different layers change as a function of environmental parameters (Chapter 2).

Our analytical results provide specific predictions for how different environmental parameters affect vertical distribution and biomass. See Chapter 2 for a table, further details, and methods used to generate these predictions. Increasing nutrient concentration in the sediments, R_{sed}, should decrease the depth of the population and increase deep layer biomass while increasing or having no effect on mixed layer biomass. Increasing nutrient input to the mixed layer, R_{inML}, should decrease or have no effect on the depth of the population and decrease or have no effect on deep layer biomass while increasing or having no effect on mixed layer biomass. Increasing background light attenuation, a_{bg}, should decrease the depth of the population and decrease or have no effect on deep layer and mixed layer biomass. Increasing mixed layer depth, z_{m}, should have no effect on the depth of the population in the deep layer and increase, decrease, or have no effect on the deep layer and mixed layer biomass. Increasing water column depth, z_{b}, should increase the depth of the population and decrease the deep layer biomass while decreasing or having no effect on mixed layer biomass. Increasing turbulent diffusion, D, should decrease the depth of the population and increase deep layer biomass while increasing or having no effect on mixed layer biomass.

II. Community (biological variation)

Several models predict that species should segregate vertically according to nutrient and light competitive abilities (Klausmeier 2000, Huisman et al. 2006, Yoshiyama et al. 2009). Klausmeier (2000) predicts that for multiple species competition, the better light competitor should reside under the better nutrient competitor in accordance with resource ratio theory (Tilman 1982). Huisman et al. (2006) predict a similar vertical zonation and show that vertical zonation patterns in the subtropi-

cal Pacific Ocean may be consistent with that prediction. Yoshiyama et al. (2009) extend this previous work to analysis of multiple species competition in stratified water columns and show that DCMs should attract one another in space due to the feedbacks the DCMs have on resource conditions. Yoshiyama et al. (2009) also show that the vertical zonation prediction from previous studies is complicated by environmental conditions. For example, a good light competitor can reside under a good nutrient competitor or it can take over the mixed layer, but these two competitive outcomes can be disjunct along an environmental axis such that the good light competitor is absent from the system for some area in environmental parameter space. This complication, along with areas in parameter space with multiple stable states, makes simple predictions difficult.

We conducted a lake survey to describe and better understand patterns in the vertical distribution of phytoplankton. The goals were to determine the variation in vertical distributions, characterize the distributions, and test model predictions about the determinants of vertical distributions across broad environmental gradients. In addition, we aimed to measure the biological variation in the communities of phytoplankton distributed along the vertical dimension within lakes and across environmental gradients between lakes. This biological variation comes in many forms including community species diversity and composition, as well as broad taxonomic groupings. We expect whole-lake and local environmental conditions to determine the taxonomic turnover and resulting phytoplankton community structure for lakes in the surveyed region.

Among the five questions we consider in the present study, questions 2) and 3) have specific predictions from prior theory (Chapter 2) associated with them on how environmental variables affect phytoplankton vertical structure. Questions 4) and 5) do not have specific predictions from prior theory associated with them, but for those questions, we provide hypotheses that are constructed from theories of multiple

species competing for nutrients and light (Klausmeier 2000, Huisman et al. 2006, Yoshiyama et al. 2009 and other general ecological studies.

The questions are the following:

1) What variation exists in vertical distributions of phytoplankton?

2) What drives this variation?

   In a particular lake, A) Can a peak form in the deep layer? B) If a peak can form in the deep layer, can a benthic layer form? C) What drives depth of peaks?

3) What determines the amount of phytoplankton biomass?

4) Why do multiple peaks of phytoplankton biomass form and what determines the number of peaks that form?

   A) How can multiple peaks exist? H1: Multiple nutrient sources (Chapter 2). Sources such as riverine inputs of different densities, lateral intrusions, and inputs from shear and other physical processes. H2: Multiple species with nutrient-light tradeoff (Yoshiyama et al. 2009). Each peak is composed of a different species from a tradeoff in competitive abilities for nutrients and light.

   B) Is the number of peaks related to resource quantity and/or resource heterogeneity? H: Resource supply must be of sufficient quantity to sustain multiple peaks but resource heterogeneity (Stevens and Carson 2002) increases number of peaks.

5) How do phytoplankton communities change with depth and what drives these changes?

   A) Is species diversity greater in the surface mixed layer niche or DCM niche and what explains diversity in these locations? H: The mixed layer provides greater

opportunities for coexistence (Huisman and Weissing 1995) because it has a wider range of resource conditions than a DCM that exists at a single depth and mixing may prevent competitive exclusion (Flöder and Sommer 1999).

B) Are communities more different within a lake or between lakes and what explains differences in communities within lakes? H: Communities are more different between lakes due to the large differences in environmental conditions between lakes and the mixing that occurs within a lake but there are likely differences in communities within lakes that are driven by habitat differentiation in local conditions.

C) Do taxonomic groups or species found in the DCM differ from taxonomic groups or species found in the mixed layer and why might they be different? H: Some taxonomic groups are known for their associations with certain vertical niches such as DCMs due to specific environmental conditions within those niches but this could depend on whole-lake environmental characteristics (Reynolds 1984).

4.3 Survey methods

4.3.1 Sampling in field

We conducted a lake survey of 30 lakes in western Michigan, sampling the lakes three to five times in four distinct sampling campaigns during the stratified season from May to October in 2007. We selected these lakes based on their similar geochemistry but wide range of mixing depths, light attenuation, and total phosphorus levels. At the deepest point in each lake, we obtained high spatial resolution (mm scale) measurements of chlorophyll *a* fluorescence and physical conditions and collected water samples at different locations throughout the water column in order to capture

chemical gradients.

We used casts from a microprofiling device (SCAMP, PME Carlsbad, CA) to measure a continuous high resolution temperature gradient, $T(z)$, which we converted to a temperature gradient spectrum so that we could obtain the turbulent kinetic energy dissipation rate by fitting a Batchelor spectrum (Luketina and Imberger 2001). We then calculated the vertical eddy diffusion coefficient, $D(z)$ from energy dissipation rate following Osborn (1980). Each cast also measured density, chlorophyll *a* fluorescence, photosynthetically active radiation (PAR) with an attached LI-COR flat sensor (LI-COR Biosciences, Lincoln, NE), and conductivity with depth. Three to six casts were obtained per visit to a lake. These casts comprise what we will refer to as a profile for a visit to a lake. We also took measurements of pH and oxygen at 1 m intervals using a Hydrolab sonde (Loveland, CO). Integrated water samples were collected with a tube sampler through the mixed layer and discrete depth water samples were collected from pronounced fluorescence peaks (DCMs), 1 m above and below each DCM, and 0.5 m above the sediments with a 10 cm diameter horizontal van Dorn sampler. All water samples were immediately placed in a dark bottle and taken to the lab for processing. We also took a vertical zooplankton net haul throughout the water column during each lake sampling using a 0.3 m diameter, 80-micron mesh net.

4.3.2 Laboratory measurements

All phytoplankton and chemical analyses were performed on the water samples from the mixed layer and DCMs. Only chemical analyses were performed on the water samples from distances above and below the DCMs and the samples 0.5 m above the sediments.

Chemical analyses

Total phosphorus was measured by using persulfate digestion and then analyzing

colorimetrically on a Shimadzu spectrophotometer UV-240PC (Shimadzu Scientific Instruments, Columbia, MD) at 880 nm. Samples for dissolved phosphorus and nitrogen were filtered through acid washed GF/F filters. Dissolved phosphorus (soluble reactive phosphorus, SRP) was measured using the orthophosphate method on Lachat Instruments Quick Chem 8500 (Lachat Instruments a Hach Co Brand, Loveland, CO). Total nitrogen was measured after persulfate digestion (Bachmann and Canfield 1996). Total nitrogen and dissolved nitrogen (nitrate) were measured by second-derivative spectroscopy (Crumpton et al. 1992).

Phytoplankton analyses

Chlorophyll *a* was measured by filtering onto a 25 mm Whatman GF/B filter, which was extracted with 95 percent ethanol and measured fluorometrically (Welschmeyer 1994). Chlorophyll *a* as measured in the lab was strongly correlated with fluorescence measured in the field (Figure 4.1).

Samples for phytoplankton identification were poured into graduated cylinders, preserved immediately using Lugols iodine, and allowed to settle for several days. These condensed samples were used for identifying and enumerating species in Palmer counting cells and settling chambers under compound and inverted microscopes, respectively. Only data from a single sampling campaign, the September campaign, were analyzed for community composition and diversity.

We counted individuals in random microscope fields until at least 400 individuals were counted but a minimum of four fields when counting at 400X. The diameters of chambers were also scanned for rare species and any species for which less than three individuals were found before was recorded. Individuals were identified to species and morphotype if possible but many could only be positively identified to genus while some were only identified to class and a few were identified just as a morphological description. We distinguished morphotypes based on whether individuals were a colony (or part of a colony) and colony size. We will use the term species throughout

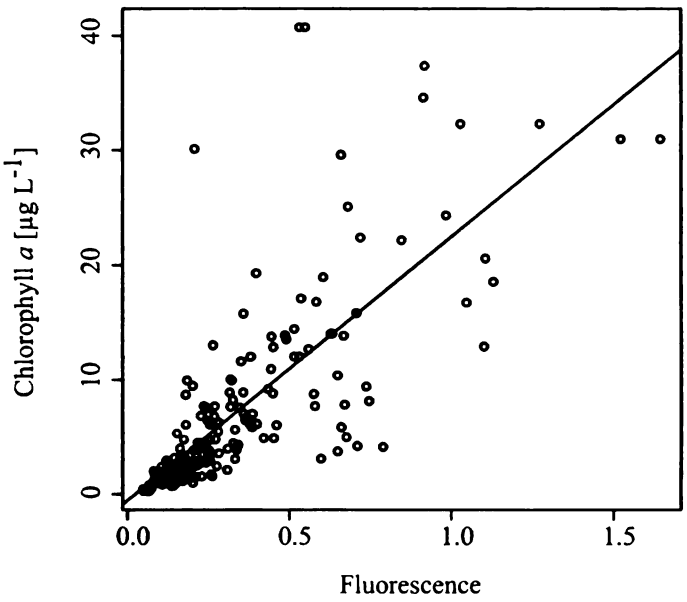

Figure 4.1: Relationship between chlorophyll a as measured in the laboratory with standard protocols using ethanol extraction and on a laboratory fluorometer and fluorescence as measured in the field using SCAMP built-in fluorometer for all lakes, times, and samples (including mixed layer and discrete depths). Regression equation: chlorophyll $a = 23\times$ fluorescence -0.55, P<0.001, $R^2_{\text{adj.}} = 0.58$.

to describe the highest level of classification used for each individual counted. In most cases, this classification represents a true species but in some cases it may just be a distinct morphotype. Phytoplankton densities are reported as individuals per mL, where individuals is generally number of single cells, number of cells in colonies for countable cells, number of colonies for very small celled colonies, and number of filaments for filamentous algae (see Appendix Table for what was considered an individual for different species). We also measured length and width of 10 individuals in each lake of the top two to five most abundant species.

Zooplankton analyses

Zooplankton samples were condensed and preserved with 95% ethanol. Later they were identified to genus and enumerated under a dissecting scope using a counting wheel to count approximately at least 200 individuals. Zooplankton densities were

calculated based on volume sampled in lakes. Densities were divided into three grazer categories for analysis: *Daphnia*, other major zooplankton grazers (calanoid copepods, *Bosmina, Diaphanisoma*, and *Ceriodaphnia*), and other zooplankton (Demott 1982, Sarnelle 2005).

4.3.3 Survey analysis

Ecosystem-level

To find peaks in chlorophyll *a* fluorescence, each cast was smoothed with a Savitzky-Golay smoothing filter (Savitzky and Golay 1964). Savitzky-Golay smoothing filters can do a better job of preserving peaks in data than other moving window smoothing techniques because they approximate the underlying function within a window by a higher order polynomial, rather than a constant (Press et al. 2001). We used a window size of 50 data points, which corresponds to a 0.8 m window.

We found the following criteria to identify significant peaks in chlorophyll *a* fluorescence and match the depths we sampled in the field. The first derivative of the smoothed profile was used to locate local maxima and minima and the second derivative was used to confirm the maxima. For a maximum to be called a peak, two other criteria must be met: 1) in the region around a maximum bounded by a minimum on each side, there must be a difference in the values of the first derivative of > 0.1, and 2) in the region around a maximum bounded by $\pm$ 1/2 window size, the standard deviation in raw fluorescence values divided by the total standard deviation in raw fluorescence values for the entire water column must be > 0.1. We also checked to see if there was a benthic layer. In order for a benthic layer layer to be present, the following criteria must be met: the first derivative of the smoothed profile has to be increasing at the bottom and that rate of increase divided by the maximum rate of increase for the whole profile had to be > 0.2. We used our multiple casts we gathered during a visit to a lake as replicates to confirm the existence of a peak; that

is, there must have been peaks within 0.35 m of one another in at least two casts. Those peak depths were then averaged across casts. We considered only peaks that occurred below the mixed layer.

Environmental variables were calculated in the following ways. Water column depth, z_b, was estimated in the field based on sonar readings and raw SCAMP casts. Mixed layer depth, z_m, was calculated as the uppermost depth where dT/dz exceeded 1 degree C/m and then was averaged across casts of a lake during a visit. Background light attenuation, a_{bg}, was calculated as total light attenuation minus chlorophyll concentration (lab measurement) multiplied by a chlorophyll attenuation coefficient of 0.01094 $m^2\ mg^{-1}$ (Kirk 1975*b*). Turbulent diffusion coefficient, D, was the average log turbulent diffusion coefficient throughout the water column averaged across all casts of a lake on the sampling date.

We $\log_{10}$ transformed all environmental variables as is commonly done when variables span several orders of magnitude. The environmental variables background light attenuation, water column depth, total phosphorus in the mixed layer, mixed layer depth, total phosphorus at the bottom, and turbulent diffusion coefficient were checked for multicollinearity by regressing each environmental variable on all the other environmental variables. Tolerance (the reciprocal of tolerance is variance inflation factor) is calculated as 1-R^2 and we used the common cut off criterion (Walker and Maddan 2005) of any tolerance less than 0.25 to indicate multicollinearity. All of the main environmental variables were within the tolerance limits.

For the statistical model of number of peaks, we used a different set of variables: deep layer span calculated as $z_b - z_m$, total phosphorus gradient in the deep layer calculated as the absolute value of (total phosphorus at the bottom−total phosphorus in the mixed layer)/ $(z_b - z_m)$, light gradient in the deep layer calculated as (light at z_m−light at z_b)/ $(z_b - z_m)$, total phosphorus at the bottom, light at z_m, and background attenuation. Total phosphorus at the bottom and total phosphorus gradient

in the deep layer are highly correlated, resulting in too low of a tolerance value to be included in the same model together, as are light at z_m and light gradient in the deep layer. Therefore, these variables were run in separate models.

Since each lake was sampled one to four times throughout the stratified season, we added the covariate day-of-year into the models as a check for temporal effects to determine whether sampling date should be explicitly modeled. Day-of-year was not significant in any of the models presented. We also checked for temporal effects with autocorrelation tests, autoregressive models, and residuals of variables at $t + 1$ vs t, but no significant effects of time were detected (although there are only a few points in time). Concluding that the environmental variables should absorb any temporal effects, we pooled the data across the season. This is consistent with Wisconsin studies that found only a small proportion of lakes sampled on one-five week intervals showing autocorrelation and little effects of that autocorrelation in the statistical results (Carpenter et al. 1989, Stow et al. 1998). Our discrete sampling campaigns were separated by > 1 month intervals, which happens to coincide with the scale of the greatest variation in primary production (Carpenter and Kitchell 1987).

We employed a multiple regression analysis, which included all environmental variables for which we have theoretical predictions, as well as day-of-year in the model to examine determinants of phytoplankton vertical distribution, biomass, and number of peaks. We used the best model to indicate what environmental variables had a significant impact on the biotic variable of interest. We found the best model using two separate methods. 1) We put all variables into the model and then removed all variables with P values > 0.05 and checked that the reduced model had a significantly lower AIC than the full model. 2) We ran a backwards step-wise regression with all variables included and used AIC values to reduce the model. In case of disagreement between these methods (two cases of disagreement), we chose the model with the lowest AIC to represent the best model (Burnham and Anderson 2002). Variables

from the best models are reported in the tables and figures. If a relationship appeared quadratic, it was also checked for significant nonlinear terms but none were found.

Community-level

Shannon-Weiner (Weaver and Shannon 1949), Simpson's (Simpson 1949), and inverse Simpson's diversity indices were calculated using species densities. We used t-tests to test for differences in diversity between the mixed layer and main DCM, where main DCM is the depth of the peak with the largest chlorophyll a fluorescence value. To explain diversity across lakes, we used regressions with the same environmental variables as in the ecosystem analyses with the addition of two zooplankton grazer variables: 1) *Daphnia* density and 2) other major grazer density.

Detrended correspondence analysis (DCA) was conducted to examine the relationships of communities to one another (Legendre and Legendre 1998). DCA was used instead of regular correspondance analysis (CA) because a CA plot exhibited an arch (Legendre and Legendre 1998). DCA was also used to examine correlations of environmental variables with community space. The Bray-Curtis dissimilarity index was used on species densities to measure community similarities (Faith et al. 1987). A Mantel statistic based on Pearson's product-moment correlation and 999 permutations was used to test for covarying dissimilarity indices (Legendre and Legendre 1998) between the mixed layer and main DCMs.

Phytoplankton were classified into seven major taxonomic groups (Watson et al. 1997): chrysophytes, cryptophytes, cyanobacteria, diatoms, dinoflagellates, euglenoids, and greens. The dominant species was simply the species with the highest density in a community. We present species densities that are $> 5\%$ of the total community densities (typically summing up to $70 - 80\%$ of the total community) for each community in the Appendix. Regressions for dissimilarity, taxonomic group relative abundance, and dominance switches were run in a similar fashion to the ecosystem models with the same model selection criteria and with all variables listed in the

captions of each table. Dissimilarity and taxonomic group relative abundance were arcsine transformed for the regression analyses. Statistical analyses were performed in *Mathematica* v7 (Wolfram Research, Inc., Champaign, IL) and *R* v2.10 (The R Foundation for Statistical Computing, Vienna, Austria).

4.4 Results

4.4.1 Ecosystem

4.4.1.1 Vertical distributions of phytoplankton

We observed considerable variation in phytoplankton distributions. In 104 profiles, 15 were not thermally stratified, and hence lacked a poorly-mixed deep layer where a peak in chlorophyll *a* fluorescence could form. Peaks were identified in 86 of the remaining 89 profiles with clearly defined deep layers. Many of the profiles had multiple peaks: 39 profiles showed single peaks, but 17 showed double, 24 showed triple, 5 showed quadruple, and 1 showed quintuplet peaks. The depth of the global fluorescence maximum (largest fluorescence value in the water column), as well as all peaks, occurred in different portions of the water column (Figure 4.2).

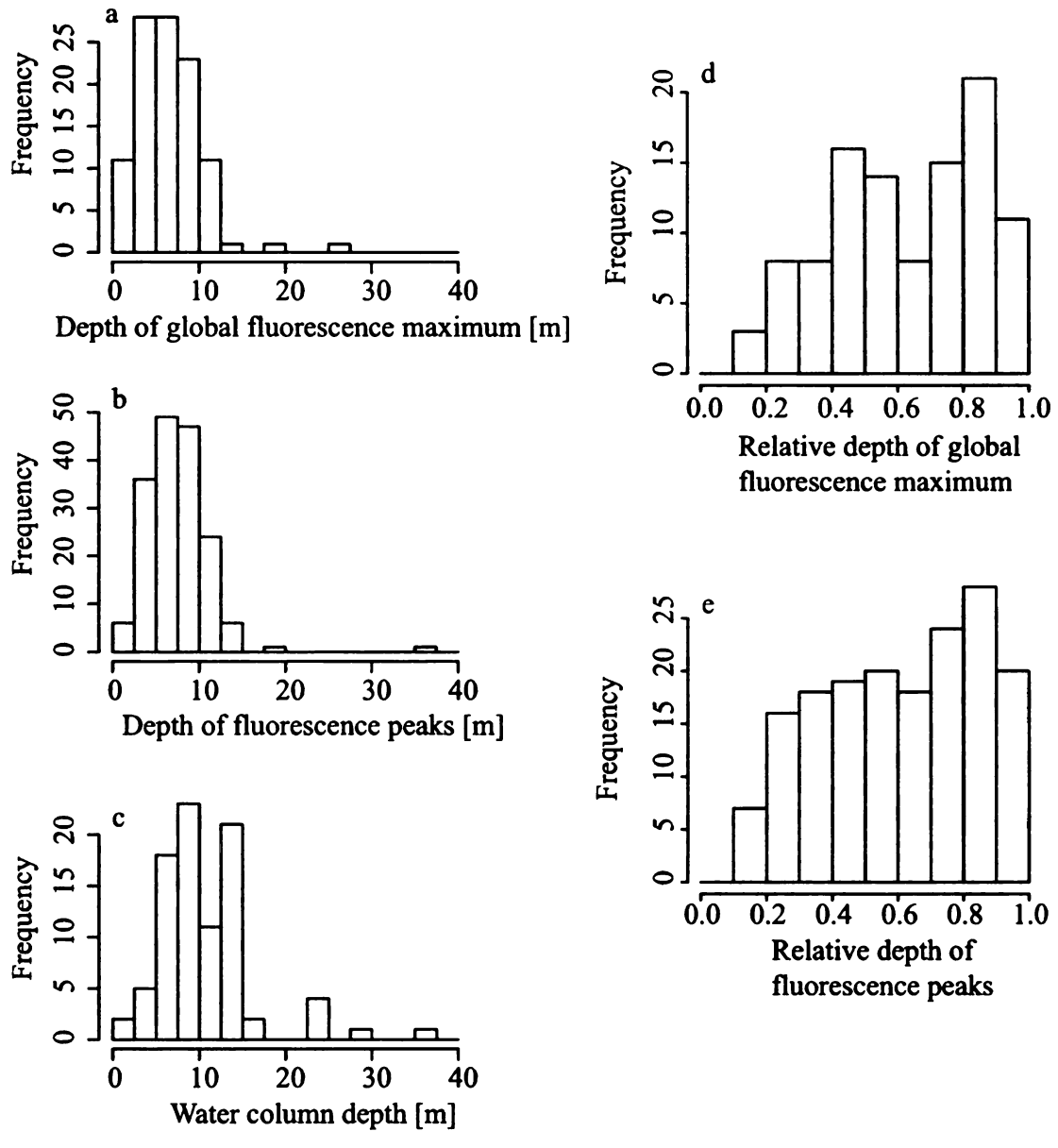

Figure 4.2: Depths of a) global fluorescence maximum, b) peaks in fluorescence, and c) water column. Depths relative to water column depth of d) global fluorescence maximum and e) peaks in fluorescence. Histograms include all lakes and times (n=104 for fluorescence maximum and water column and n=170 for all peaks).

4.4.1.2 Environmental parameters

The environmental parameters we measured in the survey lakes showed considerable variation (Table 4.1). The total nitrogen to total phosphorus ratio in the mixed layer showed significant variation (Figure 4.3a). However, overall, total nitrogen was correlated with total phosphorus across all sampling depths (Figure 4.3b).

Table 4.1: Summary of major environmental variables

	Minimum	Mean	Maximum
Water column depth [m]	1.9	9.95	35.50
Mixed layer depth [m]	1.27	3.06	17.58
Turbulent diffusion coefficient [m^2 d^{-1}]	$1.22x10^{-11}$	$6.20x10^{-5}$	$7.581x10^{-4}$
Background attenuation coefficient [m^{-1}]	0.18	0.77	3.24
Total phosphorus in mixed layer [μg P L^{-1}]	4.01	19.18	107
Total phosphorus at bottom [μg P L^{-1}]	6.88	79.44	978

The existence of phosphorus gradients was indicated by comparing concentrations of dissolved phosphorus 0.5 m above the bottom with concentrations in the mixed layer. On average, the concentration in the mixed layer was 20 μg P L^{-1} lower than the concentration 0.5 m above the bottom (Figure 4.4, paired t-test, t=2.27, P=0.013, df=105). A nutrient gradient was not detected for dissolved nitrogen (paired t-test, t=-2.09, P=0.98, df=70). We used phosphorus as the focal limiting nutrient due to the lack of a vertical gradient in nitrogen and the overall strong correlation of total nitrogen and total phosphorus.

4.4.1.3 Vertical distributions across environmental gradients

To examine phytoplankton vertical structure across environmental gradients, we first tested if algae formed a peak in the deep layer and in a benthic layer. We performed a logistic regression of presence of a peak versus the light level at the bottom of the mixed layer, but it was not significant. Together with the fact that there were only a few profiles that did not form a peak in the deep layer, there is a very high

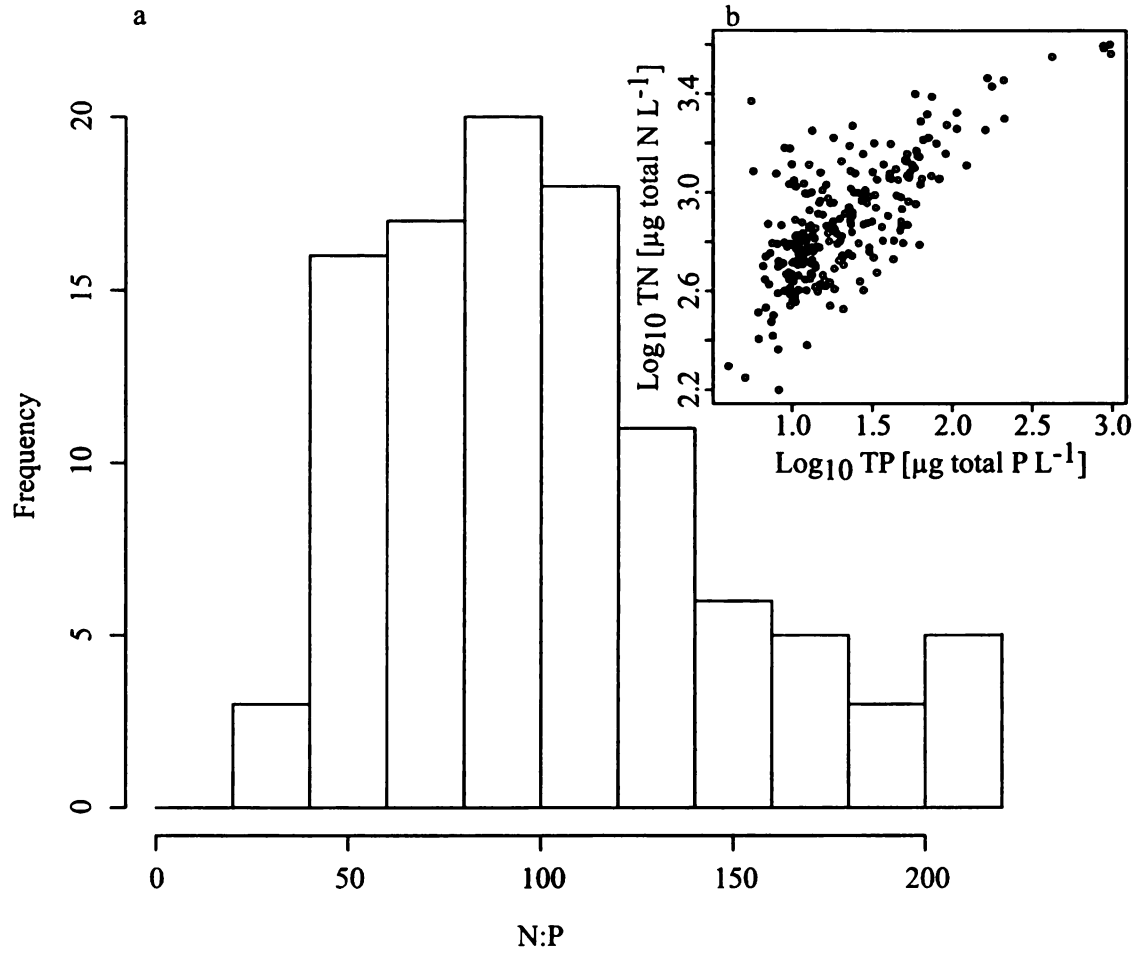

Figure 4.3: Nitrogen and phosphorus relationships in the data. a) Molar N:P ratio for total nitrogen and total phosphorus measured in the mixed layer (mean=115, median=97, minimum=35, maximum=932). b) Relationship between $\log_{10}$ Total nitrogen and $\log_{10}$ Total phosphorus for all lakes, times, and samples (including mixed layer and discrete depths). Pearson's correlation r=0.75, P <0.001, df=278).

probability that a peak can form in the deep layer in the lakes we sampled. However, the probability that a benthic layer forms depended significantly on the light level at the bottom of the water column (logistic regression, z statistic=3.57, $P<$ 0.001, Figure 4.5). Therefore, a deep layer peak is highly probable for given light conditions but a benthic layer forms only if enough light reaches the sediments.

There is a high probability of a peak forming in the deep layer but what determines the depth of these peaks? We focus on three main measures of vertical distribution of

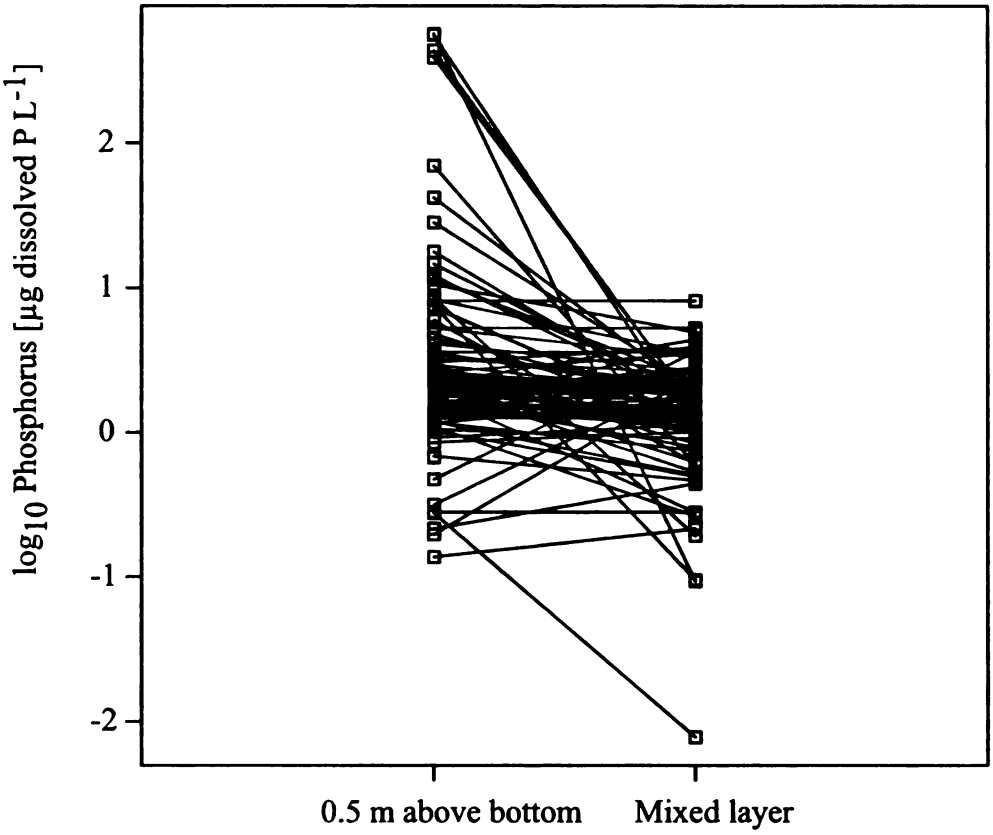

Figure 4.4: Phosphorus gradient present in most lakes and times (paired t-test, t=2.27, P=0.013, df=105). Note that in the plot, nutrient concentrations are log scaled.

the phytoplankton: 1) depth of global maximum of chlorophyll *a* fluorescence in the water column (most commonly used), 2) depths of peaks identified by fluorescence profile analysis, 3) depth of a peak for lakes that only contain a single peak (a subset of measure 2). The other measures of vertical distribution (average depth, average depth in the deep layer, mean of peak depths, and maximum of peak depths) gave very similar results to the global maximum of fluorescence measure.

Global maximum:

Depth of the global chlorophyll *a* fluorescence maximum was positively associated

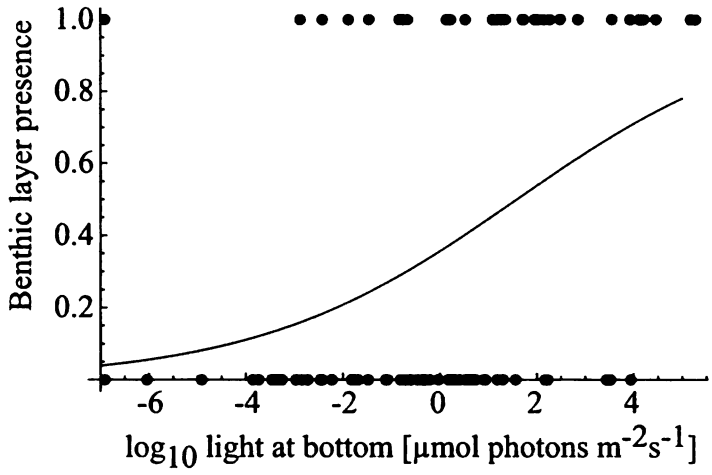

Figure 4.5: Logistic regression relating probability of a benthic layer forming to $\log_{10}$ light at the bottom of the water column (z statistic=3.57, $P< 0.001$).

with mixed layer depth and water column depth (Table 4.2), i.e. increasing mixed layer or water column depth acts to move the peak deeper in the water column. Depth of the global chlorophyll *a* fluorescence maximum was negatively associated with background light attenuation and the turbulent diffusion coefficient, i.e. increasing either of these two variables acts to move the peak shallower.

Table 4.2: Multiple linear regression results for depth of global fluorescence maximum versus all environmental variables. Only relationships from the best model were included in the table. The intercept was not significant ($P< 0.05$) so it was not included in this table.

	Coefficient (SE)	t	P-value	P_{overall}	$R^2_{\text{adj.}}$
Constant	0.2065 (0.1280)	1.613	0.1	< 0.001	0.39
$\log_{10}$ mixed layer depth	0.2722 (0.1013)	2.687	< 0.01		
$\log_{10}$ water column depth	0.2192 (0.103)	2.129	0.036		
$\log_{10}$ background light attenuation	-0.3883 (0.1107)	-3.509	< 0.001		
$\log_{10}$ turbulent diffusion coefficient	-0.030 (0.0119)	-2.532	0.013		

All peaks:

Depths of all peaks were positively associated with mixed layer depth and water column depth (Table 4.3), i.e. increasing mixed layer or water column depth acts to move the peak deeper in the water column. Depths of all peaks were negatively associ-

ated with background light attenuation, i.e. increasing background light attenuation acts to move the peak shallower.

Table 4.3: Multiple linear regression results for depths of fluorescence peaks versus all environmental variables. Only relationships from the best model were included in the table.

	Coefficient (SE)	t	P-value	P_{overall}	$R^2_{\text{adj.}}$
Constant	-0.4424 (0.0774)	5.719	< 0.001	< 0.001	0.35
$\log_{10}$ mixed layer depth	0.2532 (0.0544)	4.656	< 0.001		
$\log_{10}$ water column depth	0.2115 (0.0802)	2.639	< 0.01		
$\log_{10}$ background light attenuation	-0.3186 (0.0819)	-3.889	< 0.001		

Single peaks:

The closest association of depth distribution with environmental variables occurs in the lakes with only a single peak (Table 4.4). Single peak depth was positively associated with mixed layer depth, i.e. increasing mixed layer depth acts to move the peak deeper in the water column (Figure 4.6a, 4.7a). Single peak depth was also positively associated with water column depth (Figure 4.6b, 4.7b). Single peak depth was negatively associated with both background light attenuation (Figure 4.6c, 4.7c) and the turbulent diffusion coefficient (Figure 4.6d, 4.7d), i.e. increasing either of these two variables acts to move the peak shallower. Single peak depth was positively associated with total phosphorus in the mixed layer, i.e. was deeper with higher nutrients (Figure 4.6e, 4.7e).

Table 4.4: Multiple linear regression results for depths of single fluorescence peaks versus all environmental variables. Only relationships from the best model were included in the table.

	Coefficient (SE)	t	P-value	P_{overall}	$R^2_{\text{adj.}}$
Constant	-0.2806 (0.1354)	-2.072	0.046	< 0.001	0.8
$\log_{10}$ mixed layer depth	0.3412 (0.0932)	3.663	< 0.001		
$\log_{10}$ water column depth	0.4299 (0.0968)	4.441	< 0.001		
$\log_{10}$ TP in mixed layer	0.1942 (0.0779)	2.494	0.018		
$\log_{10}$ background light attenuation	-0.4324 (0.1132)	-3.821	< 0.001		
$\log_{10}$ turbulent diffusion coefficient	-0.0399 (0.0091)	-4.403	< 0.001		

Figure 4.6. Depth of peak of single peak lakes versus significant environmental variables. a) Relationship with mixed layer depth. The line is not a fit for the data, it is the depth of the mixed layer and denotes the upper limit of the peak depth. b) Relationship with water column depth. The line is not a fit for the data, it is the depth of the water column and denotes the lower limit of the peak depth. c) Relationship with background attenuation. The line is not a fit for the data, it is the $z_{\max}$ depth and denotes a theoretical lower limit of the peak depth and is calculated as $\log \frac{(I_{\text{in}}/I^*)}{a_{\text{bg}}}$. d) Relationship with $\log_{10}$ turbulent diffusion coefficient. e) Relationship with total phosphorus in the mixed layer.

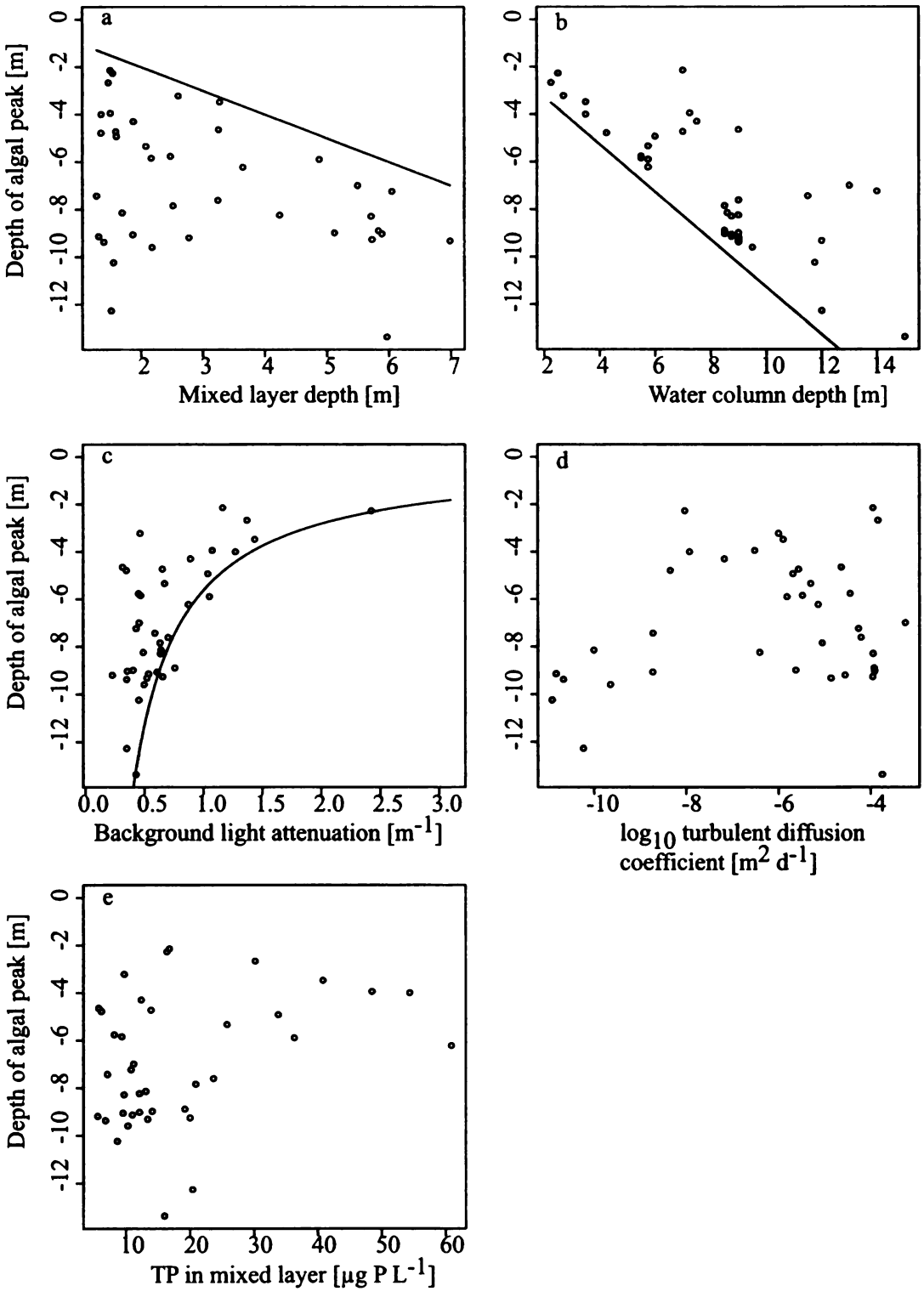

Figure 4.6: Depth of peak of single peak lakes versus environment.

Figure 4.7. The partial residual plots for the significant $\log_{10}$ transformed variables in the model of depth of peak of single peak lakes versus significant environmental variables. Note, these are the same variables as in Figure 4.6, but these are the partial residual plots and so represent the true relationship of the variable with peak depth. Lines are the slopes for the variables in the table. In these plots, depth increases along the partial residual axes (larger values are deeper).

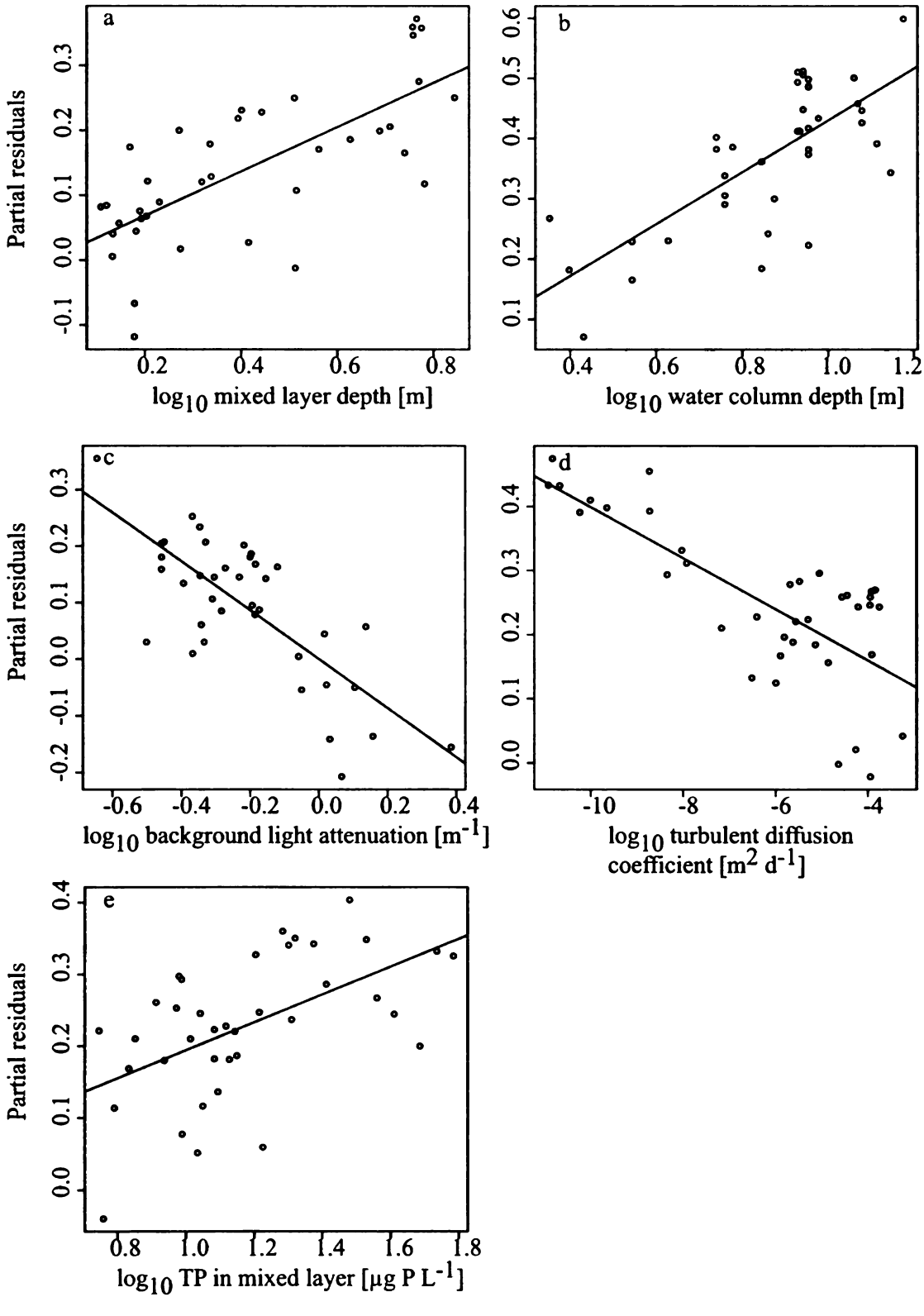

Figure 4.7: Partial residual plots for the depth of peak of single peak lakes.

4.4.1.4 Biomass

Total biomass, as measured by in-situ chlorophyll *a* fluorescence integrated throughout the water column, was positively associated with water column depth and background light attenuation (Table 4.5, Figure 4.8). Biomass in the deep layer, as measured by integrated fluorescence below the mixed layer, was positively associated with water column depth and background light attenuation, and negatively associated with mixed layer depth (Table 4.5, Figure 4.9). The mixed layer biomass, as measured by integrated fluorescence in the mixed layer, was positively associated with mixed layer depth, total phosphorus in the mixed layer, and background light attenuation (Table 4.5, Figure 4.10).

Table 4.5: Multiple linear regression results for integrated fluorescence ("biomass") versus all environmental variables. Only relationships from the best model were included in the table.

	Coefficient (SE)	t	P-value	P_{overall}	$R^2_{\text{adj.}}$
Total biomass					
Constant	-0.3771 (0.0837)	-4.506	< 0.001	< 0.001	0.6
$\log_{10}$ water column depth	0.8702 (0.1063)	8.187	< 0.001		
$\log_{10}$ total phosphorus at bottom	0.05828 (0.04178)	1.395	0.167		
$\log_{10}$ background light attenuation	0.84930 (0.11454)	7.415	< 0.001		
Deep layer biomass					
Constant	-0.7321 (0.1152)	-6.356	< 0.001	< 0.001	0.64
$\log_{10}$ water column depth	1.2291 (0.1422)	8.644	< 0.001		
$\log_{10}$ mixed layer depth	-0.4868 (0.0906)	-5.370	< 0.001		
$\log_{10}$ total phosphorus at bottom	0.08293 (0.05588)	1.484	0.142		
$\log_{10}$ background light attenuation	0.7639 (0.1556)	4.908	< 0.001		
Mixed layer biomass					
Constant	-0.7822 (0.1559)	-5.017	< 0.001	< 0.001	0.85
$\log_{10}$ mixed layer depth	1.1360 (0.0835)	13.598	< 0.001		
$\log_{10}$ total phosphorus in mixed layer	0.1923 (0.0976)	1.971	0.052		
$\log_{10}$ background light attenuation	0.8956 (0.1189)	7.531	< 0.001		
$\log_{10}$ turbulent mixing	0.0148 (0.0097)	1.528	0.13		

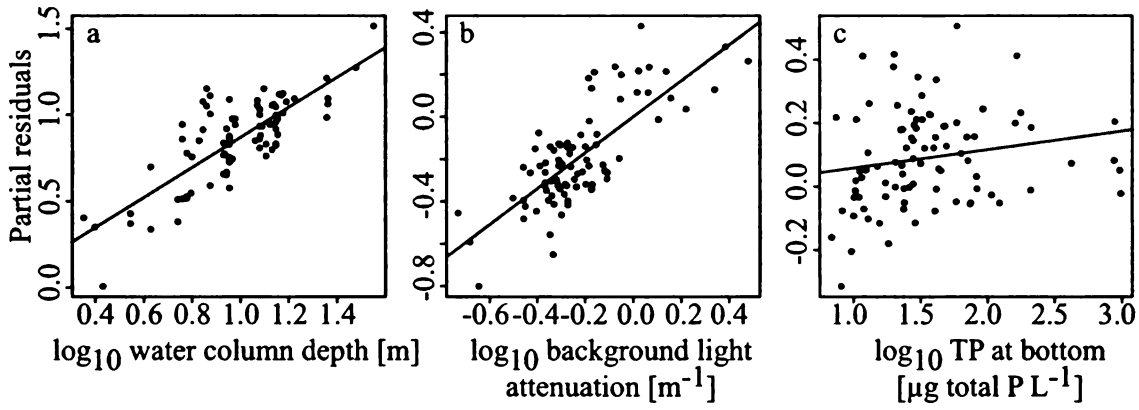

Figure 4.8: Partial residual plots for total biomass (integrated fluorescence) versus environmental variables in the best model.

4.4.1.5 Multiple peak coexistence

The light and nutrient conditions experienced by algae in the lakes were highly variable both among lakes and within a lake. For example, the light level for the average depth of the deep layer algal biomass showed considerable variation (mean=19.6, SE=4.29, minimum=0, maximum=352.80 μmol photons $m^{-2}s^{-1}$). Peaks exist along a full range of light and phosphorus levels. A type II regression of log(light) on log(dissolved phosphorus) at a peak showed a negative relationship that was highly significant (RMA method, slope=-3.94, $R^2 = 0.15$, $P < 0.001$, Figure 4.11).

4.4.1.6 Number of peaks

The number of peaks was determined by the amount of physical space in the deep layer (Table 4.6, Fig. 4.12a) and the nutrient gradient (Fig. 4.12c). The data provide some support that the light gradient also plays a role (Fig. 4.12b). All of these factors are associated with an increased number of peaks (Table 4.6).

We could not test the relative importance of resource heterogeneity versus resource quantity (Stevens and Carson 2002) because TP at the bottom has too much multicollinearity when in models with TP gradient in the deep layer (as does light at

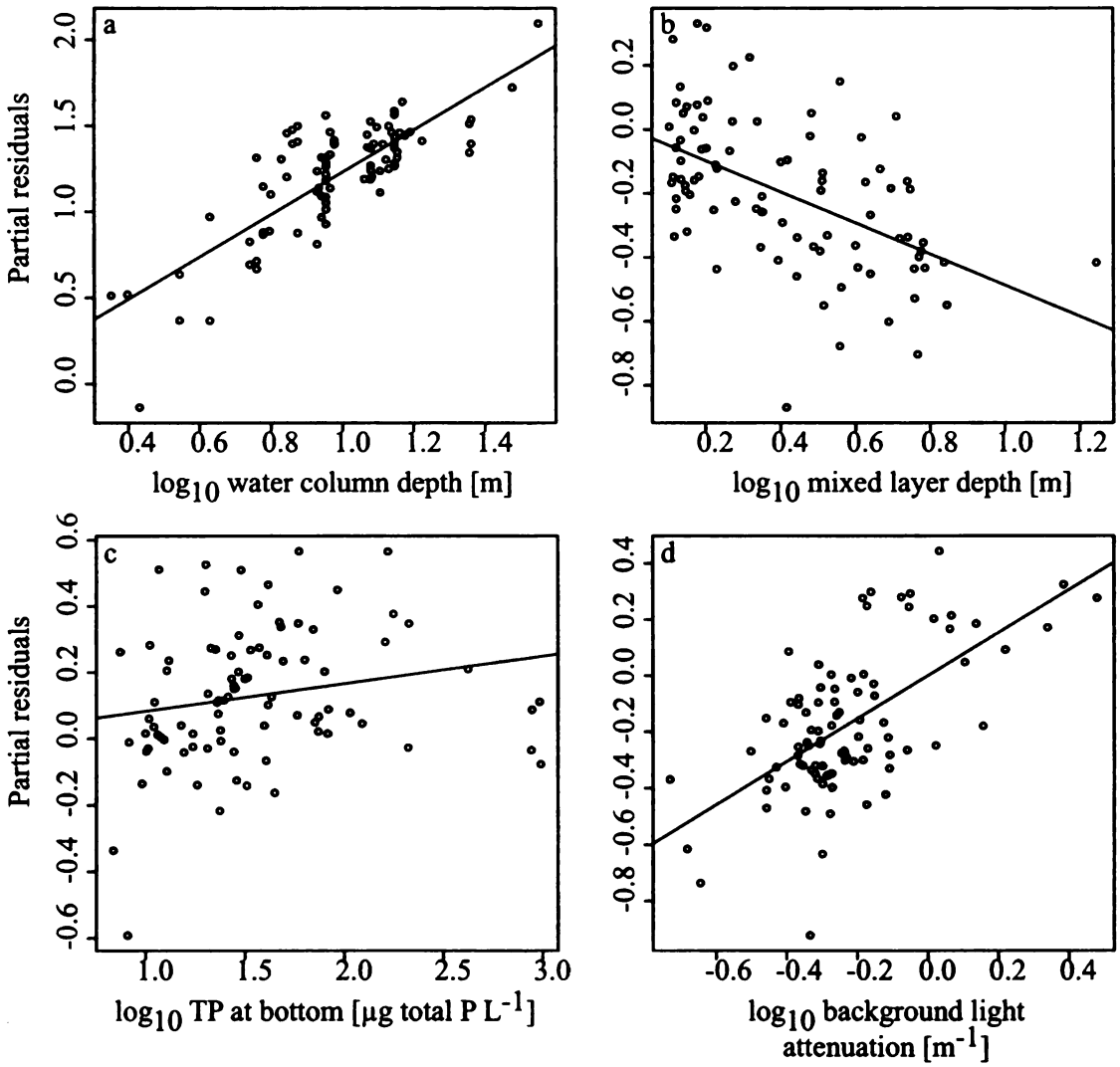

Figure 4.9: Partial residual plots for deep layer biomass (integrated fluorescence in the deep layer) versus environmental variables in the best model.

Table 4.6: Multiple linear regression results for number of peaks versus the following $\log_{10}$ transformed environmental variables: deep layer span, TP gradient in the deep layer, light gradient in the deep layer, and background light attenuation; as well as day-of-year. Only relationships from the best model were included in the table.

	Coefficient (SE)	t	P-value	P_{overall}	$R^2_{\text{adj.}}$
$\log_{10}$ deep layer span	1.5280 (0.2692)	5.677	< 0.001	< 0.001	0.28
$\log_{10}$ TP gradient	0.3165 (0.1382)	2.290	0.02		
$\log_{10}$ background light attenuation	0.9334 (0.5460)	1.709	0.09		

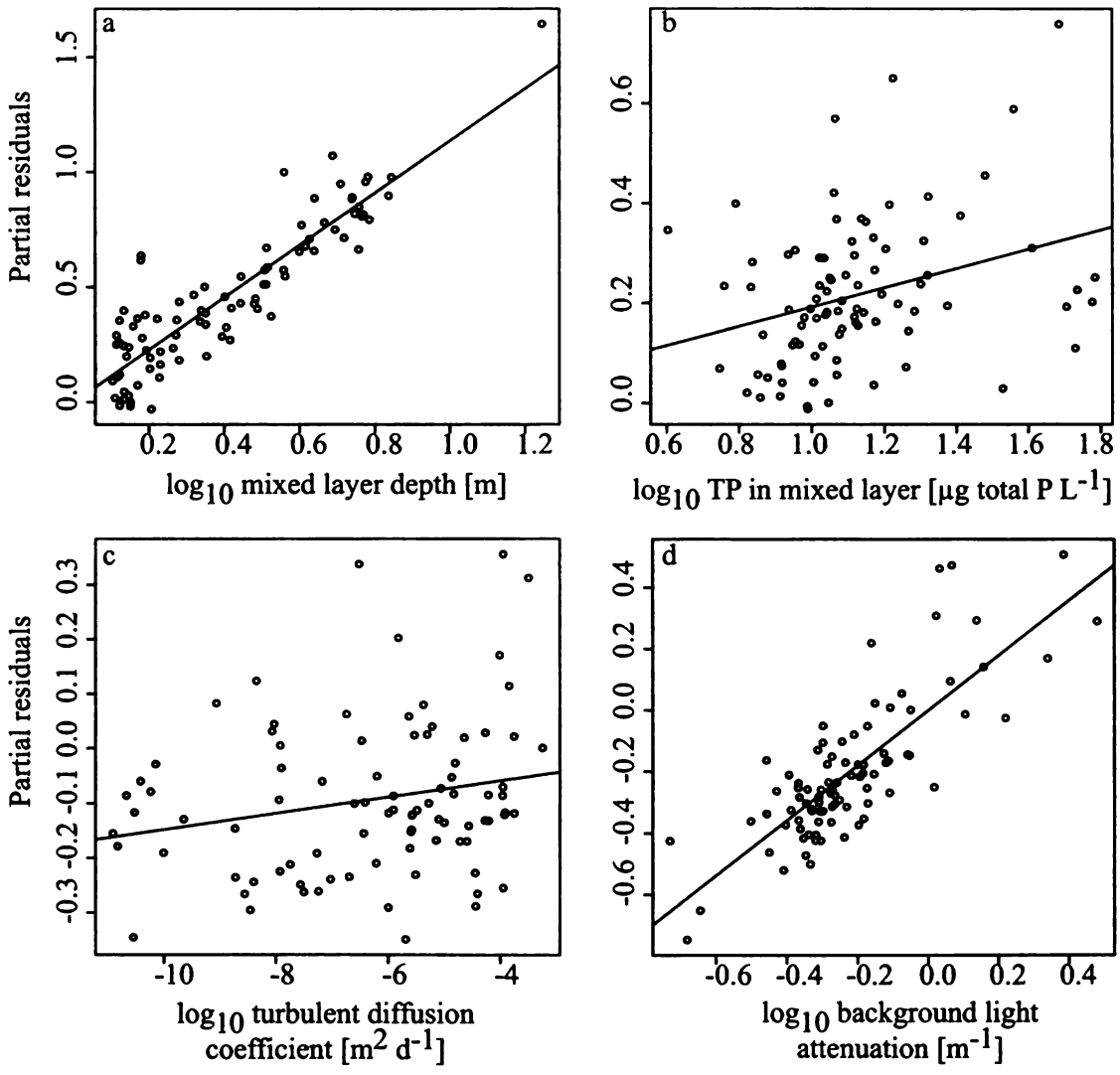

Figure 4.10: Partial residual plots for mixed layer biomass (integrated fluorescence in the mixed layer) versus environmental variables in the best model.

the mixed layer and light gradient in the deep layer). However, when we replace the gradients (vertical heterogeneity) in the above model with resource supplies (quantities), the best model to explain number of peaks becomes deep layer span and TP at the bottom with all light variables being not significant. This indicates that for nutrients, either resource heterogeneity or resource quantity is important but we cannot distinguish which is more important.

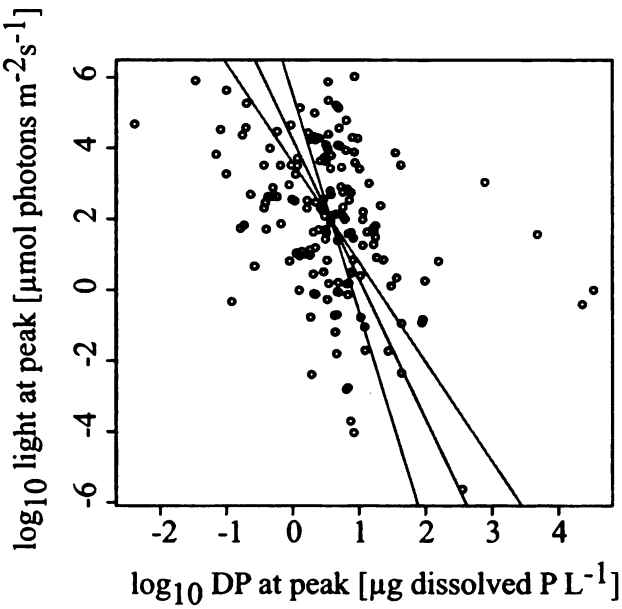

Figure 4.11: Type II regression of log light values at a peak versus log dissolved phosphorus values at a peak.

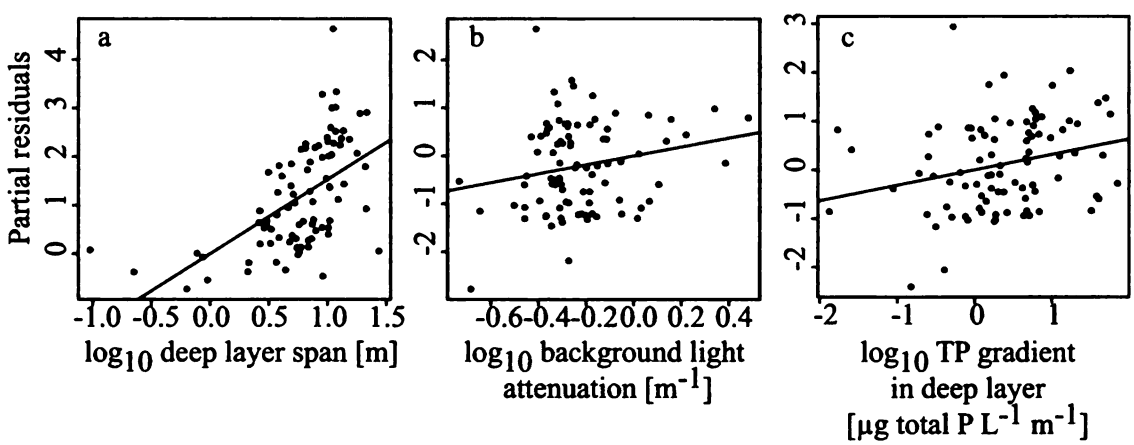

Figure 4.12: Partial residual plots for number of peaks versus environmental variables in the best model.

4.4.2 Community

4.4.2.1 Species Diversity

Phytoplankton species richness varied from 13 to 54 (mean=28, SD=9) species at a depth. The mixed layer and the main DCM (peak with the largest chlorophyll

a fluorescence value) did not differ for any measure of diversity (species richness, Shannon, Simpson's, inverse Simpson's, all paired and unpaired t-test P-values $>$ 0.1). Mixed-layer Shannon diversity was positively associated with other major (non-*Daphnia*) grazers densities, background light attenuation, total phosphorus at the bottom, and mixed layer depth and negatively associated with water column depth, *Daphnia* densities, and total phosphorus in the mixed layer (Table 4.7). Shannon diversity in the main DCM was positively associated with *Daphnia* density, total phosphorus at the bottom, mixed layer depth, and the light level at the bottom of the mixed layer and negatively associated with water column depth (Table 4.7). Species richness in the mixed layer could be explained by a subset of the variables that explained Shannon diversity in the mixed layer. Species richness in the main DCM could not be explained by a significant model.

Table 4.7: Multiple linear regression results for Shannon diversity versus all environmental variables in the best model. Environmental variables considered were the same for the mixed layer and main DCM and included: turbulent mixing, water column depth, *Daphnia* densities, other major grazers densities, background light attenuation, total phosphorus at the bottom, total phosphorus in the mixed layer, and the light level at the bottom of the mixed layer. Only relationships from the best model were included in the table.

	Coefficient (SE)	t	P-value	P_{overall}	$R^2_{\text{adj.}}$
Mixed layer Shannon diversity					
Constant	-4.8339 (1.1753)	-4.506	< 0.001	0.08	0.28
$\log_{10}$ water column depth	-1.7529 (0.7137)	-2.456	< 0.05		
$\log_{10}$ *Daphnia*	-0.4977 (0.1869)	-2.663	< 0.05		
$\log_{10}$ other major grazers	0.5670 (0.2994)	1.894	0.076		
$\log_{10}$ background light attenuation	3.0862 (1.4315)	2.156	< 0.05		
$\log_{10}$ total phosphorus at bottom	0.9239 (0.4075)	2.267	< 0.05		
$\log_{10}$ total phosphorus in mixed layer	-2.4828 (0.8995)	-2.760	< 0.05		
$\log_{10}$ mixed layer depth	1.6237 (0.6025)	2.695	< 0.05		
Main DCM Shannon diversity					
Constant	-0.2867 (0.7898)	-0.363	0.72	< 0.05	0.42
$\log_{10}$ water column depth	0.0684 (0.02459)	-2.785	< 0.05		
$\log_{10}$ *Daphnia*	0.0197 (0.0067)	2.924	< 0.05		
$\log_{10}$ total phosphorus at bottom	0.0017 (0.00064)	2.709	< 0.05		
$\log_{10}$ mixed layer depth	3.1778 (0.9393)	3.383	< 0.005		
$\log_{10}$ light at bottom of mixed layer	0.6616 (0.2957)	2.237	< 0.05		

4.4.2.2 Whole-community comparisons

Detrended correspondence analysis plot indicated variation between some communities while also showing conspicuous community overlap (Figure 4.13). For some of the lakes, communities from different depths within a lake clustered in multidimensional community space, indicating similarity within a lake. Furthermore, examination of correlations between environmental variables and axes illustrated that communities differentiated along several nutrient, light, and grazing axes.

The Bray-Curtis community dissimilarity index also showed that communities within a lake (mean dissimilarity=0.57, SE=0.03, Fig. 4.14a) appear to be much more similar to each other than communities across lakes (mean dissimilarity=0.84, SE=0.003, Fig. 4.14b). Furthermore, both mixed layers and the main DCMs showed a lot of dissimilarity across lakes (Fig. 4.14c and d respectively) indicating that within each of these environments, the communities were not the same across lakes. Main DCMs (mean dissimilarity=0.79, SE=0.01, minimum=0.25, maximum=0.996) appear to be slightly more similar to one another on average than mixed layers (mean dissimilarity=0.84, SE=0.009, minimum=0.09, maximum=1) and have a smaller range in variation. In addition, main DCMs and mixed layers covary across lakes, meaning that if a mixed layer community differs from all the other mixed layer communities, the main DCM community will differ from all the other main DCM communities in a similar fashion (Mantel test, $r = 0.55$, $P<0.001$, Fig. 4.14e). Dissimilarity between paired samples of mixed layer and main DCM shows a large amount of variation (mean dissimilarity=0.63, minimum=0, maximum=0.97, Fig. 4.14f).

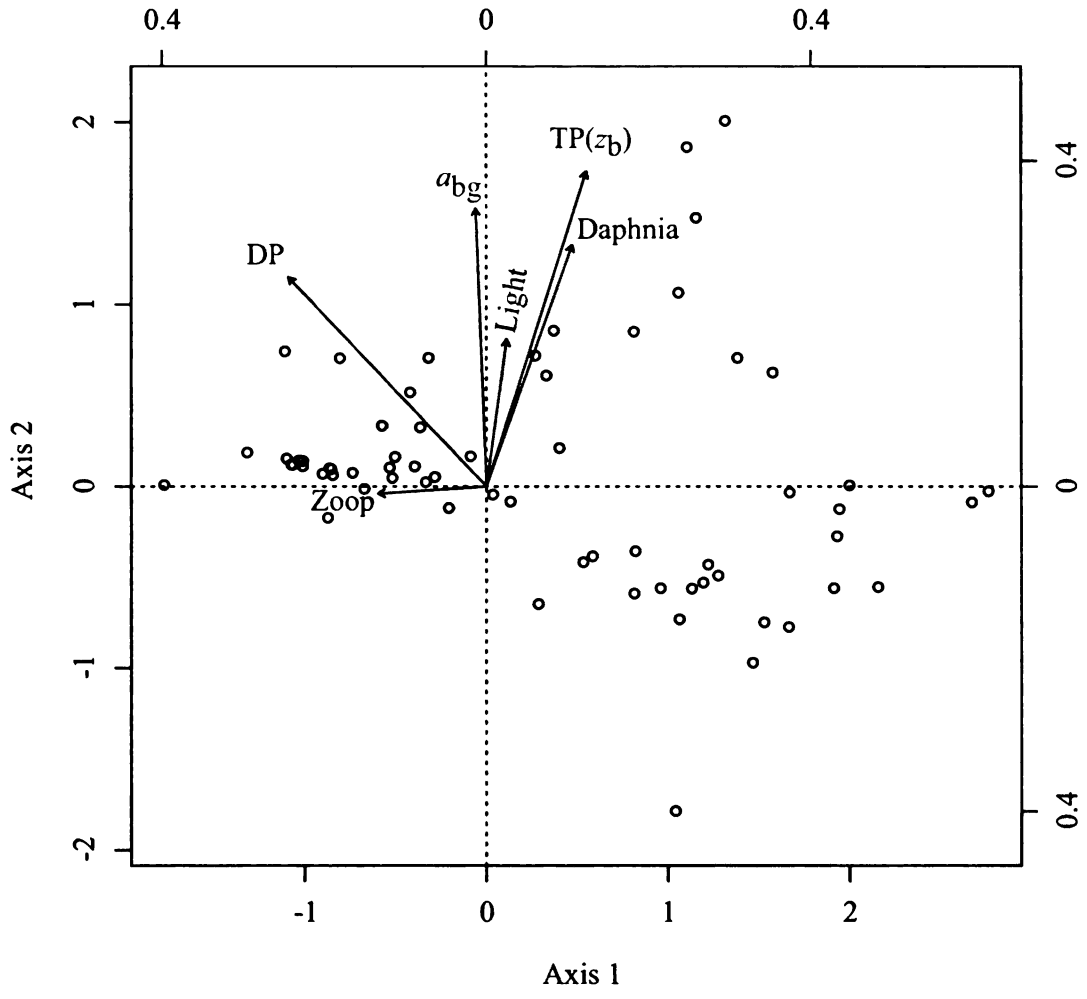

Figure 4.13: Detrended correspondence analysis plot (DCA) of all communities (all lakes and depths). Also plotted are environmental vectors for $\log_{10}$ transformed environmental variables that did not overlap too strongly with another variable (excluded turbulent mixing coefficient because it overlapped with a_{bg} and TP measured at the depth of the sample because it overlapped with TP measured at the bottom). Other variables and their scores (vectors scaled by correlation coefficient) for axis 1 and 2 respectively: DP is soluble reactive phosphorus (-0.24397522, 0.257411923) and light is irradiance (0.02501621, 0.181052901) at the depth of the community sample, a_{bg} is background light attenuation (-0.01306323, 0.341490988), TP(z_b) is total phosphorus measured at the bottom (0.12299715, 0.387226041), Daphnia is *Daphnia* density (0.10589080, 0.297177857), and Zoop is density of other major grazers (-0.13330044, -0.008967929).

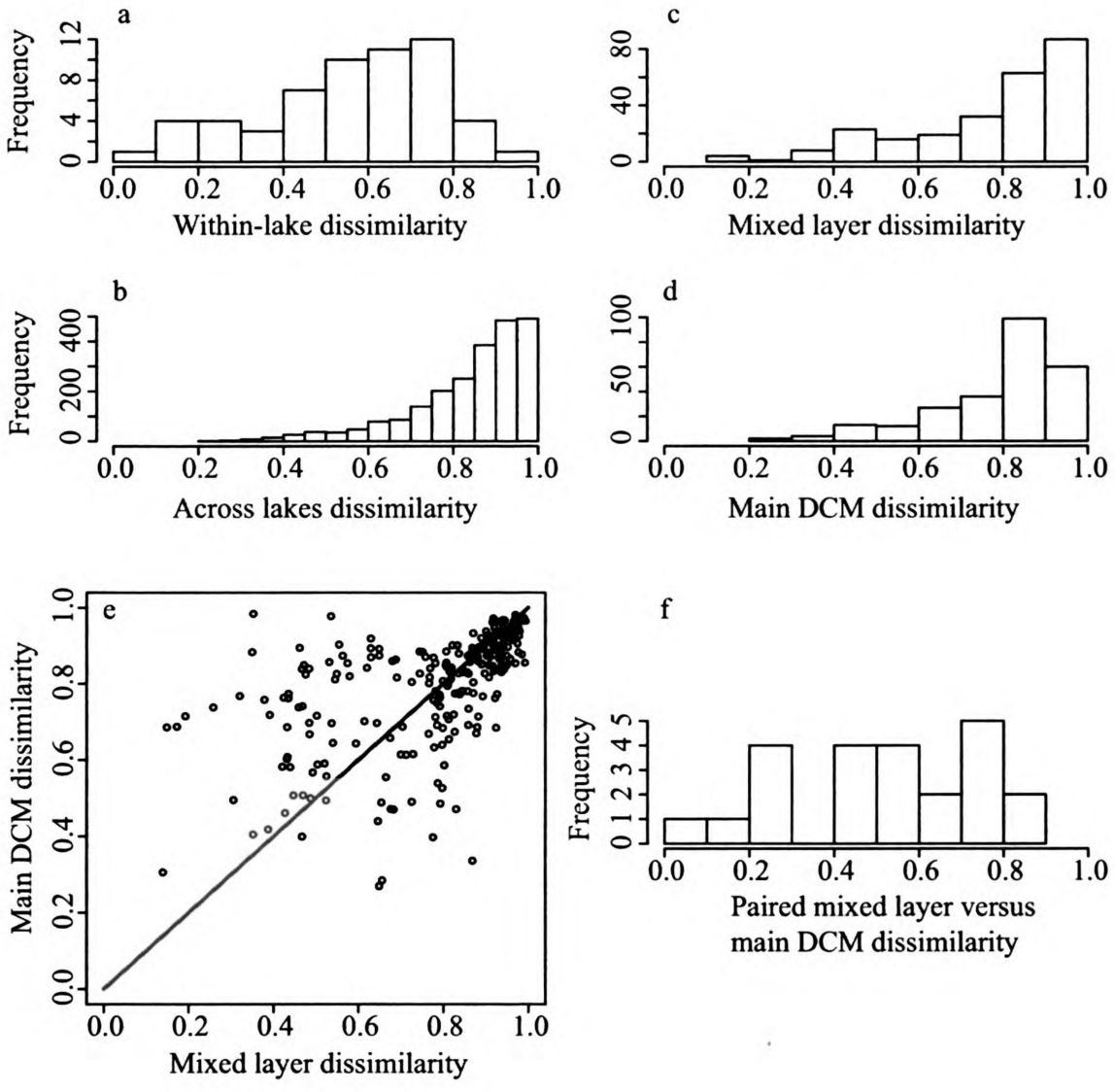

Figure 4.14: Frequency distributions for Bray-Curtis community dissimilarity indices of different community samples. Dissimilarity is maximum at a value of 1. a) Dissimilarity for samples taken within a lake. b) Across lake dissimilarity for communities. c) Dissimilarity of mixed layer communities compared to other mixed layer communities. d) Dissimilarity of main DCM communities compared to other main DCM communities. e) Correlation between dissimilarity of mixed layer communities (part c) and dissimilarity of main DCM communities (part e). f) Dissimilarity between paired mixed layer and main DCM samples for each lake.

The dissimilarity between communities in the mixed layer and main DCM could

best be explained by two environmental variables (Table 4.8): background light attenuation appeared to make the communities more similar (Fig. 4.15a) and total phosphorus at the bottom appeared to make the communities less similar (Fig. 4.15b) although note that the overall model is not significant (P=0.15).

Table 4.8: Multiple linear regression results for dissimilarity versus the following $\log_{10}$ environmental variables as indicated by the DCA to potentially play a role: TP at the bottom, and a_{bg}, *Daphnia*, and other major grazers. Only relationships from the best model were included in the table. Note that TP at the bottom in the best model could be replaced by TP gradient in the deep layer (P=0.05) but the model cannot include both due to multicollinearity.

	Coefficient (SE)	t	P-value	$P_{overall}$	$R^2_{adj.}$
$\log_{10}$ TP at the bottom	0.1892 (0.1287)	1.470	0.16	0.17	0.08
$\log_{10}$ a_{bg}	-0.5218 (0.2879)	-1.812	0.085		

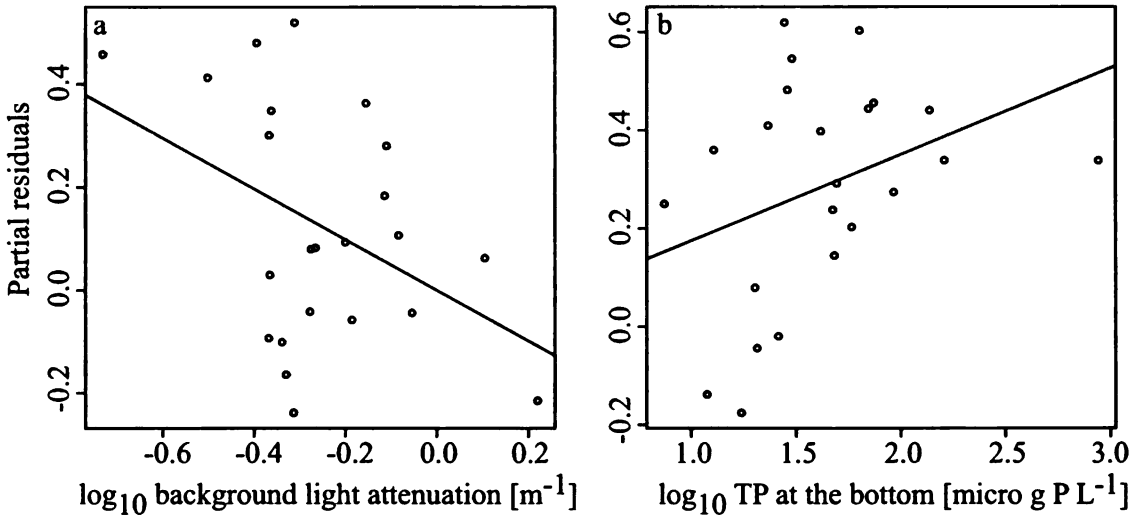

Figure 4.15: Partial residual plots for community dissimilarity between the mixed layer and main DCM versus environmental variables in the best model.

4.4.2.3 Taxonomic group and species

DCMs were not all dominated by the same taxonomic group or genus (Appendix Table). In fact, dominance by taxonomic group and genus shows as much variation

in DCMs as in the mixed layer. Thus, the DCM niche can be filled by a number of different taxonomic groups and species.

Cyanobacteria appear to be the most abundant group across all lakes (Fig. 4.16). Taxonomic group relative abundances showed some relationships with lake characteristics across lakes (Fig. 4.16, Table 4.9). Chrysophytes increased with turbulent mixing and decreased with mixed layer depth and *Daphnia* density. Cryptophytes decreased with total phosphorus in the mixed layer. Cyanobacteria increased with *Daphnia* density and appeared to decrease with other major grazers density. Diatoms increased with other major grazers density and decreased with water column depth and total phosphorus in the mixed layer. Dinoflagellates increased with background light attenuation. Euglenoids decreased with other major grazers density. Greens decreased with background light attenuation.

Figure 4.16. Relative abundance of taxonomic groups across lakes and with depth within lakes for the 23 lakes from which multiple samples were taken with depth. Each plot is a single lake and the communities from all the depths sampled are arrayed in the vertical dimension of each according to depth (surface is top and deepest depth is bottom). Plots are arrayed roughly in 2 dimensional environmental space: *Daphnia* density increases along the horizontal axis across lakes and background light attenuation increases along the vertical axis across lakes. a) Pleasant, b) Lime, c) Gravel, d) Little Long, e) Big Glen, f) Baker, g) Donnell, h) Lawrence, i) Long, j) Gun, k)Fine, l) Hogsett, m) Bristol, n) Baldwin, o) Warner, p) Bassett, q) Cloverdale, r) Little Mill, s) Pine, t) Sherman, u) Hess, v) Brooks, w) Wintergreen.

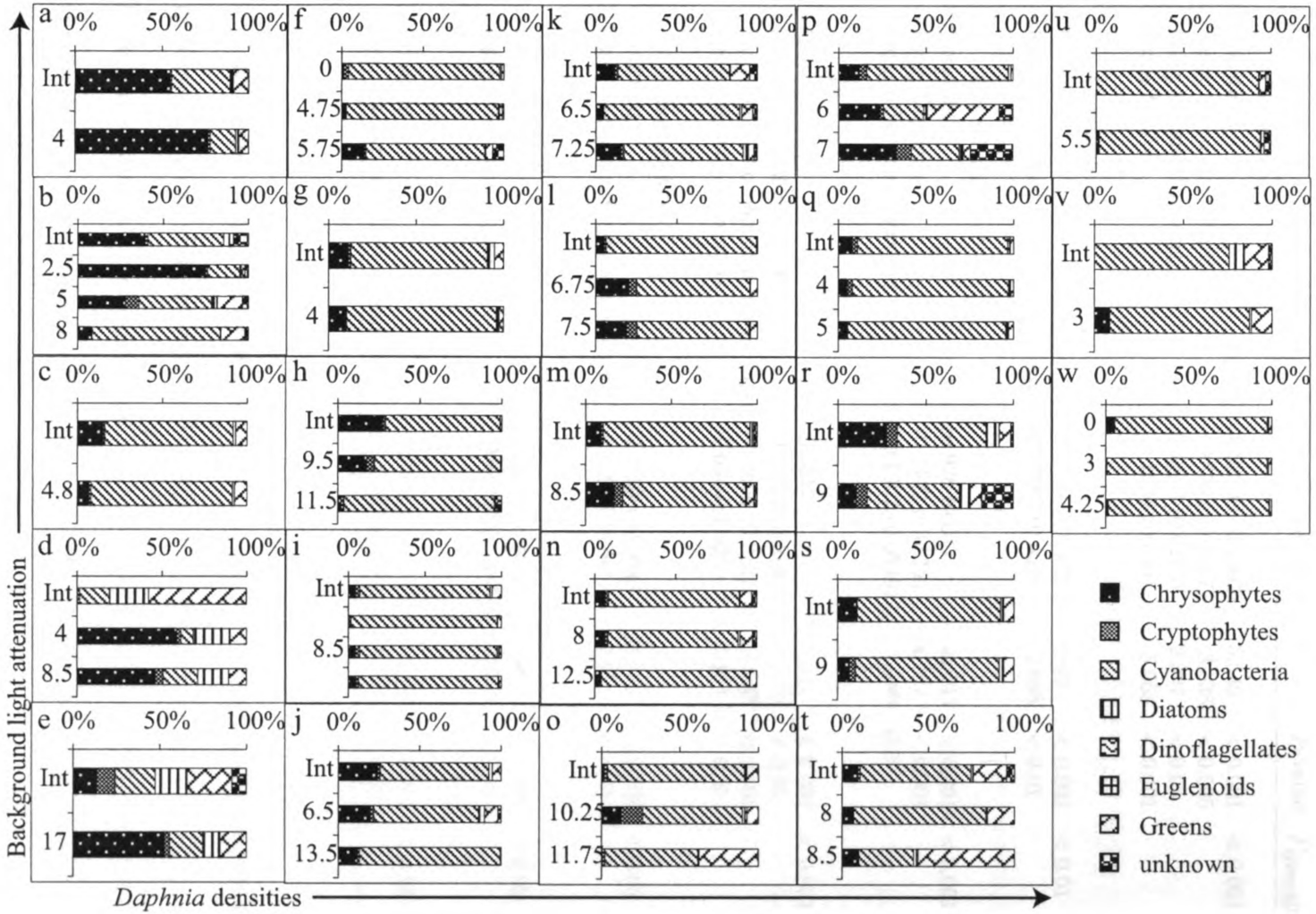

Figure 4.16: Relative abundance of taxonomic groups across lakes and with depth.

Table 4.9: Multiple linear regression results for relative abundance of taxonomic groups versus all environmental variables in the best model. Environmental variables considered were: turbulent mixing, mixed layer depth, water column depth, *Daphnia* densities, other major grazers densities, background light attenuation, total phosphorus at the bottom, total phosphorus in the mixed layer.

	Coefficient (SE)	t	P-value	P_{overall}	$R^2_{\text{adj.}}$
Chrysophytes					
Constant	0.92238 (0.1662)	5.549	< 0.001	< 0.001	0.38
$\log_{10}$ mixed layer depth	-0.4061 (0.1217)	-3.338	< 0.005		
$\log_{10}$ turbulent mixing	0.0538 (0.0225)	2.397	< 0.05		
$\log_{10}$ *Daphnia*	-0.1976 (0.039)	-5.068	< 0.001		
Cryptophytes					
Constant	0.2526 (0.03827)	6.60	< 0.001	< 0.01	0.09
$\log_{10}$ total phosphorus in mixed layer	-0.0887 (0.0329)	-2.698	< 0.01		
Cyanobacteria					
Constant	0.928 (0.04)	23.212	< 0.001	< 0.001	0.28
$\log_{10}$ *Daphnia*	0.2449 (0.0512)	4.787	< 0.001		
$\log_{10}$ other major grazers	-0.1002 (0.0545)	-1.840	0.07		
Diatoms					
Constant	0.5617 (0.1012)	5.551	< 0.001	< 0.001	0.31
$\log_{10}$ water column depth	-0.1434 (0.059)	-2.430	< 0.05		
$\log_{10}$ total phosphorus in mixed layer	-0.2666 (0.0537)	-4.963	< 0.001		
$\log_{10}$ other major grazers	0.0545 (0.023)	2.373	< 0.05		
Dinoflagellates					
Constant	0.0433 (0.0054)	8.069	< 0.001	< 0.05	0.06
$\log_{10}$ background light attenuation	0.039 (0.0164)	2.371	< 0.05		
Euglenoids					
Constant	0.0326 (0.00505)	6.468	< 0.001	< 0.05	0.046
$\log_{10}$ other major grazers	-0.01431 (0.00704)	-2.031	< 0.05		
Greens					
Constant	0.2098 (0.0290)	7.229	< 0.001	< 0.05	0.05
$\log_{10}$ background light attenuation	-0.1932 (0.0889)	-2.173	< 0.05		

Taxonomic group relative abundances appear to change significantly with depth in some lakes but differed relatively little in other lakes (Fig. 4.16). Fig. 4.16 shows that diatoms mostly decreased with depth, cryptophytes mostly increased with depth, chrysophytes, cyanobacteria, and greens both increased and decreased with depth, and other groups were roughly equal with depth across lakes. Analysis of how local

resource conditions correlated with relative abundance of taxonomic groups showed that some groups have significant relationships with local resource conditions while others showed no relationship (Table 4.10). Chrysophytes show a positive relationship with light measured at the depth of the sample. Cyanobacteria show a negative relationship with light measured at the depth of the sample. Diatoms show a positive relationship with light measured at the depth of the sample and euglenoids show a negative relationship with light measured at the depth of the sample. All other taxonomic groups (cryptophytes, dinoflagellates, and greens) show no relationship with local resource conditions.

Out of the 30 lakes sampled in September for community composition analyses, 23 had multiple depths sampled because those lakes were stratified and a DCM was present. The identity of the dominant species switched between depths in the water column in 15 of those 23 lakes, making a dominance switch a common occurrence (Appendix Table). Dominance switches appear to be more likely in deeper lakes (Table 4.11).

4.5 Discussion

4.5.1 Variation in phytoplankton vertical distributions

We established that there is considerable variation in phytoplankton vertical distributions. Lakes varied in the depths of their chlorophyll *a* fluorescence peaks. In addition, we found many lakes with multiple peaks, in agreement with Fee (1976), who showed that usually a considerable amount of biomass exists in a peak below the mixed layer.

Numerous hypotheses have been proposed to explain vertical distributions of phytoplankton, and in particular DCMs. However, we focused on several hypotheses related to light, nutrients, and mixing: low turbulence and sufficient light penetra-

Table 4.10: Multiple linear regression results for relative abundance of taxonomic groups versus local environmental variables in the best model. Environmental variables considered were: light at the sample depth and dissolved phosphorus at the sample depth. For integrated mixed layer samples, the light level at the bottom of the mixed layer was used as the light at the sample depth. NS indicates that the best model was not significant ($P< 0.1$).

	Coefficient (SE)	t	P-value	P_{overall}	$R^2_{\text{adj.}}$
Chrysophytes					
Constant	0.2185 (0.0654)	3.342	< 0.005	< 0.05	0.07
$\log_{10}$ light	0.0977 (0.0398)	2.454	< 0.05		
$\log_{10}$ dissolved phosphorus	0.1078 (0.071)	1.519	0.13		
Cryptophytes					
NS					
Cyanobacteria					
Constant	1.1303 (0.0773)	14.625	< 0.001	0.09	0.04
$\log_{10}$ light	-0.0935 (0.0470)	-1.988	0.05		
$\log_{10}$ dissolved phosphorus	-0.1254 (0.084)	-1.494	0.14		
Diatoms					
Constant	0.0793 (0.0285)	2.778	< 0.01	< 0.05	0.056
$\log_{10}$ light	0.0419 (0.0186)	2.248	< 0.05		
Dinoflagellates					
NS					
Euglenoids					
Constant	0.04439 (0.007996)	5.552	< 0.001	< 0.05	0.08
$\log_{10}$ light	-0.01364 (0.005217)	-2.615	< 0.05		
Greens					
NS					

tion are necessary for a DCM to persist (Fee 1976), while the light and nutrient gradients may control the vertical position of the peak (Fee 1976, Klausmeier and Litchman 2001). We considered how these hypotheses may contribute to not just formation of DCMs but the variation in DCM vertical positions as well, and the overall variation in phytoplankton vertical distributions across environmental gradients. Our model (Chapter 2) details how these hypothesized processes should work for a

Table 4.11: Logistic regression results for whether a lake switches identity of the dominant species within the water column (by comparing all samples within a water column) versus the following $\log_{10}$ environmental variables: water column depth, mixed layer depth, turbulent mixing coefficient, background light attenuation, TP at the bottom, and TP in the mixed layer. Only relationships from the best model were included in the table.

	Coefficient (SE)	z	P-value	P_{overall}
Constant	-5.772 (3.364)	-1.716	0.086	0.15
$\log_{10}$ water column depth	6.381 (3.400)	1.877	0.06	

particular algal physiology and provides specific predictions that we tested.

4.5.2 Depth of algae

Most of the profiles had peaks in the deep layer indicating that enough light penetrated to the deep layer for a peak to form. Consistent with our theoretical predictions, our data show that light availability determines whether or not a peak forms at the bottom (Figure 4.5).

When considering profiles with only a single peak, multiple regression models explained much more of the variance ($R^2_{\text{adj.}} = 0.8$) than the models of multiple peaks ($R^2_{\text{adj.}} = 0.35$) or the global maximum ($R^2_{\text{adj.}} = 0.39$). In addition, more variables predict peak depths for single peak profiles. For single peaks, five environmental variables have significant effects, including total phosphorus. Fewer environmental variables can explain the variation in algal distribution in profiles with multiple peaks (three variables) or for the global maximum (four variables), and it appears that nutrients are unimportant.

A statistical model that considers all of the multiple peaks, or ignores all but one, has decreased predictive power for vertical distribution. This is likely because each peak alters resource conditions for all the other peaks due to nutrient depletion and shading. In addition, peaks can be composed of different species and interactions

between them may alter their vertical distribution. These modified distributions based on species interactions are a common phenomenon, which may be driven by habitat partitioning in the aquatic environment (Werner and Hall 1977, Werner et al. 1983, Leibold 1991) and especially among phytoplankton (Carney et al. 1988).

Relationships between depth of the single peaks and environmental variables generally agree with model predictions. Greater background light attenuation should result in a shallower peak due to increased light limitation. Support for this prediction is shown in Figure 4.7c. As predicted, greater turbulent diffusion results in a a shallower peak because the increases in turbulent diffusion may have increased nutrient flux from near the sediments to the biomass peak (Figure 4.7d). As predicted, a deeper water column results in a deeper peak, likely because the nutrient source is deeper (Figure 4.7b).

However, effects of two of the predictor variables differ in directionality from our predictions. We predicted mixed layer depth to have no effect on depth of the peak, however, depth of the peak was deeper with greater mixed layer depths. It is possible that this result is more of an artifact of the definition of peaks (a peak in this analysis must be below the mixed layer) but the global fluorescence maximum model also shows that a deeper mixed layer depth results in a deeper peak (Table 4.2). Another possibility is that peaks are composed of actively motile species that preferentially seek lower turbulent mixing locations (Franks 2001, Incze et al. 2001) or species that sink to fluid of equal density (Condie and Bormans 1997) below the mixed layer.

Additionally, total phosphorus in the mixed layer had a different effect on peak depth than predicted. Peaks are deeper with increasing TP in the mixed layer. We predicted increasing nutrient input to the mixed layer to move the depth of the peak shallower because biomass in the mixed layer increases and shades the biomass in the peak in the deep layer. However, there may be little mixed-layer biomass because the biomass there is limited by another factor such as grazing or washout. In these

cases, excess nutrients may be available to the deep layer peak that is deeper and hence closer to the nutrient source at the bottom than predicted because of the extra mortality above it. More data is needed from other lakes to determine the robustness of this unexpected pattern (next paragraph).

Although it is likely that different factors may have different relative importance between lakes, a handful of environmental variables can explain much of the variation in the single peak depth distribution. Other studies have shown similar variables to be important. Barbiero and Tuchman (2001) show that light attenuation regulates DCMs in the Laurentian Great Lakes. Longhi and Beisner (2009) also show shallower peaks with greater background attenuation. However, they show the opposite trend for TP in the mixed layer. In their data, the peak occurs shallower with more TP in the mixed layer. Their result is also more similar to Lake Geneva, where a reduction in phosphorus inputs to the surface led to a deepening of the depth of the DCM (Anneville and Leboulanger 2001).

Other studies have shown factors other than what we considered here to be important in determining depth distribution. Peaks have been shown to track the sulfide-oxygen boundary (Gasol et al. 1992). Grazing can also shape or limit the upper boundary of the peak and peaks have also been shown to track the silica gradient (Barbiero and McNair 1996). Previous studies have also shown that the depth of the peak roughly tracks the light level that is 1% of the surface irradiance. However, the 1% light level, and hence the depth of the 1% light level often used to delineate the euphotic zone, can fluctuate significantly due to differences in surface irradiance and processes operating within the water column so it is not clear why algae would follow this light level (Banse 2004).

4.5.3 Amount and distribution of biomass

Total biomass can be determined by a number of factors (e.g. Lampert et al. 1986, Schindler 1977, Diehl et al. 2002), but results support some model predictions. Total biomass showed a positive relationship with water column depth (Figure 4.8a), more likely the result of integrating biomass over the entire water column. Total biomass showed a positive relationship with background light attenuation (Figure 4.8a) but we predicted background light attenuation to decrease or have no effect on biomass. If it merely had no effect, then a conclusion might be that biomass was never really light-limited. However, because it increased, another explanation is needed. It is possible that another variable, such as an essential or supplemental resource is correlated with background attenuation that we did not consider in the model.

Deep layer biomass shows some predicted relationships with environmental variables. Biomass in the deep layer decreased with mixed layer depth (Figure 4.9b) in line with model predictions, but it increased with water column depth (Figure 4.9b), which is opposite of what we predicted. Relationships with water column depth and mixed layer depth could be an artifact, however, because they delineate the boundaries for integrating deep layer biomass. Background light attenuation increased deep layer biomass (Figure 4.9d) and we predicted it should have no effect or decrease biomass but this could be for the same reasons background attenuation impacted total biomass.

Mixed layer biomass followed many of the predicted relationships with environmental variables. Biomass in the mixed layer increased with total phosphorus in the mixed layer (Figure 4.10b). Biomass in the mixed layer increased with mixed layer depth (Figure 4.10a), which we predicted it could do depending on the state of the population, although this could be an artifact of integrating over the mixed layer to calculate mixed layer depth. Background light attenuation increased mixed layer

biomass (Figure 4.9d) and we predicted it should have no effect or decrease it, but once again, this could be for the same reasons background attenuation impacted total biomass.

4.5.4 Multiple peaks and the environment

We frequently found multiple algal peaks within a water column. How can multiple peaks exist? For a single species in opposing gradients of nutrients and light, theory predicts a single best location in the water column (Klausmeier and Litchman 2001). However, multiple peaks can be caused by multiple nutrient sources (Ch. 2), but for this to be the case, all peaks but the deepest one must be nutrient limited. A plot of light versus nutrient conditions at the peaks should yield little scatter along the nutrient axis, resulting in a vertical regression line. However, a plot of light versus nutrient conditions show a lot of variation in nutrient and light levels and exhibits a strong negative relationship between the light and nutrient levels (Figure 4.11). A nutrient-light competitive tradeoff has been proposed to explain coexistence of species in well-mixed (Huisman and Weissing 1995), poorly-mixed (Huisman et al. 2006), and stratified environments (Yoshiyama et al. 2009). Some empirical evidence exists for such a tradeoff (Carney et al. 1988, Strzepek and Harrison 2004, but see Passarge et al. 2006) making its existence likely (Litchman and Klausmeier 2008). The negative relationship between light and nutrient levels at peaks is consistent with the hypothesis of a nutrient-light tradeoff in species that comprise the peaks. Our community composition data demonstrated that indeed, separate peaks within a lake are dominated by different species. We suggest that the changes in species dominance between peaks are partly due to a tradeoff in competitive abilities for nutrients and light.

We found that multiple peaks can be present simultaneously. The number of peaks *is* determined by physical space, the strength of the light gradient, and the strength

of the nutrient gradient (Figure 4.12). The amount of physical space available for peaks to form may be analogous to general species-area relationships (Smith et al. 2005), and likely there is some minimal amount of space required for multiple peaks to exist. However, Yoshiyama et al. (2009) predict peaks to attract one another and we have also observed multiple peaks within very small (< 1 m) depth spans. Two measures of resource heterogeneity also acted to increase number of peaks, which is consistent with the heterogeneity hypothesis of maintaining diversity (Stevens and Carson 2002). Increasing background light attenuation, a measure of the strength of the light gradient, also acts to increase the number of peaks. Increasing the change in total phosphorus with depth in the deep layer also acts to increase the number of peaks. However, this phosphorus gradient is correlated with phosphorus supply. Phosphorus supply was significant in an alternative model, ultimately making it difficult to distinguish between the heterogeneity and energy hypothesis (Stevens and Carson 2002) for nutrients.

4.5.5 Community

Somewhat surprisingly, species diversity did not differ within the water column even though strong environmental gradients existed and the mixed layer and the DCM are unique niches that are physically isolated from one another. To our knowledge, this is the first study that compares phytoplankton species diversity at different depths in a water column. Although diversity was not different between the mixed layer and main DCM, the environmental variables that explain diversity differ between these two locations. Both locations had significant variables that describe in-situ conditions. For example, total phosphorus in the mixed layer affected mixed layer diversity but not DCM diversity and light at the bottom of the mixed layer (supply rate to deep layer) explained DCM diversity but not mixed layer diversity (Table 4.7).

Although it may be expected that communities within a lake are more similar to

one another than communities across lakes, with large landscape-level driven differences in environmental conditions between lakes, discrete depths within a lake were often quite dissimilar to one another (Fig. 4.14a) relative to overall dissimilarity (Fig. 4.14b). Although a relatively small suite of species has been found in DCMs (Padisák 2004), we have shown that communities inhabiting the DCM niche are as dissimilar from one another as communities in mixed layers (Fig. 4.14c,d). Keeping this in mind, and that species diversity did not differ between the mixed layer and DCM, it is perhaps not surprising that mixed layer and DCM communities varied similarly across lakes (Fig. 4.14e). Two environmental variables, acting in opposition to one another, may have been related to the dissimilarity between mixed layer and DCM communities (Table 4.8, Fig. 4.15a,b). Although the overall model is not significant ($P > 0.05$), the trends in this best model are worth discussing. For example, the difference between light and nutrient effects indicates that light may be more important for determining which community can exist in the deep layer while nutrients may be abundant enough in the water column that they become an important axis of community divergence.

Some taxonomic groups are known in particular for forming DCMs (e.g. flagellates) and some groups are known in particular for growing in the mixed layer or forming surface blooms (e.g. cyanobacteria, green algae) but we found these groups in both niches (Fig. 4.16). Dominance of taxonomic groups varied as much in DCMs as in the mixed layer. Often, a single taxonomic group dominated at all depths of a lake. This result may indicate that our model that considers an aggregate community may be a good approximation in some situations.

Across lakes, the relationships between taxonomic group relative abundance and environmental variables (Table 4.9) mostly conform to understood patterns in taxonomic group abundances (Reynolds 1984). For example, cyanobacteria increased with *Daphnia* abundance because they are not grazed as heavily by *Daphnia* as some

other groups (Sarnelle 1992) and green algae decreased with background attenuation because they often have a high light competitive strategy (Richardson et al. 1983, Schwaderer et al. submitted). Some caution is warranted about concluding too much from the taxonomic group abundance across lakes because lakes with more samples are weighted heavier in the analyses. Nonetheless, because we are documenting the across-lake and within-lake community structure, we considered all (sampled) depths that have peaks in biomass. These results shed light on communities in the whole lake (Longhi and Beisner 2009) rather than just the mixed layer (Duarte and Canfield 1992, Watson et al. 1997).

Taxonomic groups showed some correlation with local conditions of light and dissolved phosphorus in a lake (Table 4.10). Although it does not fully explain the vertical zonation observed (Fig. 4.16), there is indication that different taxonomic groups have different requirements and impacts on their environment. Cyanobacteria and euglenoids actually declined in the community with increasing light possibly due to competition or a physiological or ecological tradeoff that allows them to grow in low light conditions. Chrysophytes and diatoms increased in the community with increasing light. Although the dissolved phosphorus term was not significant ($P > 0.05$) in any of the models, it was in the best model for two groups. The amount of dissolved phosphorus may be a better measure of the impact on the resource levels, rather than the requirements (Tilman 1982).

A single niche, such as the mixed layer or a DCM within a lake, is usually rather diverse in species richness but almost always heavily dominated by a single species. The identity of that dominant species changed with depth in most of the lakes (Appendix Table), begging the classic community ecology question, why do we find different species across habitats?

We measured whether species were found in different habitats by whether the dominance switched within the water column (mixed layer to DCM or DCM to DCM)

and showed that the only predictor of dominance switch was water column depth. Water column depth can determine the number of peaks due to the effect it has on the deep layer span, which was shown to be a significant predictor. Thus with more peaks, the switch in dominance is more likely.

It is difficult to generalize too much about patterns in species abundances with depth because of the large regional species pool, few samples with the same species dominating, and whole lake and within lake interacting environmental factors. Nevertheless, it appears that size changes with depth in some genera and that bigger species tend to be deeper (Appendix Table). Bigger species may be poorer nutrient competitors (Pasciak and Gavis 1974), have higher sinking rates (Vogel 1994), and/or be more resistant to grazing (Sarnelle 1992), resulting in size segregation within the water column even if they are poorer light competitors (Finkel et al. 2004, Schwaderer et al. submitted). It also appears that filamentous cyanobacteria are in greater abundance at depth, which is likely because they are good light competitors (Schwaderer et al. submitted). There appeared to be no real trend in evenness or diversity in the mixed layer versus DCMs based on the dominant (> 5% of community) species, either can be much greater than other (Appendix Table).

One final interesting result is that several species appear to exhibit a bimodal distribution within the water column. For example, a Chroococcus species was abundant at a shallow depth, disappeared at a deeper depth, and then reappeared at an even deeper depth in Lime lake and Fine lake. Theory predicts that for this to occur, either the limiting environmental factor has to be the same in both locations or the species must be phenotypically different in each location (simulation results not shown). It is likely that some of these morphologically identical species are actually different physiologically so our resolution of classification could not distinguish between these cryptospecies or different strains of the same species. In such a case, closely related species may partition the vertical niche more than distantly related species, analagous

to divergent selection at the tips of a phylogenetic tree rather than deeper in the tree (Losos et al. 2003).

4.5.6 Future work

Environmental filtering of phytoplankton between lakes and then phytoplankton sorting within lakes may not exist in a strict hierarchy due to interactions with the scale of taxonomic resolution. Scale is important (Levin 1992) for examining community structure across landscapes of lakes and with depth within lakes. Species within each taxonomic group we considered can be very different (Reynolds 1984), so these broad taxonomic groups can overlap in niche space. This suggests that the division of niche space across and within lakes can happen at the species level. Unfortunately, species-specific environmental niche data is sparse, both in this study due to the large regional species pool and turnover between lakes and depths, and in other studies, so it is difficult to describe species-level spatial distribution patterns let alone ascribe these patterns to environmental conditions. To further complicate matters, environmental conditions are mediated by the interactions of species themselves. Future research should consider this sorting of different taxonomic resolutions at different spatial scales in the environment (landscape versus within a lake) and with explicit consideration of the feedbacks on the environment created by different phytoplankton. This also highlights the importance of examining traits rather than taxonomic classifications. A community aggregated light-competitive-ability trait was not related to light conditions for communities in this study (results not shown) but more species-specific trait data are needed to examine relationships between phytoplankton traits and the environment.

4.5.7 Further importance and conclusions

Nutrient concentration measured at the sediment interface was a better predictor for many biotic variables than nutrient concentration measured in the mixed layer, as indicated by presence and absence of these variables in the best models. Specifically, total biomass and mixed layer diversity, as well as deep layer biotic variables such as deep layer biomass, diversity and number of peaks had total phosphorus measured at the bottom in their best models. Yet, most studies do not measure this variable, rather, they measure total phosphorus at the surface. If a researcher is interested in explaining population and community structure, the results of this study indicate that nutrients at the bottom of the water column may be a better measure of potential ecosystem processes. This highlights the importance of studying spatial coupling in ecosystems, as some locations may be more tightly coupled with distant locations than their local environment.

This study addresses crucial ideas in ecology, including, understanding and predicting spatial distributions of organisms, matching the strategies of the organisms with their environments, and demonstrating how biological and physical components of an ecosystem are coupled, using the plankton community as an example. Climate change strongly affects physical processes operating in lakes in the Great Lakes region (Kling et al. 2003) and worldwide (Fee et al. 1996, Schindler 1997, Livingstone 2003, O'Reilly et al. 2003, Verburg et al. 2003). Understanding how physical processes operating in lakes impact plankton communities is imperative to predict how future climate change may alter freshwater ecosystems.

4.6 Appendix

Table 4.12: Appendix Table of dominant species for all samples. Shown are relative abundances for species densities that are > 5% of the total community density of a sample.

Lake	Date	Depth[m]	Taxonomic	Species	Abund.
Brooks	19-Sep	Integrated	Cyanobacteria	*Chroococcus* small (cells)	0.47
			Cyanobacteria	*Aphanocapsa* (small colony)	0.19
			Diatom	*Cyclotella michiganiana* (sm)	0.07
			Green	*Oocystis* (cells)	0.06
Brooks	19-Sep	3	Cyanobacteria	*Aphanocapsa* (small colony)	0.43
			Cyanobacteria	*Chroococcus* small (cells)	0.22
			Cyanobacteria	*Anabaena* (cells)	0.06
			Chrysophyte	*Chrysochromulina*	0.06
			Green	*Oocystis* (cells)	0.05
Little Long	6-Sep	Integrated	Green	Coccoid Green 5um	0.43
			Diatom	*Cyclotella michiganiana* (sm)	0.23
			Cyanobacteria	*Aphanocapsa incerta*	0.08
			Green	Green Flagellate	0.06
Little Long	6-Sep	4	Chrysophyte	Chrysophyte ~5-7um	0.54
			Diatom	*Cyclotella michiganiana* (sm)	0.20
			Cyanobacteria	*Aphanocapsa* (small colony)	0.06
Little Long	6-Sep	8.5	Chrysophyte	*Chrysochromulina*	0.25
			Diatom	*Cyclotella michiganiana* (sm)	0.17
			Chrysophyte	Chrysophyte ~5-7um	0.16
			Cyanobacteria	*Chroococcus* small (cells)	0.10
			Cyanobacteria	*Aphanocapsa* (small colony)	0.09
			Green	*Oocystis* (cells)	0.06
Big Fisher	26-Sep	Integrated	Cyanobacteria	*Chroococcus* small (cells)	0.49
			Dinoflagellate	Dinoflagellate, most w/o shell	0.10
			Diatom	*Cyclotella michiganiana* (sm)	0.08
			Cyanobacteria	*Aphanocapsa incerta*	0.07
Little Glen	26-Sep	Integrated	Chrysophyte	*Chrysochromulina*	0.29
			Cyanobacteria	*Chroococcus* small (cells)	0.21
			Cyanobacteria	*Aphanocapsa* (small colony)	0.14
			Cryptophyte	*Rhodomonas minuta*	0.07
			Unidentified	Rod shaped cells	0.07

Table 4.12 continued

Lake	Date	Depth[m]	Taxonomic	Species	Abund.
Little Fisher	26-Sep	Integrated	Chrysophyte	*Chrysochromulina*	0.43
			Diatom	*Cyclotella michiganiana* (sm)	0.14
			Cyanobacteria	*Chroococcus* med (cells)	0.13
			Cyanobacteria	*Aphanocapsa* (small colony)	0.05
			Green	Green Flagellate	0.05
Warner	13-Sep	Integrated	Cyanobacteria	*Chroococcus* small (cells)	0.57
			Cyanobacteria	*Chroococcus* med (cells)	0.11
			Cyanobacteria	*Chroococcus* large (cells)	0.06
Warner	13-Sep	10.25	Cyanobacteria	*Aphanocapsa* (small colony)	0.32
			Cyanobacteria	*Chroococcus* small (cells)	0.16
			Chrysophyte	*Chrysochromulina*	0.10
			Cryptophyte	*Rhodomonas minuta*	0.09
			Cyanobacteria	*Chroococcus* med (cells)	0.06
			Cryptophyte	*Cryptomonas*	0.05
Warner	13-Sep	11.75	Green	*Synechococcus*	0.37
			Cyanobacteria	*Pseudanabaena* (cells)	0.27
			Cyanobacteria	*Chroococcus* small (cells)	0.18
Pine	13-Sep	Integrated	Cyanobacteria	*Chroococcus* small (cells)	0.67
			Chrysophyte	*Chrysochromulina*	0.07
			Cyanobacteria	*Aphanocapsa* (small colony)	0.05
Pine	13-Sep	9	Cyanobacteria	*Chroococcus* small (cells)	0.50
			Cyanobacteria	*Aphanocapsa* (small colony)	0.19
Little Mill	5-Sep	Integrated	Cyanobacteria	*Chroococcus* small (cells)	0.31
			Chrysophyte	Chrysophyte ~5-7um	0.14
			Chrysophyte	*Chrysochromulina*	0.11
			Cyanobacteria	*Aphanocapsa* (small colony)	0.07
			Cryptophyte	*Rhodomonas minuta*	0.06
			Cyanobacteria	*Anabaena* (cells)	0.06

Table 4.12 continued

Lake	Date	Depth[m]	Taxonomic	Species	Abund.
Little Mill	5-Sep	9	Cyanobacteria	*Chroococcus* small (cells)	0.23
			Green	coccoid green clusters	0.16
			Cyanobacteria	*Aphanocapsa* (small colony)	0.06
			Cyanobacteria	*Chroococcus* med (cells)	0.06
			Cyanobacteria	*Pseudanabaena* (strands)	0.06
			Diatom	*Fragilaria crotonensis*	0.05
			Chrysophyte	*Chrysochromulina*	0.05
Big Glen	26-Sep	Integrated	Green	Coccoid Green <3um	0.15
			Cyanobacteria	*Chroococcus* small (cells)	0.14
			Diatom	*Cyclotella michiganiana* (sm)	0.13
			Chrysophyte	*Ochromonas*	0.09
			Cryptophyte	*Rhodomonas minuta*	0.08
			Cyanobacteria	*Aphanocapsa incerta*	0.08
			Green	*Oocystis* (cells)	0.07
			Cyanobacteria	Filamentous	0.05
Big Glen	26-Sep	17	Chrysophyte	*Chrysochromulina*	0.23
			Chrysophyte	Chrysophyte ~5-7um	0.20
			Cyanobacteria	*Aphanocapsa* (small colony)	0.08
			Green	*Oocystis* (cells)	0.07
			Chrysophyte	*Ochromonas*	0.06
			Diatom	*Cyclotella comta* (large)	0.06
			Cyanobacteria	*Chroococcus* small (cells)	0.05
Shaw	12-Sep	Integrated	Cyanobacteria	*Chroococcus* small (cells)	0.64
			Cyanobacteria	*Aphanocapsa* (small colony)	0.07
			Cyanobacteria	*Chroococcus* med (cells)	0.06
			Chrysophyte	*Chrysochromulina*	0.05
Baldwin	21-Sep	Integrated	Cyanobacteria	*Chroococcus* small (cells)	0.67
			Chrysophyte	*Chrysochromulina*	0.06
			Cyanobacteria	*Aphanocapsa* (small colony)	0.05
Baldwin	21-Sep	8	Cyanobacteria	*Chroococcus* small (cells)	0.65
			Cyanobacteria	*Aphanocapsa* (small colony)	0.07
Baldwin	21-Sep	12.5	Cyanobacteria	*Pseudanabaena* (cells)	0.62
			Cyanobacteria	*Chroococcus* small (cells)	0.18
			Cyanobacteria	*Aphanocapsa* (small colony)	0.07

Table 4.12 continued

Lake	Date	Depth[m]	Taxonomic	Species	Abund.
Wintergreen	4-Sep	0	Cyanobacteria	*Woronichinia* # in colony	0.58
			Cyanobacteria	*Woronichinia*	0.28
Wintergreen	4-Sep	3	Cyanobacteria	*Woronichinia*	0.92
Wintergreen	4-Sep	4.25	Cyanobacteria	*Woronichinia*	0.84
			Cyanobacteria	*Woronichinia* # in colony	0.10
Pleasant	5-Sep	Integrated	Chrysophyte	Chrysophyte ~8um	0.45
			Cyanobacteria	*Aphanocapsa* (small colony)	0.20
			Cyanobacteria	*Microcystis* (colony, cells)	0.12
			Green	*Staurastrum*	0.06
Pleasant	5-Sep	4	Chrysophyte	Chrysophyte ~8um	0.62
			Cyanobacteria	*Aphanocapsa* (small colony)	0.12
			Chrysophyte	Chrysophyte ~5-7um in col.	0.06
Baker	12-Sep	0	Cyanobacteria	*Woronichinia* # in colony	0.50
			Cyanobacteria	*Woronichinia*	0.29
Baker	12-Sep	4.75	Cyanobacteria	*Woronichinia* # in colony	0.51
			Cyanobacteria	*Woronichinia*	0.19
			Cyanobacteria	*Aphanocapsa* (small colony)	0.13
Baker	12-Sep	5.75	Cyanobacteria	*Woronichinia* # in colony	0.34
			Cyanobacteria	*Woronichinia*	0.15
			Chrysophyte	Chrysophyte ~5-7um	0.08
			Cyanobacteria	*Merismopedia* (small cells)	0.08
			Cyanobacteria	*Aphanizemenon*	0.07
			Cyanobacteria	*Aphanocapsa* (small colony)	0.06
Cloverdale	11-Sep	Integrated	Cyanobacteria	*Woronichinia*	0.44
			Cyanobacteria	*Aphanocapsa* (small colony)	0.18
			Cyanobacteria	*Woronichinia* # in colony	0.09
			Chrysophyte	Chrysophyte ~5-7um	0.07
Cloverdale	11-Sep	4	Cyanobacteria	*Woronichinia* # in colony	0.35
			Cyanobacteria	*Woronichinia*	0.25
			Cyanobacteria	*Aphanizomenon*	0.17

Table 4.12 continued

Lake	Date	Depth[m]	Taxonomic	Species	Abund.
Cloverdale	11-Sep	5	Cyanobacteria	*Aphanizomenon*	0.48
			Cyanobacteria	*Microcystis* (colony, cells)	0.16
			Cyanobacteria	*Woronichinia*	0.13
			Cyanobacteria	*Aphanocapsa* (small colony)	0.08
Bassett	12-Sep	Integrated	Cyanobacteria	*Aphanizomenon*	0.57
			Cyanobacteria	*Planktolyngbya* (straight)	0.18
			Chrysophyte	Chrysophyte ~<5 um	0.11
Bassett	12-Sep	6	Green	*Sphaerocystis* (cells, colony)	0.30
			Chrysophyte	Chrysophyte ~<5 um	0.24
			Green	*Chlamydomonas*	0.11
			Cyanobacteria	*Aphanocapsa* (small colony)	0.10
			Unidentified	long thin transparent rod	0.08
			Cyanobacteria	*Aphanizomenon*	0.05
			Cyanobacteria	*Planktothrix*	0.05
Bassett	12-Sep	7	Chrysophyte	Chrysophyte ~<5 um	0.33
			Unidentified	long thin transparent rod	0.24
			Cyanobacteria	*Cyanobium*	0.13
			Cyanobacteria	*Planktothrix*	0.10
			Cryptophyte	*Rhodomonas minuta*	0.05
Hess	19-Sep	Integrated	Cyanobacteria	*Aphanocapsa* (small colony)	0.71
			Cyanobacteria	*Chroococcus* small (cells)	0.14
			Cyanobacteria	*Planktolyngbya* (straight)	0.06
Hess	19-Sep	5.5	Cyanobacteria	*Aphanocapsa* (small colony)	0.55
			Cyanobacteria	*Chroococcus* small (cells)	0.24
Lawrence	4-Sep	Integrated	Cyanobacteria	*Woronichinia* # in colony	0.36
			Cyanobacteria	*Woronichinia*	0.23
			Chrysophyte	*Tribonema*	0.16
			Chrysophyte	Chrysophyte ~5-7um	0.06
Lawrence	4-Sep	9.5	Cyanobacteria	*Aphanocapsa* (small colony)	0.68
			Chrysophyte	Chrysophyte ~5-7um in colon	0.13

Table 4.12 continued

Lake	Date	Depth[m]	Taxonomic	Species	Abund.
Lawrence	4-Sep	11.5	Cyanobacteria	*Aphanocapsa* large cells (col.)	0.43
			Cyanobacteria	*Aphanocapsa* (small colony)	0.14
			Cyanobacteria	*Cyanobacterium*	0.14
			Cyanobacteria	*Aphanocapsa* large cells (cells	0.12
			Cyanobacteria	*Arthrospira*	0.05
Sherman	10-Sep	Integrated	Cyanobacteria	*Woronichinia* # in colony	0.50
			Green	*Sphaerocystis* (cells, colony)	0.16
			Chrysophyte	Chrysophyte ~<5 um	0.06
Sherman	10-Sep	8	Cyanobacteria	*Woronichinia* # in colony	0.61
			Green	*Sphaerocystis* (unicells)	0.12
			Cyanobacteria	*Aphanocapsa* (small colony)	0.06
			Chrysophyte	Chrysophyte ~<5 um	0.05
			Cyanobacteria	*Chroococcus* small (cells)	0.05
Sherman	10-Sep	8.5	Green	*Staurastrum*	0.30
			Green	*Sphaerocystis* (unicells)	0.15
			Cyanobacteria	*Woronichinia*	0.13
			Cyanobacteria	*Chroococcus* small (cells)	0.10
			Chrysophyte	Chrysophyte ~<5 um	0.05
Long	12-Sep	Integrated	Cyanobacteria	*Woronichinia* # in colony	0.30
			Cyanobacteria	*Aphanocapsa* large cells (col.)	0.27
			Cyanobacteria	*Woronichinia*	0.10
			Cyanobacteria	*Aphanocapsa* (small colony)	0.05
Long	12-Sep	7.5	Cyanobacteria	*Woronichinia* # in colony	0.41
			Cyanobacteria	*Aphanocapsa* (small colony)	0.25
			Cyanobacteria	*Chroococcus* med (cells)	0.11
			Cyanobacteria	*Chroococcus* small (cells)	0.08
			Cyanobacteria	*Woronichinia*	0.07
Long	12-Sep	8.5	Cyanobacteria	*Woronichinia* # in colony	0.44
			Cyanobacteria	*Aphanocapsa* (small colony)	0.25
			Cyanobacteria	*Chroococcus* med (cells)	0.09

Table 4.12 continued

Lake	Date	Depth[m]	Taxonomic	Species	Abund.
Lawrence	4-Sep	11.5	Cyanobacteria	*Aphanocapsa* large cells (col.)	0.43
			Cyanobacteria	*Aphanocapsa* (small colony)	0.14
			Cyanobacteria	*Cyanobacterium*	0.14
			Cyanobacteria	*Aphanocapsa* large cells (cells	0.12
			Cyanobacteria	*Arthrospira*	0.05
Sherman	10-Sep	Integrated	Cyanobacteria	*Woronichinia* # in colony	0.50
			Green	*Sphaerocystis* (cells, colony)	0.16
			Chrysophyte	Chrysophyte ~<5 um	0.06
Sherman	10-Sep	8	Cyanobacteria	*Woronichinia* # in colony	0.61
			Green	*Sphaerocystis* (unicells)	0.12
			Cyanobacteria	*Aphanocapsa* (small colony)	0.06
			Chrysophyte	Chrysophyte ~<5 um	0.05
			Cyanobacteria	*Chroococcus* small (cells)	0.05
Sherman	10-Sep	8.5	Green	*Staurastrum*	0.30
			Green	*Sphaerocystis* (unicells)	0.15
			Cyanobacteria	*Woronichinia*	0.13
			Cyanobacteria	*Chroococcus* small (cells)	0.10
			Chrysophyte	Chrysophyte ~<5 um	0.05
Long	12-Sep	Integrated	Cyanobacteria	*Woronichinia* # in colony	0.30
			Cyanobacteria	*Aphanocapsa* large cells (col.)	0.27
			Cyanobacteria	*Woronichinia*	0.10
			Cyanobacteria	*Aphanocapsa* (small colony)	0.05
Long	12-Sep	7.5	Cyanobacteria	*Woronichinia* # in colony	0.41
			Cyanobacteria	*Aphanocapsa* (small colony)	0.25
			Cyanobacteria	*Chroococcus* med (cells)	0.11
			Cyanobacteria	*Chroococcus* small (cells)	0.08
			Cyanobacteria	*Woronichinia*	0.07
Long	12-Sep	8.5	Cyanobacteria	*Woronichinia* # in colony	0.44
			Cyanobacteria	*Aphanocapsa* (small colony)	0.25
			Cyanobacteria	*Chroococcus* med (cells)	0.09

Table 4.12 continued

Lake	Date	Depth[m]	Taxonomic	Species	Abund.
Long	12-Sep	10.25	Cyanobacteria	*Aphanocapsa* (small colony)	0.36
			Cyanobacteria	*Chroococcus* small (cells)	0.21
			Cyanobacteria	*Pseudanabaena* (strands)	0.10
			Cyanobacteria	*Chroococcus* med (cells)	0.08
			Cyanobacteria	*Arthrospira*	0.06
Lime	19-Sep	Integrated	Cyanobacteria	*Chroococcus* small (cells)	0.30
			Chrysophyte	Chrysophyte ~<5 um	0.22
			Chrysophyte	Chrysophyte ~8um	0.09
			Unidentified	small unicells (unclassifiable)	0.08
			Chrysophyte	Chrysophyte ~5-7um	0.07
			Cyanobacteria	*Gomphosphaeria* (cells)	0.05
Lime	19-Sep	2.5	Chrysophyte	Chrysophyte ~8um	0.59
			Chrysophyte	Chrysophyte ~<5 um	0.13
			Cyanobacteria	*Gomphosphaeria* (cells)	0.07
			Cyanobacteria	*Aphanocapsa* (small colony)	0.06
Lime	19-Sep	5	Chrysophyte	Chrysophyte ~<5 um	0.21
			Cyanobacteria	*Aphanocapsa* (small colony)	0.20
			Cyanobacteria	*Gomphosphaeria* (cells)	0.12
			Green	*Dictyosphaerium* (cells)	0.11
			Chrysophyte	Chrysophyte ~5-7um	0.07
			Cryptophyte	*Cryptomonas*	0.05
Lime	19-Sep	8	Cyanobacteria	*Chroococcus* small (cells)	0.20
			Cyanobacteria	*Gomphosphaeria* (cells)	0.18
			Cyanobacteria	*Pseudanabaena* (strands)	0.15
			Cyanobacteria	*Chroococcus* med (cells)	0.13
			Green	*Dictyosphaerium* (cells)	0.12
			Cyanobacteria	*Aphanocapsa* (small colony)	0.07
Fine	5-Sep	Integrated	Cyanobacteria	*Chroococcus* small (cells)	0.34
			Cyanobacteria	*Chroococcus* med (cells)	0.15
			Cyanobacteria	*Aphanocapsa* (small colony)	0.10
			Chrysophyte	Chrysophyte ~<5 um	0.07
			Green	*Sphaerocystis* (cells, colony)	0.06
			Cyanobacteria	*Aphanothece* (small colony)	0.06

Table 4.12 continued

Lake	Date	Depth[m]	Taxonomic	Species	Abund.
Fine	5-Sep	6.5	Cyanobacteria	*Microcystis* (colony, cells)	0.55
			Cyanobacteria	*Aphanocapsa* (small colony)	0.15
			Cyanobacteria	*Aphanocapsa* large cells (col.)	0.07
Fine	5-Sep	7.25	Cyanobacteria	*Aphanocapsa* (small colony)	0.23
			Cyanobacteria	*Microcystis* (colony, cells)	0.15
			Cyanobacteria	*Woronichinia* # in colony	0.15
			Cyanobacteria	*Aphanocapsa* large cells (col.)	0.11
			Cyanobacteria	*Chroococcus* small (cells)	0.07
Bristol	5-Sep	Integrated	Cyanobacteria	*Microcystis* (colony, cells)	0.53
			Cyanobacteria	*Aphanocapsa* (small colony)	0.09
			Cyanobacteria	*Woronichinia* # in colony	0.09
			Cyanobacteria	*Aphanocapsa* large cells (col.)	0.06
			Chrysophyte	Chrysophyte ~<5 um	0.06
Bristol	5-Sep	8.5	Cyanobacteria	*Woronichinia* # in colony	0.42
			Cyanobacteria	*Aphanocapsa* (small colony)	0.14
			Chrysophyte	Chrysophyte ~<5 um	0.11
			Chrysophyte	Chrysophyte ~5-7um	0.05
Gun	24-Sep	Integrated	Cyanobacteria	*Aphanocapsa* large cells (col.)	0.29
			Cyanobacteria	*Aphanocapsa* (small colony)	0.23
			Chrysophyte	Chrysophyte ~<5 um	0.18
			Cyanobacteria	*Chroococcus* small (cells)	0.07
Gun	24-Sep	6.5	Cyanobacteria	*Aphanocapsa* (small colony)	0.24
			Cyanobacteria	*Chroococcus* small (cells)	0.20
			Chrysophyte	Chrysophyte ~<5 um	0.16
			Cyanobacteria	*Aphanocapsa* large cells (col.)	0.12
Gun	24-Sep	13.5	Cyanobacteria	*Chlorogloea*	0.22
			Cyanobacteria	*Cyanobacterium*	0.21
			Cyanobacteria	*Chroococcus* small (cells)	0.18
			Cyanobacteria	*Aphanocapsa* (small colony)	0.12
			Chrysophyte	Chrysophyte ~<5 um	0.11
			Cyanobacteria	*Chroococcus* med (cells)	0.11

Table 4.12 continued

Lake	Date	Depth[m]	Taxonomic	Species	Abund.
Hogsett	21-Sep	Integrated	Cyanobacteria	*Chroococcus* small (cells)	0.46
			Cyanobacteria	*Microcystis* (medium)	0.37
Hogsett	21-Sep	6.75	Cyanobacteria	*Chroococcus* small (cells)	0.37
			Cyanobacteria	*Aphanocapsa* (small colony)	0.16
			Chrysophyte	Chrysophyte ~<5 um	0.15
			Cyanobacteria	*Microcystis* (colony, cells)	0.05
			Chrysophyte	Chrysophyte ~5-7um	0.05
Hogsett	21-Sep	7.5	Cyanobacteria	*Aphanocapsa* large cells (col.)	0.19
			Cyanobacteria	*Chroococcus* small (cells)	0.17
			Chrysophyte	Chrysophyte ~<5 um	0.15
			Cyanobacteria	*Aphanocapsa* (small colony)	0.13
			Cyanobacteria	*Planktothrix*	0.08
			Cryptophyte	*Rhodomonas minuta*	0.05
Swan	17-Sep	Integrated	Chrysophyte	Chrysophyte ~<5 um	0.31
			Cyanobacteria	*Aphanizomenon*	0.25
			Cyanobacteria	*Aphanocapsa* (small colony)	0.18
			Chrysophyte	Chrysophyte ~5-7um	0.08
			Cyanobacteria	*Planktolyngbya* (straight)	0.05
Little Tom	17-Sep	Integrated	Chrysophyte	*Chrysochromulina*	0.51
			Cyanobacteria	*Aphanocapsa* (small colony)	0.17
			Cyanobacteria	*Chroococcus* small (cells)	0.12
Spring	24-Sep	Integrated	Cyanobacteria	*Pseudanabaena* (strands)	0.29
			Chrysophyte	*Chrysochromulina*	0.18
			Cyanobacteria	*Planktolyngbya* (straight)	0.08
			Cyanobacteria	*Aphanocapsa* (small colony)	0.07
			Cyanobacteria	*Planktolyngbya* (curved)	0.07
Donnell	21-Sep	Integrated	Cyanobacteria	*Chroococcus* small (cells)	0.69
			Chrysophyte	*Chrysochromulina*	0.09
			Cyanobacteria	*Aphanocapsa* (small colony)	0.06
Donnell	21-Sep	4	Cyanobacteria	*Chroococcus* small (cells)	0.71
			Cyanobacteria	*Aphanocapsa* (small colony)	0.09
			Chrysophyte	*Chrysochromulina*	0.08

Table 4.12 continued

Lake	Date	Depth[m]	Taxonomic	Species	Abund.
Gravel	21-Sep	Integrated	Cyanobacteria	*Chroococcus* small (cells)	0.44
			Cyanobacteria	*Chroococcus* large (cells)	0.24
			Chrysophyte	*Chrysochromulina*	0.13
Gravel	21-Sep	4.8	Cyanobacteria	*Chroococcus* small (cells)	0.42
			Cyanobacteria	*Chroococcus* large (cells)	0.31
			Chrysophyte	*Chrysochromulina*	0.05

Bibliography

Bibliography

Anneville, O. and Leboulanger, C. 2001. Long-term changes in the vertical distribution of phytoplankton biomass and primary production in Lake Geneva: a response to the oligotrophication. Alti Associazione Italiana Oceanologia Limnologia 14:25–35.

Arvola, L., Ojala, A., Barbosa, F., and Heaney, S. 1991. Migration behavior of 3 cryptophytes in relation to environmental gradients - an experimental approach. British Phycological Journal 26:361–373.

Bachmann, R. W. and Canfield, D. E. 1996. Use of an alternative method for monitoring total nitrogen concentrations in Florida lakes. Hydrobiologia 323:1–8.

Banse, K. 2004. Should we continue to use the 1% light depth convention for estimating the compensation depth of phytoplankton for another 70 years? Limnology & Oceanography Bulletin 13:49–52.

Barbiero, R. P. and McNair, C. M. 1996. The dynamics of vertical chlorophyll distribution in an oligomesotrophic lake. Journal of Plankton Research 18:225–237.

Barbiero, R. P. and Tuchman, M. L. 2001. Results from the US EPA's biological open water surveillance program of the Laurentian Great Lakes: II. Deep chlorophyll maxima. Journal of Great Lakes Research 27:155–166.

Beckmann, A. and Hense, I. 2007. Beneath the surface: Characteristics of oceanic ecosystems under weak mixing conditions - A theoretical investigation. Progress in Oceanography 75:771–796.

Brown, J. H. 1984. On the relationship between abundance and distribution of species. American Naturalist 124:255–279.

Brown, P. N., Byrne, G. D., and Hindmarsh, A. C. 1989. VODE- a Variable-coefficient ODE Solver. SIAM Journal on Scientific & Statistical Computing 10:1038–1051.

Burnham, K. and Anderson, D., 2002. Model selection and multimodel inference: a practical information-theoretic approach. Springer Science+Business Media, Inc.

Burrough, P. A. 1981. Fractal dimensions of landscapes and other environmental data. Nature 294:240–242.

Camacho, A. 2006. On the occurrence and ecological features of deep chlorophyll maxima (DCM) in Spanish stratified lakes. Limnetica 25:453–478.

Carney, H. J., Richerson, P. J., Goldman, C. R., and Richards, R. C. 1988. Seasonal phytoplankton demographic-processes and experiments on interspecific competition. Ecology 69:664–678.

Carpenter, S. R. 1996. Microcosm experiments have limited relevance for community and ecosystem ecology. Ecology 77:677–680.

Carpenter, S. R., Frost, T. M., Heisey, D., and Kratz, T. K. 1989. Randoomized intervention analysis and the interpretation of whole-ecosystem experiments. Ecology 70:1142–1152.

Carpenter, S. R. and Kitchell, J. F. 1987. The temporal scale of variance in limnetic primary production. American Naturalist 129:417–433.

Christensen, D. L., Carpenter, S. R., and Cottingham, K. L. 1995. Predicting chlorophyll vertical-distribution in response to epilimnetic nutrient enrichment in small stratified lakes. Journal of Plankton Research 17:1461–1477.

Clegg, M., Maberly, S., and Jones, R. 2007. Behavioral response as a predictor of seasonal depth distribution and vertical niche separation in freshwater phytoplanktonic flagellates. Limnology & Oceanography 52:441–455.

Condie, S. A. and Bormans, M. 1997. The influence of density stratification on particle settling, dispersion and population growth. Journal of Theoretical Biology 187:65–75.

Coon, T. G., Lopez, M., Richerson, P. J., Powell, T. M., and Goldman, C. R. 1987. Summer dynamics of the deep chlorophyll maximum in Lake Tahoe. Journal of Plankton Research 9:327–344.

Crumpton, W. G., Isenhart, T. M., and Mitchell, P. D. 1992. Nitrate and organic n analyses with 2nd-derivative spectroscopy. Limnology And Oceanography 37:907–913.

Crumpton, W. G. and Wetzel, R. G. 1982. Effects of differential growth and mortality in the seasonal succession of phytoplankton populations in Lawrence Lake, Michigan. Ecology 63:1729–1739.

Cullen, J. J. and MacIntyre, J. G., 1998. Physiological ecology of harmful algal blooms, Chapter. Springer-Verlag, Berlin, Heidelberg.

Cullen, J. J., Reid, F. M. H., and Stewart, E. 1982. Phytoplankton in the surface and chlorophyll maximum off southern California in August, 1978. Journal of Plankton Research 4:665–694.

Demott, W. R. 1982. Feeding selectivities and relative ingestion rates of daphnia and bosmina. Limnology & Oceanography 27:518–527.

Depinto, J. V. and Verhoff, F. H. 1977. Nutrient regeneration from aerobic decomposition of green-algae. Environmental Science & Technology 11:371–377.

Diehl, S. 2002. Phytoplankton, light, and nutrients in a gradient of mixing depths: Theory. Ecology 83:386–398.

Diehl, S., Berger, S., Ptacnik, R., and Wild, A. 2002. Phytoplankton, light, and nutrients in a gradient of mixing depths: Field experiments. Ecology 83:399–411.

Du, Y. and Hsu, S.-B. 2008. Concentration phenomena in a nonlocal quasi-linear problem modelling phytoplankton II: Limiting profile. SIAM Journal on Mathematical Analysis 40:1441–1470.

Duarte, C. M. and Canfield, D. E. 1992. Patterns in phytoplankton community structure in florida lakes. Limnology & Oceanography 37:155–161.

Eppley, R. W., Swift, E., Redalje, D. G., Landry, M. R., and Haas, L. W. 1988. Subsurface chlorophyll maximum in August-September 1985 in the climax area of the North Pacific. Marine Ecology-Progress Series 42:289–301.

Faith, D. P., Minchin, P. R., and Belbin, L. 1987. Compositional dissimilarity as a robust measure of ecological distance. Vegetatio 69:57–68.

Falkowski, P. G., Barber, R. T., and Smetacek, V. 1998. Biogeochemical controls and feedbacks on ocean primary production. Science 281:200–206.

Fee, E. J. 1976. Vertical and seasonal distribution of chlorophyll in lakes of Experimental-Lakes-Area, Northwestern Ontario implications for primary production estimates. Limnology & Oceanography 21:767–783.

Fee, E. J., Hecky, R. E., Kasian, S. E. M., and Cruikshank, D. R. 1996. Effects of lake size, water clarity, and climatic variability on mixing depths in Canadian Shield lakes. Limnology & Oceanography 41:912–920.

Fennel, K. and Boss, E. 2003. Subsurface maxima of phytoplankton and chlorophyll: steady-state solutions from a simple model. Limnology & Oceanography 48:1521–1534.

Field, C. B., Behrenfeld, M. J., Randerson, J. T., and Falkowski, P. 1998. Primary production of the biosphere: Integrating terrestrial and oceanic components. Science 281:237–240.

Finkel, Z. V., Irwin, A. J., and Schofield, O. 2004. Resource limitation alters the 3/4 size scaling of metabolic rates in phytoplankton. Marine Ecology-Progress Series 273:269–279.

Flöder, S. and Sommer, U. 1999. Diversity in planktonic communities: An experimental test of the intermediate disturbance hypothesis. Limnology & Oceanography 44:1114–1119.

Fogg, G. E. and Thake, B., 1987. Algal cultures and phytoplankton ecology. University of Wisconsin Press.

Franks, P. J. S. 1995. Thin-layers of phytoplankton - a model of formation by near-inertial wave shear. Deep-Sea Research Part I-Oceanographic Research Papers 42:75–91.

Franks, P. J. S. 2001. Turbulence avoidance: An alternate explanation of turbulence-enhanced ingestion rates in the field. Limnology & Oceanography 46:959–963.

Garside, C. 1985. The vertical-distribution of nitrate in open ocean surface-water. Deep-Sea Research Part A- Oceanographic Research Papers 32:723–732.

Gasol, J. M., Garciacantizano, J., Massana, R., Peters, F., Guerrero, R., and Pedrosalio, C. 1991. Diel changes in the microstratification of the metalimnetic community in Lake Ciso. Hydrobiologia 211:227–240.

Gasol, J. M., Guerrero, R., and Pedrosalio, C. 1992. Spatial and temporal dynamics of a metalimnetic Cryptomonas peak. Journal of Plankton Research 14:1565–1579.

Gervais, F. 1998. Ecology of cryptophytes coexisting near a freshwater chemocline. Freshwater Biology 39:61–78.

Gonsiorczyk, T., Casper, P., and Koschel, R. 1998. Phosphorus-binding forms in the sediment of an oligotrophic and an eutrophic hardwater lake of the Baltic lake district (Germany). Water Science & Technology 37:51–58.

Gross, H. P., Wurtsbaugh, W. A., Luecke, C., and Budy, P. 1997. Fertilization of an oligotrophic lake with a deep chlorophyll maximum: Predicting the effect on primary productivity. Canadian Journal of Fisheries & Aquatic Sciences 54:1177–1189.

Grover, J. P. 2009. Is storage an adaptation to spatial variation in resource availability? American Naturalist 173:E44–E61.

Guillard, R. 1975. Culture of phytoplankton for feeding marine invertebrates. Plenum Pub Corp proceedings.

Hartmann, J., Kunimatsu, T., and Levy, J. K. 2008. The impact of Eurasian dust storms and anthropogenic emissions on atmospheric nutrient deposition rates in forested Japanese catchments and adjacent regional seas. Global & Planetary Change 61:117–134.

Hastings, A., Byers, J. E., Crooks, J. A., Cuddington, K., Jones, C. G., Lambrinos, J. G., Talley, T. S., and Wilson, W. G. 2007. Ecosystem engineering in space and time. Ecology Letters 10:153–164.

Hays, G. C., Richardson, A. J., and Robinson, C. 2005. Climate change and marine plankton. Trends in Ecology & Evolution 20:337–344.

Hodges, B. A. and Rudnick, D. L. 2004. Simple models of steady deep maxima in chlorophyll and biomass. Deep-Sea Research Part I- Oceanographic Research Papers 51:999–1015.

Holopainen, A. L., Niinioja, R., and Rämö, A. 2003. Seasonal succession, vertical distribution and long term variation of phytoplankton communities in two shallow forest lakes in eastern Finland. Hydrobiologia 506:237–245.

Huisman, J. 1999. Population dynamics of light-limited phytoplankton: Microcosm experiments. Ecology 80:202–210.

Huisman, J., Arrayas, M., Ebert, U., and Sommeijer, B. 2002. How do sinking Phytoplankton species manage to persist? American Naturalist 159:245–254.

Huisman, J., Jonker, R. R., Zonneveld, C., and Weissing, F. J. 1999*a*. Competition for light between phytoplankton species: Experimental tests of mechanistic theory. Ecology 80:211–222.

Huisman, J., Sharples, J., Stroom, J. M., Visser, P. M., Kardinaal, W. E. A., Verspagen, J. M. H., and Sommeijer, B. 2004. Changes in turbulent mixing shift competition for light between phytoplankton species. Ecology 85:2960–2970.

Huisman, J. and Sommeijer, B. 2002. Maximal sustainable sinking velocity of phytoplankton. Marine Ecology-Progress Series 244:39–48.

Huisman, J. and Sommeijer, B. 2002. Population dynamics of sinking phytoplankton in light-limited environments: simulation techniques and critical parameters. Journal of Sea Research 48:83–96.

Huisman, J., Thi, N. N. P., Karl, D. M., and Sommeijer, B. 2006. Reduced mixing generates oscillations and chaos in the oceanic deep chlorophyll maximum. Nature 439:322–325.

Huisman, J., van Oostveen, P., and Weissing, F. 1999*b*. Species dynamics in phytoplankton blooms: Incomplete mixing and competition for light. American Naturalist 154:46–68.

Huisman, J., van Oostveen, P., and Weissing, F. J. 1999*c*. Critical depth and critical turbulence: Two different mechanisms for the development of phytoplankton blooms. Limnology & Oceanography 44:1781–1787.

Huisman, J. and Weissing, F. J. 1994. Light-limited growth and competition for light in well-mixed aquatic environments: an elementary model. Ecology 75:507–520.

Huisman, J. and Weissing, F. J. 1995. Competition for nutrients and light in a mixed water column - a theoretical-analysis. American Naturalist 146:536–564.

Hutchinson, G. E., 1957. A Treatise on Limnology. John Wiley & Sons.

Hutchinson, G. E. 1961. The paradox of the plankton. American Naturalist 95:137–145.

Incze, L. S., Hebert, D., Wolff, N., Oakey, N., and Dye, D. 2001. Changes in copepod distributions associated with increased turbulence from wind stress. Marine Ecology-Progress Series 213:229–240.

Jaeger, C. G., Diehl, S., and Emans, M. 2010. Physical determinants of phytoplankton production, algal stoichiometry, and vertical nutrient fluxes. American Naturalist 175:E51–E104.

Jaeger, C. G., Diehl, S., and Schmidt, G. M. 2008. Influence of water-column depth and mixing on phytoplankton biomass, community composition, and nutrients. Limnology & Oceanography 53:2361–2373.

Jöhnk, K. D., Huisman, J., Sharples, J., Sommeijer, B., Visser, P. M., and Stroom, J. M. 2008. Summer heatwaves promote blooms of harmful cyanobacteria. Global Change Biology 14:495–512.

Johnsen, G. H. and Jakobsen, P. J. 1987. The effect of food limitation on vertical migration in Daphnia-Longispina. Limnology & Oceanography 32:873–880.

Karlsson, J., Byström, P., Ask, J., Ask, P., Persson, L., and Jansson, M. 2009. Light limitation of nutrient-poor lake ecosystems. Nature 460:506–509.

Kirk, J. T. O. 1975*a*. Theoretical-analysis of contribution of algal cells to attenuation of light within natural-waters. 1. General treatment of suspensions of pigmented cells. New Phytologist 75:11–20.

Kirk, J. T. O. 1975*b*. Theoretical-analysis of contribution of algal cells to attenuation of light within natural-waters. 2. spherical cells. New Phytologist 75:21–36.

Klausmeier, C. A. 1999. Regular and irregular patterns in semiarid vegetation. Science 284:1826–1828.

Klausmeier, C. A., 2000. Ph.D. thesis, University of Minnesota.

Klausmeier, C. A. and Litchman, E. 2001. Algal games: The vertical distribution of phytoplankton in poorly mixed water columns. Limnology & Oceanography 46:1998–2007.

Kling, G. W., Hayhoe, K., Johnson, L. B., Magnuson, J. J., Polasky, S., Robinson, S. K., Shuter, B. J., Wander, M. M., Wuebbles, D. J., Zak, D. R., Lindroth, R. L., Moser, S. C., and Wilson, M. L. 2003. Confronting climate change in the great lakes region: impacts on our communities and ecosystems. Union of Concerned Scientists, Cambridge, Massachusetts, and Ecological Society of America, Washington, DC .

Krause-Jensen, D. and Sand-Jensen, K. 1998. Light attenuation and photosynthesis of aquatic plant communities. Limnology & Oceanography 43:396–407.

Kunz, T. J. and Diehl, S. 2003. Phytoplankton, light and nutrients along a gradient of mixing depth: a field test of producer-resource theory. Freshwater Biology 48:1050–1063.

Laland, K. N., Odling-Smee, F. J., and Feldman, M. W. 1999. Evolutionary consequences of niche construction and their implications for ecology. Proceedings Of The National Academy Of Sciences Of The United States Of America 96:10242–10247.

Lampert, W., Fleckner, W., Rai, H., and Taylor, B. E. 1986. Phytoplankton control by grazing zooplankton - a study on the spring clear-water phase. Limnology & Oceanography 31:478–490.

Lampert, W., McCauley, E., and Manly, B. F. J. 2003. Trade-offs in the vertical distribution of zooplankton: ideal free distribution with costs? Proceedings of the Royal Society of London Series B-Biological Sciences 270:765–773.

Legendre, P. and Legendre, L., 1998. Numerical Ecology. Elsevier Science B.V.

Leibold, M. A. 1990. Resources and predators can affect the vertical distributions of zooplankton. Limnology & Oceanography 35:938–944.

Leibold, M. A. 1991. Trophic interactions and habitat segregation between competing daphnia species. Oecologia 86:510–520.

Leibold, M. A., Holyoak, M., Mouquet, N., Amarasekare, P., Chase, J. M., Hoopes, M. F., Holt, R. D., Shurin, J. B., Law, R., Tilman, D., Loreau, M., and Gonzalez, A. 2004. The metacommunity concept: a framework for multi-scale community ecology. Ecology Letters 7:601–613.

Levin, S. A. 1976. Population dynamic-models in heterogeneous environments. Annual Review of Ecology and Systematics 7:287–310.

Levin, S. A. 1992. The problem of pattern and scale in ecology. Ecology 73:1943–1967.

Levin, S. A. 1994. Patchiness in marine and terrestrial systems - from individuals to populations. Philosophical Transactions of the Royal Society of London Series B-Biological Sciences 343:99–103.

Levins, R. 1979. Coexistence in a variable environment. American Naturalist 114:765–783.

Lindholm, T. 1992. Ecological role of depth maxima of phytoplankton. Archiv für Hydrobiologie-Beiheft Ergebnisse der Limnologie 35:33–45.

Litchman, E. and Klausmeier, C. A. 2008. Trait-Based Community Ecology of Phytoplankton. Annual Review of Ecology, Evolution, and Systematics 39:615–639.

Livingstone, D. M. 2003. Impact of secular climate change on the thermal structure of a large temperate central European lake. Climate Change 57:205–225.

Longhi, M. L. and Beisner, B. E. 2009. Environmental factors controlling the vertical distribution of phytoplankton in lakes. Journal of Plankton Research 31:1195–1207.

Loreau, M., Mouquet, N., and Gonzalez, A. 2003*a*. Biodiversity as spatial insurance in heterogeneous landscapes. Proceedings Of The National Academy Of Sciences Of The United States Of America 100:12765–12770.

Loreau, M., Mouquet, N., and Holt, R. D. 2003*b*. Meta-ecosystems: a theoretical framework for a spatial ecosystem ecology. Ecology Letters 6:673–679.

Lorenzen, M. and Mitchell, R. 1973. Theoretical effects of artificial destratification on algal production in impoundments. Environmental Science & Technology 7:939–944.

Losos, J. B., Leal, M., Glor, R. E., de Queiroz, K., Hertz, P. E., Schettino, L. R., Lara, A. C., Jackman, T. R., and Larson, A. 2003. Niche lability in the evolution of a Caribbean lizard community. Nature 424:542–545.

Lucas, L. V., Cloern, J. E., Koseff, J. R., Monismith, S. G., and Thompson, J. K. 1998. Does the sverdrup critical depth model explain bloom dynamics in estuaries? Journal of Marine Research 56:375–415.

Luketina, D. and Imberger, R. 2001. Determining turbulent kinetic energy dissipation from Batchelor curve fitting. Journal of Atmospheric and Oceanic Technology 18:100–113.

MacArthur, R., 1972. Geographical ecology: patterns in the distribution of species. Harper & Row.

MacIntyre, S., Flynn, K. M., Jellison, R., and Romero, J. R. 1999. Boundary mixing and nutrient fluxes in Mono Lake, California. Limnology & Oceanography 44:512–529.

Magnuson, J. J., Webster, K. E., Assel, R. A., Bowser, C. J., Dillon, P. J., Eaton, J. G., Evans, H. E., Fee, E. J., Hall, R. I., Mortsch, L. R., Schindler, D. W., and Quinn, F. H. 1997. Potential effects of climate changes on aquatic systems: Laurentian Great Lakes and Precambrian Shield Region. Hydrological Processes 11:825–871.

Mann, K. H. and Lazier, J. R. N., 1996. Dynamics of marine ecosystems: biological-physical interacting in the oceans. Blackwell Science.

Marsden, M. W. 1989. Lake restoration by reducing external phosphorus loading - the influence of sediment phosphorus release. Freshwater Biology 21:139–162.

Mazumder, A., Taylor, W. D., McQueen, D. J., and Lean, D. R. S. 1990. Effects of fish and plankton on lake temperature and mixing depth. Science 247:312–315.

McCann, K. S., Rasmussen, J. B., and Umbanhowar, J. 2005. The dynamics of spatially coupled food webs. Ecology Letters 8:513–523.

Moll, R. A. and Stoermer, E. F. 1982. A hypothesis relating trophic status and subsurface chlorophyll maxima of lakes. Archiv für Hydrobiologie 94:425–440.

Monsi, M. and Saeki, T. 1953. On the factor light in plant communities and its importance for matter production. Japanese Journal of Botany 14:22–52.

Neff, J. C., Ballantyne, A. P., Farmer, G. L., Mahowald, N. M., Conroy, J. L., Landry, C. C., Overpeck, J. T., Painter, T. H., Lawrence, C. R., and Reynolds, R. L. 2008. Increasing eolian dust deposition in the western United States linked to human activity. Nature Geoscience 1:189–195.

Okubo, A., 1980. Diffusion and ecological problems: mathematical models. Springer-Verlag.

O'Reilly, C. M., Alin, S. R., Plisnier, P. D., Cohen, A. S., and McKee, B. A. 2003. Climate change decreases aquatic ecosystem productivity of Lake Tanganyika, Africa. Nature 424:766–768.

Osborn, T. R. 1980. Estimates of the local-rate of vertical diffusion from dissipation measurements. Journal of Physical Oceanography 10:83–89.

Padisák, J., 2004. Phytoplankton, in The Lakes Handbook: Limnology and limnetic ecology, Pages 251–308. Wiley-Blackwell.

Paerl, H. W. 1988. Nuisance phytoplankton blooms in coastal, estuarine, and inland waters. Limnology & Oceanography 33:823–847.

Pannard, A., Bormans, M., Lefebvre, S., Claquin, P., and Lagadeuc, Y. 2007. Phytoplankton size distribution and community structure: influence of nutrient input and sedimentary loss. Journal of Plankton Research 29:583–598.

Pasciak, W. J. and Gavis, J. 1974. Transport limitation of nutrient uptake in phytoplankton. Limnology and Oceanography 19:881–898.

Passarge, J., Hol, S., Escher, M., and Huisman, J. 2006. Competition for nutrients and light: Stable coexistence, alternative stable states, or competitive exclusion? Ecological Monographs 76:57–72.

Peeters, F., Straile, D., Lorke, A., and Ollinger, D. 2007. Turbulent mixing and phytoplankton spring bloom development in a deep lake. Limnology & Oceanography 52:286–298.

Peters, R. H. and Rigler, F. H. 1973. Phosphorus release by Daphnia. Limnology & Oceanography 18:821–839.

Portielje, R. and Lijklema, L. 1999. Estimation of sediment-water exchange of solutes in Lake Veluwe, the Netherlands. Water Research 33:279–285.

Press, W. H., Flannery, B. P., Teukolsky, S. A., and Vetterling, W. T., 2001. Numerical recipes in Fortran 77: the art of scientific computing. Cambridge University Press.

Ptacnik, R., Diehl, S., and Berger, S. 2003. Performance of sinking and nonsinking phytoplankton taxa in a gradient of mixing depths. Limnology & Oceanography 48:1903–1912.

Reynolds, C. S., 1984. The ecology of freshwater phytoplankton. Cambridge University Press.

Reynolds, C. S. 1998. What factors influence the species composition of phytoplankton in lakes of different trophic status? Hydrobiologia 370:11–26.

Richardson, K., Beardall, J., and Raven, J. A. 1983. Adaptation of unicellular algae to irradiance- an analysis of strategies. New Phytologist 93:157–191.

Riley, G. A. 1942. The relationship of vertical turbulence and spring diatom flowerings. Journal of Marine Research 5:67–87.

Ross, O. N. and Sharples, J. 2007. Phytoplankton motility and the competition for nutrients in the thermocline. Marine Ecology-Progress Series 347:21–38.

Ryabov, A. B., Rudolf, L., and Blasius, B. 2009. Vertical distribution and composition of phytoplankton under the influence of an upper mixed layer. Journal of Theoretical Biology .

Sand-Jensen, K. and Borum, J. 1991. Interactions among phytoplankton, periphyton, and macrophytes in temperate freshwaters and estuaries. Aquatic Botany 41:137–175.

Sarnelle, O. 1992. Nutrient enrichment and grazer effects on phytoplankton in lakes. Ecology 73:551–560.

Sarnelle, O. 2005. Daphnia as keystone predators: effects on phytoplankton diversity and grazing resistance. Journal of Plankton Research 27:1229–1238.

Savitzky, A. and Golay, M. J. E. 1964. Smoothing + differentiation of data by simplified least squares procedures. Analytical Chemistry 36:1627–&.

Schindler, D. W. 1977. Evolution of phosphorus limitation in lakes. Science 195:260–262.

Schindler, D. W. 1997. Widespread effects of climatic warming on freshwater ecosystems in north america. Hydrological Processes 11:1043–1067.

Sharp, J. H., Perry, M. J., Renger, E. H., and Eppley, R. W. 1980. Phytoplankton rate processes in the oligotrophic waters of the Central North Pacific Ocean. Journal of Plankton Research 2:335–353.

Sharpley, A., Daniel, T. C., Sims, J. T., and Pote, D. H. 1996. Determining environmentally sound soil phosphorus levels. Journal of Soil & Water Conservation 51:160–166.

Simpson, E. H. 1949. Measurement of diversity. Nature 163:688.

Skellam, J. 1951. Random dispersal in theoretical populations. Biometrika 38:196–218.

Smith, V. H. 1986. Light and nutrient effects on the relative biomass of blue-green algae in lake phytoplankton. Canadian Journal of Fisheries & Aquatic Sciences 43:148–153.

Smith, V. H., Foster, B. L., Grover, J. P., Holt, R. D., Leibold, M. A., and deNoyelles, F. 2005. Phytoplankton species richness scales consistently from laboratory microcosms to the world's oceans. Proceedings of The National Academy of Sciences of The USA 102:4393–4396.

Smith, W. O. 1982. The relative importance of chlorophyll, dissolved and particulate material, and sea-water to the vertical extinction of light. Estuarine Coastal and Shelf Science 15:459–465.

Sommer, U. and Gliwicz, Z. M. 1986. Long-range vertical migration of Volvox in tropical Lake Cahora Bassa (Mozambique). Limnology & Oceanography 31:650–653.

Spaulding, S. A., McKnight, D. M., Smith, R. L., and Dufford, R. 1994. Phytoplankton population-dynamics in perennially ice-covered Lake Fryxell, Antarctica. Journal of Plankton Research 16:527–541.

Steele, J. 1974. Spatial heterogeneity and population stability. Nature 248:83.

Steele, J. H., 1978. Spatial pattern in plankton communities. NATO Conference Series IV: Marine Sciences Vol. 3., Pages 1–20. Plenum Press, New York.

Sterner, R. W. and Elser, J. J., 2002. Ecological stoichiometry: the biology of elements from molecules to the biosphere. Princeton University Press, Princeton NJ.

Stevens, M. H. H. and Carson, W. P. 2002. Resource quantity, not resource heterogeneity, maintains plant diversity. Ecology Letters 5:420–426.

Stow, C. A., Carpenter, S. R., Webster, K. E., and Frost, T. M. 1998. Long-term environmental monitoring: Some perspectives from lakes. Ecological Complexity 8:269–276.

Strzepek, R. F. and Harrison, P. J. 2004. Photosynthetic architecture differs in coastal and oceanic diatoms. Nature 431:689–692.

Suess, E. 1980. Particulate organic-carbon flux in the oceans - surface productivity and oxygen utilization. Nature 288:260–263.

Sverdrup, H. U. 1953. On conditions for the vernal blooming of phytoplankton. Journal du Conseil 18:287–295.

Tilman, D., 1982. Resource competition and community structure. Princeton University Press, Princeton NJ.

Tilman, D. and Kareiva, P. M., 1997. Spatial ecology: the role of space in population dynamics and interspecific interactions. Princeton University Press, Princeton NJ.

Tittel, J., Bissinger, V., Zippel, B., Gaedke, U., Bell, E., Lorke, A., and Kamjunke, N. 2003. Mixotrophs combine resource use to outcompete specialists: Implications for aquatic food webs. Proceedings Of The National Academy Of Sciences Of The United States Of America 100:12776–12781.

van de Koppel, J., Gascoigne, J. C., Theraulaz, G., Rietkerk, M., Mooij, W. M., and Herman, P. M. J. 2008. Experimental evidence for spatial self-organization and its emergent effects in mussel bed ecosystems. Science 322:739–742.

Verburg, P., Hecky, R. E., and Kling, H. 2003. Ecological consequences of a century of warming in Lake Tanganyika. Science 301:505–507.

Visser, P. M., Ibelings, B. W., vanderVeer, B., Koedood, J., and Mur, L. R. 1996. Artificial mixing prevents nuisance blooms of the cyanobacterium Microcystis in Lake Nieuwe Meer, the Netherlands. Freshwater Biology 36:435–450.

Vogel, S., 1994. Life in Moving Fluids. Princeton University Press, Princeton NJ.

Waite, A., Fisher, A., Thompson, P. A., and Harrison, P. J. 1997. Sinking rate versus cell volume relationships illuminate sinking rate control mechanisms in marine diatoms. Marine Ecology-Progress Series 157:97–108.

Walker, J. T. and Maddan, S., 2005. Statistics in criminology and criminal justice: analysis and interpretation. Jones & Bartlett Learning.

Watson, S. B., McCauley, E., and Downing, J. A. 1997. Patterns in phytoplankton taxonomic composition across temperate lakes of differing nutrient status. Limnology & Oceanography 42:487–495.

Weaver, W. and Shannon, C. E., 1949. The Mathematical Theory of Communication. University of Illinois, Urbana, Illinois.

Welschmeyer, N. A. 1994. Fluorometric analysis of chlorophyll-a in the presence of chlorophyll-b and pheopigments. Limnology & Oceanography 39:1985–1992.

Werner, E. E., Gilliam, J. F., Hall, D. J., and Mittelbach, G. G. 1983. An experimental test of the effects of predation risk on habitat use in fish. Ecology 64:1540–1548.

Werner, E. E. and Hall, D. J. 1977. Competition and habitat shift in 2 sunfishes (Centrarchidae). Ecology 58:869–876.

Wetzel, R. G., 1975. Limnology. W.B. Saunders Company.

Williamson, C. E., Sanders, R. W., Moeller, R. E., and Stutzman, P. L. 1996. Utilization of subsurface food resources for zooplankton reproduction: Implications for diel vertical migration theory. Limnology & Oceanography 41:224–233.

Wüest, A., Piepke, G., and Van Senden, D. C. 2000. Turbulent kinetic energy balance as a tool for estimating vertical diffusivity in wind-forced stratified waters. Limnology & Oceanography 45:1388–1400.

Yoshiyama, K., Mellard, J. P., Litchman, E., and Klausmeier, C. A. 2009. Phytoplankton competition for nutrients and light in a stratified water column. American Naturalist 174:190–203.

Yoshiyama, K. and Nakajima, H. 2002. Catastrophic transition in vertical distributions of phytoplankton: Alternative equilibria in a water column. Journal of Theoretical Biology 216:397–408.